SPACED CLEAVAGE DEVELOPMENT IN THE METAGREYWACKES OF THE GOLDENVILLE FORMATION, MEGUMA GROUP, NOVA SCOTIA

SPACED CLEAVAGE DEVELOPMENT IN THE METAGREYWACKES OF THE GOLDENVILLE FORMATION, MEGUMA GROUP, NOVA SCOTIA

By

FRANK FUETEN

A Thesis

Submitted to the School of Graduate Studies

in Partial Fulfilment of the Requirements

for the Degree

Master of Science

McMaster University

November, 1984

MASTER OF SCIENCE (1984) McMASTER UNIVERSITY
(Geology) Hamilton, Ontario

TITLE: Spaced Cleavage Development in the Metagreywackes of the Goldenville Formation, Meguma Group, Nova Scotia

AUTHOR: Frank Fueten, B.Sc. (McMaster University)

SUPERVISORS: Drs. P.M. Clifford and J.H. Crocket

NUMBER OF PAGES: ix, 145

Abstract

The greywackes of the Goldenville Formation, Meguma Group, Nova Scotia display a well developed spaced cleavage. The cleavage is characterized by zones of mica enrichment and associated quartz depletion and forms a network of anastomosing cleavage rhombs. Parallelism between cleavage and water escape structures suggests that the cleavage was emplaced perpendicular to bedding early in the deformational history of the rocks. Subsequent passive rotation of cleavage and water escape strucures reduced the bedding-cleavage angle to its present values.

XRF whole rock analyses of cleavage planes and lithons from two different sample locations show that the cleavage is depleted in SiO_2, CaO, Na_2O and enriched in Al_2O_3, Fe_2O_3, MgO, K_2O, TiO_2, MnO and P_2O_5 relative to lithons. Mass balance calculations based on the Gresens (1967) approach indicate that the cleavage with respect to the lithon represents a 40%-60% volume loss. Using the volume loss it can be shown that the cleavage lost SiO_2, Na_2O, CaO, MnO, P_2O_5, Pb, Sr, Nb and Y and gained MgO, K_2O, Ba, Rb and W during its formation. TiO_2, Al_2O_3, Fe_2O_3 and Zr remain relatively immobile during the cleavage forming processes. The behavior of Au, Sb, As, Ce, Nd, and La can not be discerned.

The cleavage was initiated by pressure solution at grain contacts. However, several of the above mentioned chemical migrations increased the solubility of quartz and therefore greatly enhanced the development of the cleavage.

Acknowledgments

I would like to thank Dr. P. M. Clifford for supervising my second thesis as well as my first one. I especially would like to thank him for the many stimulating conversations we had, some of which were actually about geology. Thank you also to Dr. J. H. Crocket, my "other" supervisor. Although Jim was difficult to find at times, his advise proved to be well worth the time invested searching for him. Dr. J. R. Henderson, who was my "boss" for two field seasons and his wife, Mariette, have been extremely helpful over these two years, especially by helping me maintain my sanity. Additionally I want to thank them for repeatedly letting me abuse their hospitality. Thank you to Dr. P. Y. Robin who added many helpful suggestions.

I have been fortunate enough to farm out significant portions of my work as bachelors theses. For doing an excellent job on those I want to thank Joanne Thompson and Lynn Pryer. Lynn was also a good field assistant. Thank you also to the other people who worked with us in Nova Scotia and contributed.

I am grateful to Abdul Kabir and Ota Mudrock for helping me with the analytical gadgets they so expertly run. Len Zwicker's skill for preparing excellent thin sections and apple cider, as well as his willingness to provide his lab as a hiding place from undergraduates and supervisors is

greatly appreciated. Many thanks are extended to Jack Whorwood, for his expert photography and for lending me all those books which I very much enjoyed reading while Lynn and Joanne were doing their theses.

I want to thank Andy Fyon for being my geochemical advisor and computer consultant. Thank you to Libby Fyon for helping me to put this thesis together and to Eric Fyon for leaving his mom alone long enough to do just that. Finally I would like to thank my friends for putting up with me over the last two years and for answering to the call "DINNER !?!".

This project was funded by the Geological Survey of Canada under SSC-DEMR Grant # 22ST-23233-3-0354.

Table of Contents

List of Figures

List of Tables

1. Introduction

In 1863 Sorby stated: "Limestone completely surrounded and pervaded by calcium carbonate saturated water dissolves, where the pressure is greatest and crystallizes, where it is least." (Sorby 1863 p.805) In 1908 he named this phenomenon "Pressure solution". He was thus the first person to recognize the effects of dissolution of minerals under non-hydrostatic stress and so opened up a field that has since become an area of interest to many geologists.

Non-hydrostatic thermodynamics (Gibbs, 1877) provided the theoretical groundwork for the understanding of why pressure solution should occur. It showed that a chemical potential gradient exists between the stressed and the stress-free interface of a solid. Material is therefore dissolved at areas of high chemical potential and migrates towards areas of lower chemical potential.

Observational evidence for pressure solution in rocks has been summarized in terms of 14 pressure solution contacts in 1968 by Trurnit. These contacts may be sutured, stylolitic or smooth, depending on the relative solubility of the partners involved. The less soluble partner always penetrates the more soluble one.

Pressure solution has been cited as the reason for the formation of stylolites or for the welding of granular material in limestones, dolomites and sandstones (Durney

1972). Others , for example Cosgrove (1974), and Gray (1979), regard pressure solution as one of the processes which yield crenulation cleavage in pelitic rocks. More mobile quartz is thought to have been dissolved away, leaving more phyllosilicate rich domains. Alvarez et al. (1978) and Engelder (1979) describe a spaced cleavage in limestones, where pressure solution is responsible for the removal of carbonate, producing a shortening of beds of up to 50%. This cleavage anastomoses and mean cleavage spacing decreases as the amount of shortening increases.

Williams (1972) and Boulter (1979) describe spaced and anastomosing pressure solution cleavages in greywackes. Williams (1972) discusses the development of the phyllosilicate rich domains in terms of selective removal of quartz. He considers the preferred orientation of the phyllosilicates parallel to the foliation to be due to grain rotation during cleavage development. Boulter (1979) argues for the development of an early, prefolding spaced pressure solution cleavage which is initially perpendicular to bedding. The bedding-cleavage angle is then reduced by passive rotation of the cleavage during folding. Despite the large amount of attention that spaced pressure solution has received, relatively little is known about its propagation or its chemical evolution.

Fletcher (1981) proposed an anticrack model for the propagation of pressure solution surfaces. In it large isotropic compressive stresses are set up at the tips of

solution surfaces as material is dissolved and removed. The solution surface propagates through the rock, largely as a result of these compressive stresses which promote further solution.

Several chemical reactions which enhance silica solubility and therefore aid in the formation of a spaced cleavage, have been proposed by Beach (1979), who considers the breakdown of feldspar to be of great importance for the formation of a spaced cleavage. He also suggests that the recrystallization of clays into muscovite, chlorite and biotite may help to increase silica solubility.

Robin (1979) addresses the problem of silica migration in rocks. He shows that the difference between the minimum and maximum principal stress is greater in the quartz rich layers than in the mica rich layers. When interlayer difussion is possible, silica will migrate to the low pressure interfaces in the quartz rich layers.

Little analytical work has been done on samples of real rocks. Gratier (1983) has attempted to use chemistry to estimate the volume changes occurring in a heterogeneously deformed layer. Although only a few analyses underlie his calculations, he concludes that the chemically estimated volume changes are compatible with the general strain patterns observed in the layer. Only one set of chemical analyses of individual cleavages and lithons are available in the literature (Glasson and Keays, 1978). These are used to estimate if the amount of precious metals released during

cleavage formation can account for the amounts of precious metals found in the local deposits. Unfortunately, that study restricts itself to answering that question and does not address the nature of the chemical migrations of other elements during cleavage formation.

This study will concentrate on the chemical changes which occurred in the greywackes of the Meguma Group of Nova Scotia during cleavage formation. The aim of this study is to develop a model for spaced cleavage formation, which integrates the observed physical and chemical changes. Preliminary results of this study have been published in Geological Survey of Canada, Current Research Part B, 1983.

2. Geological setting

The metasediments of the Meguma Group underly approximately 16200 square kilometres of Nova Scotia. The Cambro-Ordovician Meguma Group extends from the Atlantic coastal islands to its northern boundary, the Cobequid-Chedabucto fault zone (figure 2.1). Axial surface traces of the folds in the Meguma Group extend for tens of kilometres. The axial surfaces of these folds are subvertical and are often offset in an en echelon fashion (Henderson, 1983)

The Meguma Group itself is divided into two formations. The older Goldenville Formation consists mostly of quartz-rich greywackes and interbedded slates, deposited by turbidity currents (Schenk,1970). Primary structures, found in the Goldenville Formation, include graded bedding, cross-bedding, ripple marks, flute marks, groove casts and water escape structures (Schenk,1970). Recent sedimentological work by Waldron (1984) describes the Goldenville formation as part of a submarine fan.

The Halifax Formation, which overlies the Goldenville Formation, consists of thinly laminated slate with minor amounts of siltstones and argillites (Shenk,1970). Primary structures include ripple marks ,scours and worm burrows. The contact between the Goldenville and Halifax Formations is conformable, but varies from sharp to gradational over several tens of

Figure 2.1

Areal extent of the Meguma Group

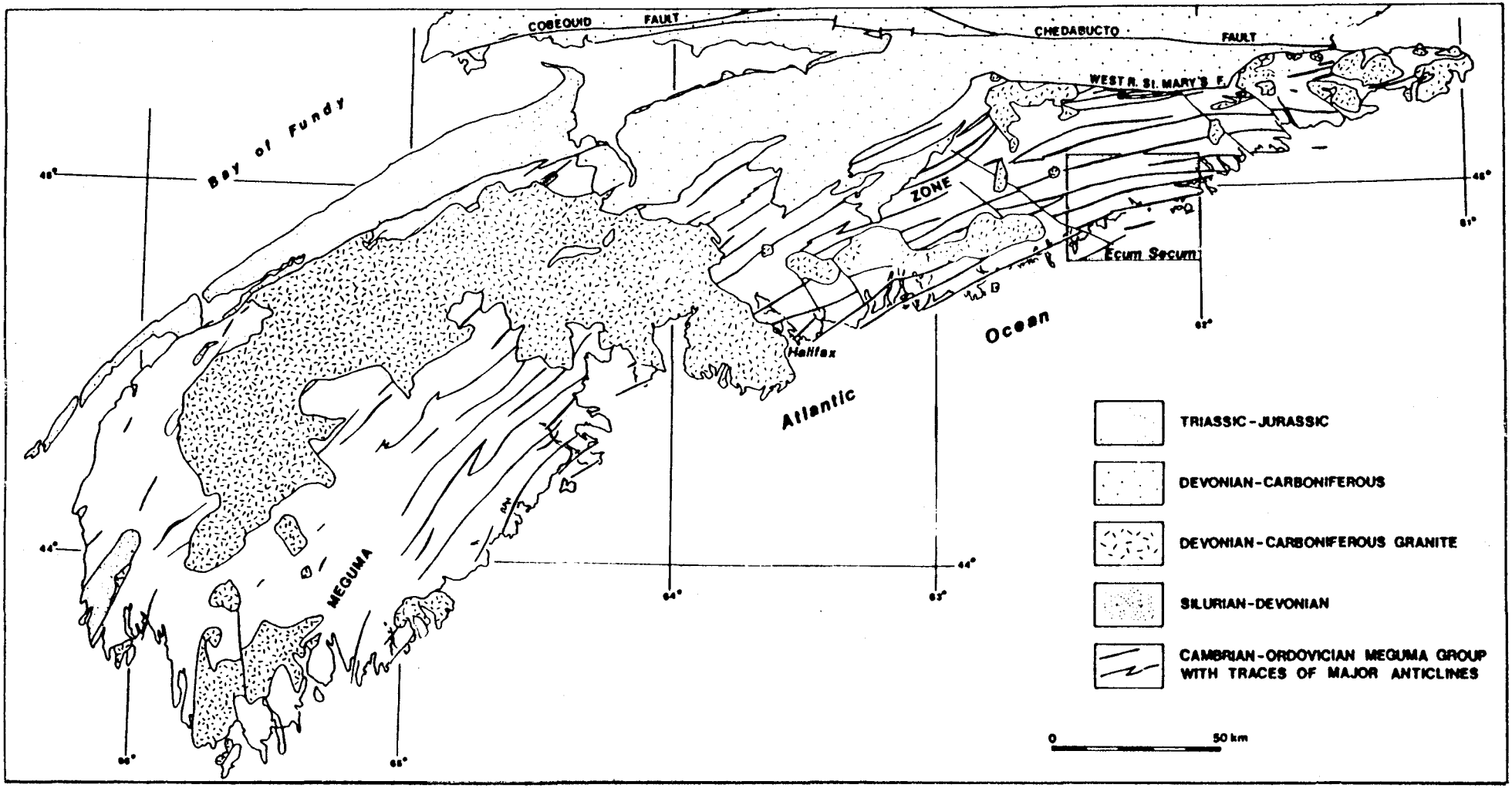
COBEQUID FAULT
CHEDABUCTO FAULT
WEST R. ST. MARY'S F.
Bay of Fundy
ZONE
Ecum Secum
Halifax
Atlantic
Ocean
MEGUMA
TRIASSIC-JURASSIC
DEVONIAN-CARBONIFEROUS
DEVONIAN-CARBONIFEROUS GRANITE
SILURIAN-DEVONIAN
CAMBRIAN-ORDOVICIAN MEGUMA GROUP WITH TRACES OF MAJOR ANTICLINES
0
50 km

metres.

The area mapped as part of this study lies between 62.00 and 62.30W, and extends from the Atlantic coast to the West River-St.Mary's Fault, which forms its northern boundary. The metamorphic grade in this area increases northward from chlorite grade greenschist facies at the coast to staurolite grade amphibolite facies at its northern boundary. The area was originally mapped by E.R. Faribault (1893, 1895a,b, 1896, 1897a,b) and more recently by J.R. Henderson (1983). In 1982, a detailed map of the Ruth Falls Syncline (Fig. 2.2) was prepared, prior to sampling at various sites in the Syncline.

Figure 2.2a

Generalized structure map of Ruth Falls Syncline

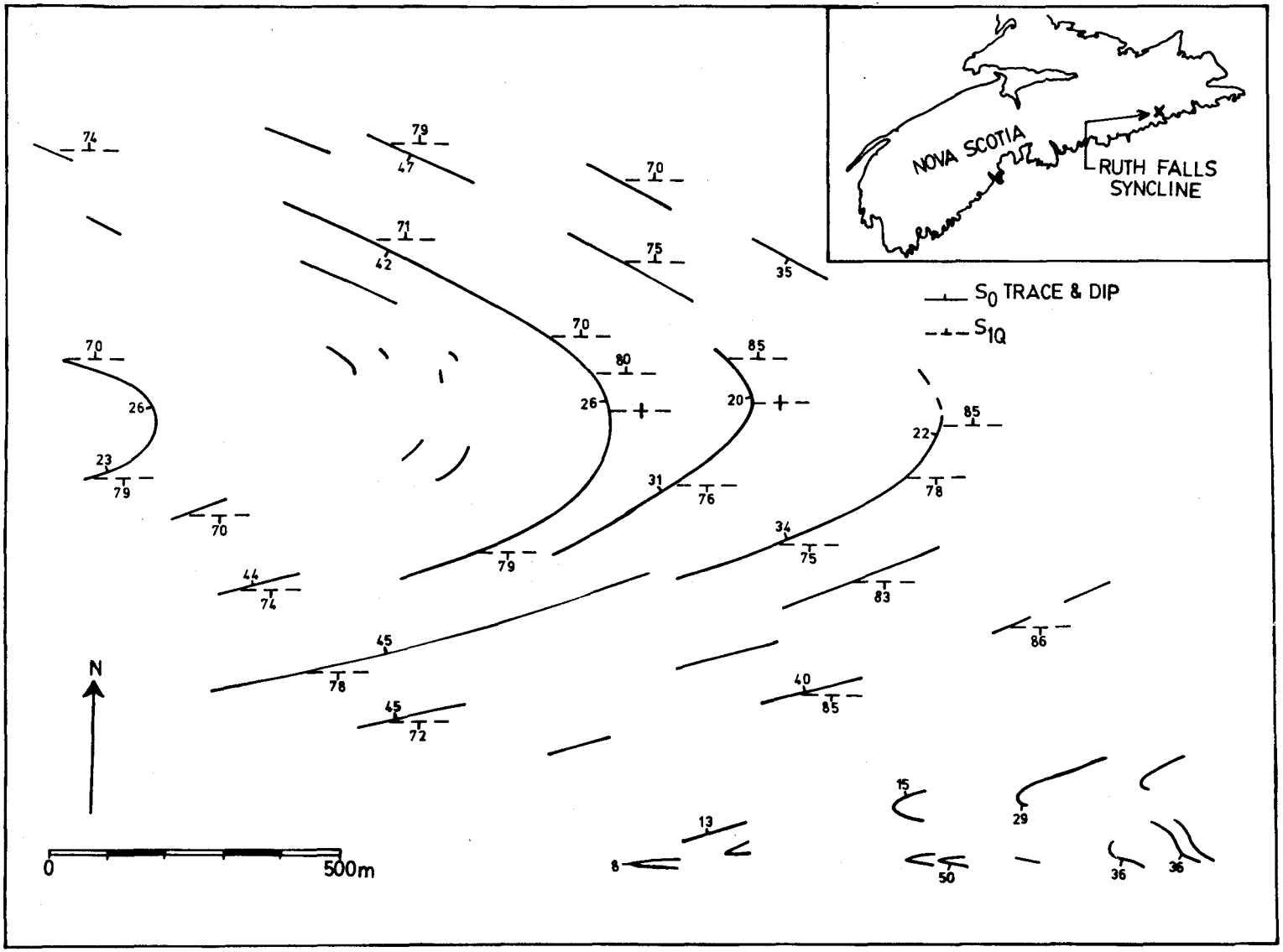
NOVA SCOTIA
RUTH FALLS SYNCLINE
S_0 TRACE & DIP
S_{1Q}
N
0
500m

Figure 2.2b

Air photo of Ruth Falls Syncline showing outcrop ridges of greywacke beds. Long axis of Lake is 500 m.


A.80301-110

3.1 Cleavage, Field Description

The greywackes of the Goldenville Formation display a spaced cleavage, which is thought to be a pressure solution cleavage. This cleavage has an anastomosing character, much as the solution cleavage in pelagic limestones described by Alvarez (1978). Throughout the area the strike of the cleavage is consistently sub-parallel, east-west, but the dip and dip direction varies. In general on a south dipping limb the cleavage dips north and vice versa. Only in areas of overturned bedding does the greywacke cleavage dip in the same direction as bedding. The dip of the cleavage varies with the dip of bedding. Figures 3.1a,b,c,d depict the bedding cleavage relationships in different parts of the map area. Data for fig. 3.1a were taken only from the Ruth Falls syncline alone, since it provided the largest data set for a small area. Figures 3.1b,c,d incorporate data from the remainder of the area. All four graphs follow the same trend. For bedding dips of 0 to approximately 20 degrees the bedding-cleavage angle is roughly 90 degrees. With increasing bedding dips the bedding-cleavage angle steadily decreases to between 5 and 20 degrees for vertical bedding.

Water escape stuctures are ubiquitous throughout the area. These consist of dewatering pipes capped by sand volcanoes and dewatering sheet structures. Both pipes and

Figure 3.1

a - Ruth Falls

b - Island and Coast

c - Center Section

d - North Section

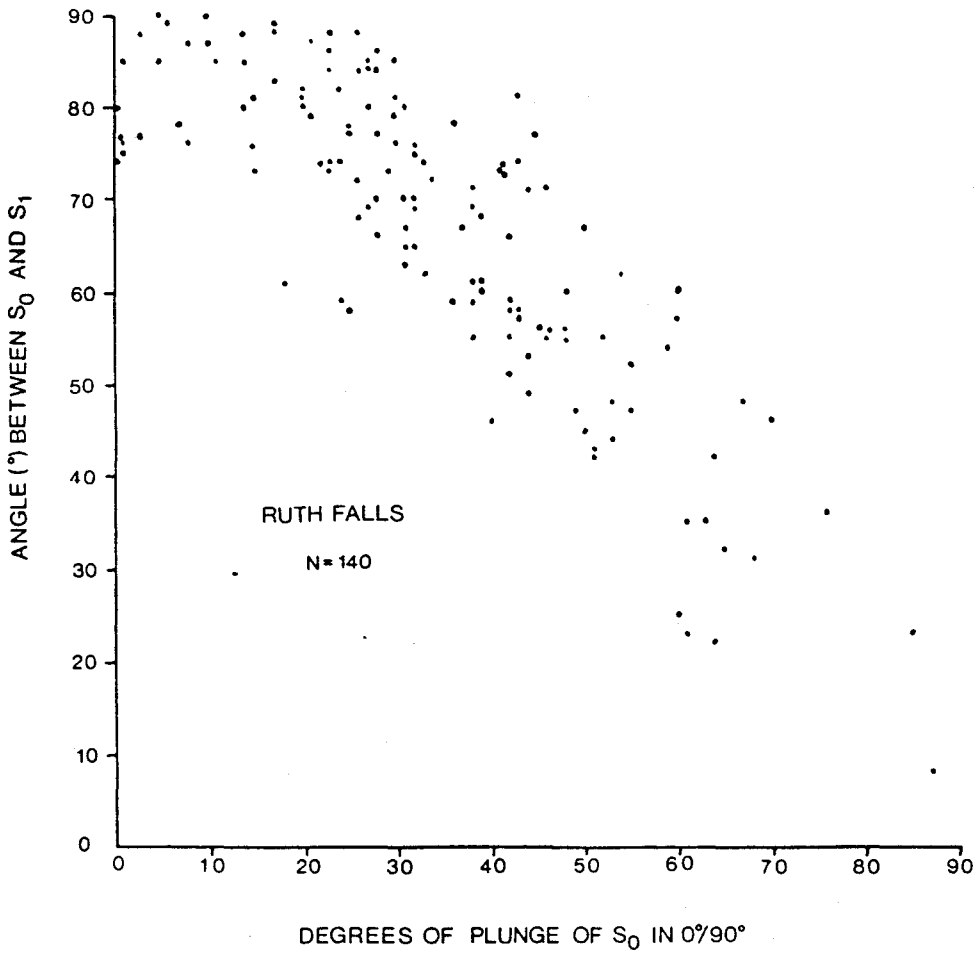
ANGLE (°) BETWEEN S_0 AND S_1
90
80
70
60
50
40
30
20
10
0
RUTH FALLS
N = 140
0
10
20
30
40
50
60
70
80
90
DEGREES OF PLUNGE OF S_0 IN 0°/90°

Figure 3.1a

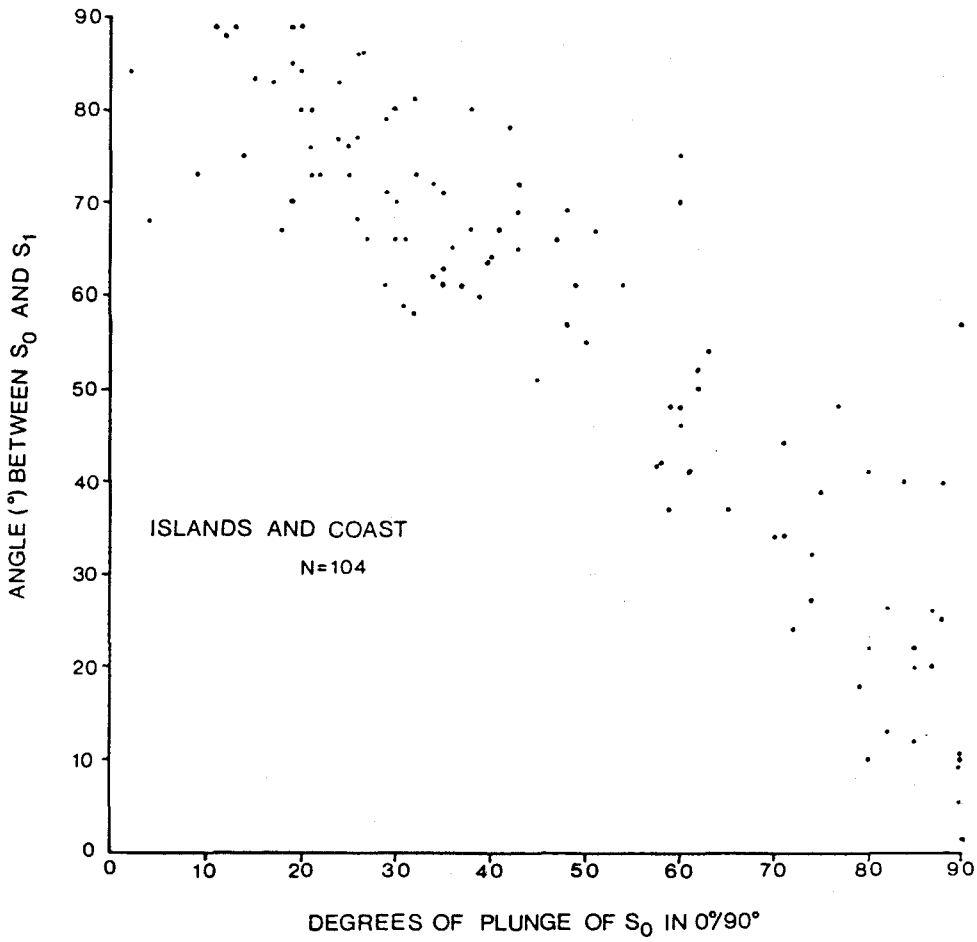
ANGLE (°) BETWEEN S_0 AND S_1
DEGREES OF PLUNGE OF S_0 IN 0°/90°
ISLANDS AND COAST
N=104
0
10
20
30
40
50
60
70
80
90

Figure 3.1b

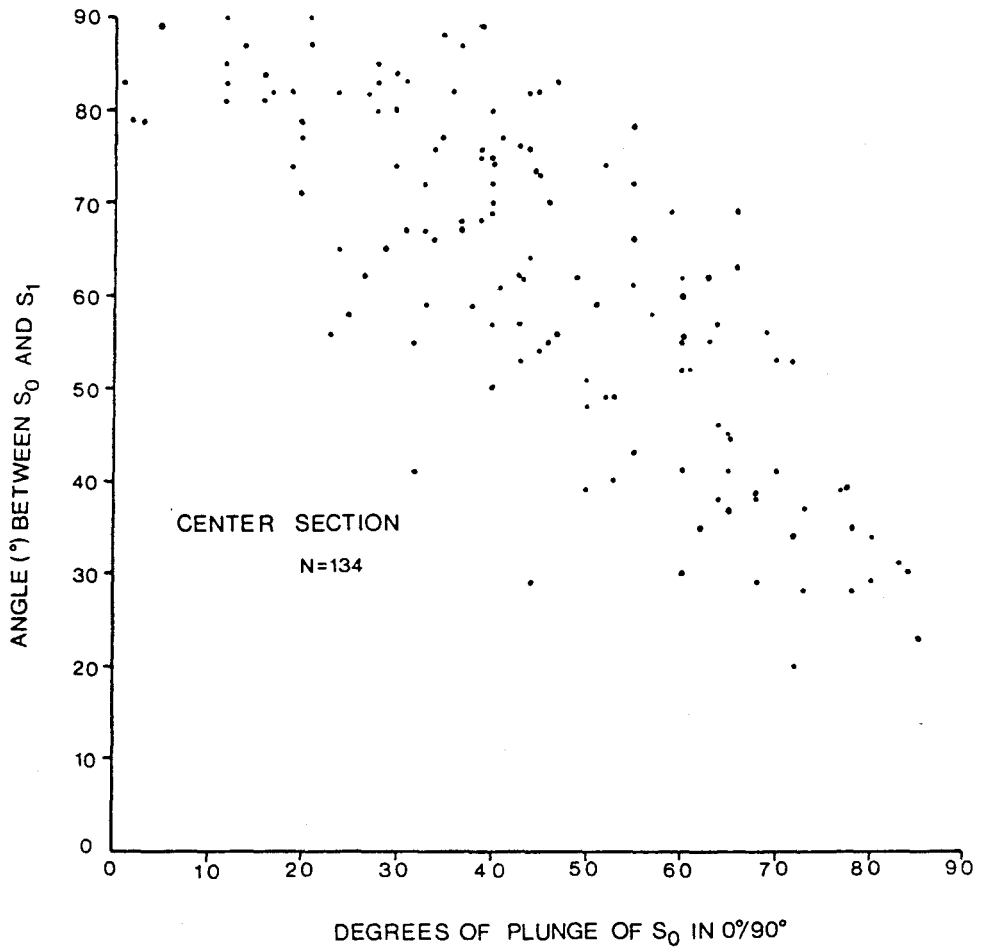
ANGLE (°) BETWEEN S_0 AND S_1
DEGREES OF PLUNGE OF S_0 IN 0°/90°
CENTER SECTION
N=134
0
10
20
30
40
50
60
70
80
90

Figure 3.1c

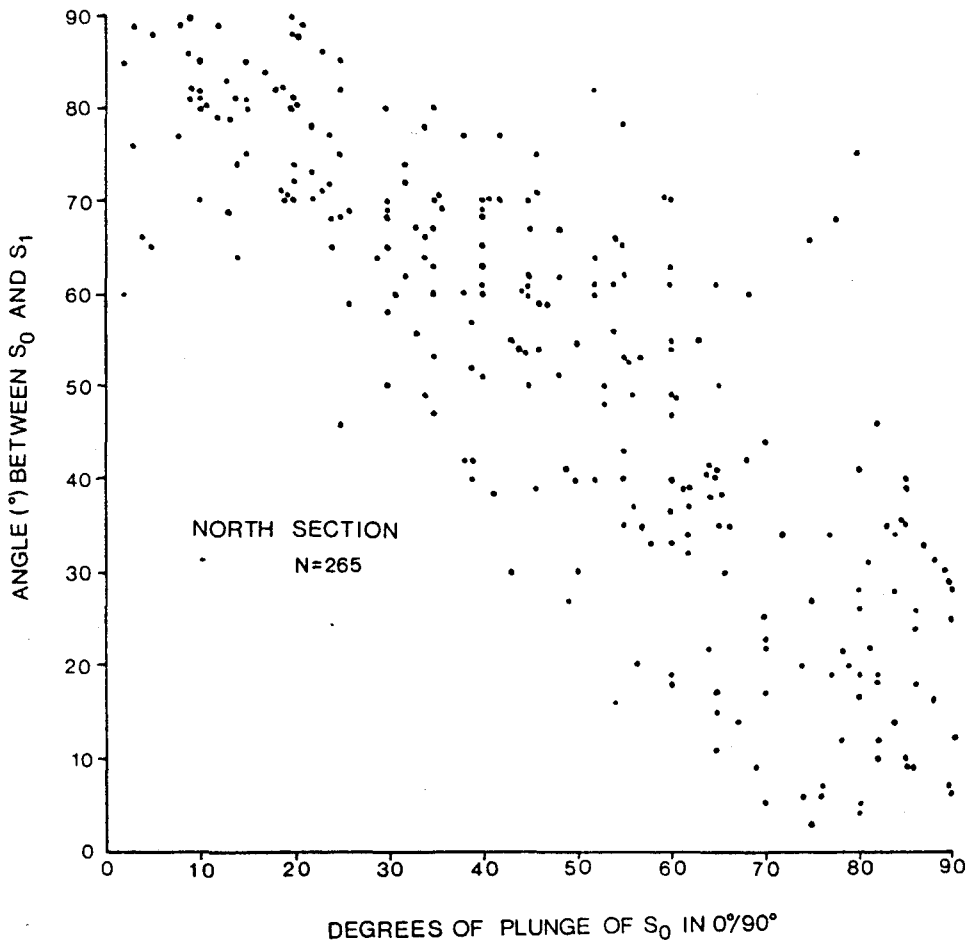
ANGLE (°) BETWEEN S_0 AND S_1
DEGREES OF PLUNGE OF S_0 IN 0°/90°
NORTH SECTION
N=265
0
10
20
30
40
50
60
70
80
90

Figure 3.1d

sheets originally were perpendicular to horizontal bedding. Wherever pipes are exposed, they and the cleavage are parallel, and are perpendicular to bedding only in fold hinge regions where bedding remains subhorizontal.

In order to quantify cleavage spacing, detailed measurements were made in the Ruth Falls syncline (figure 2.2a,b). In the field the intensity of the cleavage was measured as the number of cleavage planes per metre (C/m) visible along a line perpendicular to the lineation produced by the intersection of cleavage planes with bedding surfaces. A dip correction, which projected the field measurements onto a horizontal surface was later made. Measurements for rocks of approximately the same grain size ranged from approximately 80 C/M in the limb of a fold to approximately 120 C/M in the core of the fold (table 3.1). In a single bed increases of 15 - 51 cleavage planes can be detected.

Quantification of the anastomosing character of the cleavage in the same area was attempted by measuring the lengh-width dimensions of individual rhombs as outlined by cleavage planes, in the bedding plane as well as in the ac plane of the fold. However the outlines of the rhombs are commonly hard to discern, making the measurement very subjective. Also, even though the widths of the rhombs are linked to the C/m measurement, the lengths of the rhombs varys greatly within one outcrop. No useful quantitative results could therefore be obtained by this method.

Table 3.1

Cleavage density in Ruth Falls Syncline

Core	Limb
117 ± 4	85 ± 5
133 ± 7	82 ± 6
62 ± 4	47 ± 4
104 ± 3	67 ± 3

Cleavage Planes per metre (C/M) given as averages of three separate counts.

3.2 Cleavage: Thin Section Description

The samples that were studied in this project come from two principle locations. One set of samples were taken in the previously mentioned Ruth Falls syncline. The second set of samples used were pieces of drill core, taken from holes drilled in the Goldenville anticline. The drill core was supplied by Barry Jones of Goldenville Exploration LTD.

Both sample sets display the same general mineralogy and grain size. However, they differ in the degree to which the spaced cleavage is developed. On average, the spaced cleavage seams in the Goldenville samples are much wider and contain less quartz than those in the Ruth Falls samples.

3.2.1 Mineralogy

Detailed modal analyses (table 3.2) of the Goldenville samples, (Thompson, 1984) shows that the rocks contain approximately 60% - 70% quartz. The bulk of the remaining rock is formed by phyllosilicates, chlorite, muscovite and biotite being present. Approximately 5% - 10% of the rock is composed of detrital feldspar, rock fragments, carbonates, tourmaline and opaques. Microprobe analyses (J. Henderson, 1984 pers. com.) determined that the feldspar is pure albite and the carbonate is pure calcite. In the probed sections, ilmenite is the only opaque mineral observed; but arsenopyrite has been observed in other samples. The occasional grain of detrital pyroxene (< 0.01%) has been found. The rock fragments are predominantly of

Table 3.2

Modal Analyses from Point Count Data

Sample	Quartz	White Mica	Dark Mica	Opaques	Carbonate	Feldspar
G19-354 AC	68.3	23.0	2.7	1.0	3.6	1.3
G19-354 BC	68.0	20.4	6.2	0.8	3.5	1.0
G20-753 AC	67.0	23.5	4.9	1.6	1.4	1.4
G20-753 BC	73.2	17.7	4.5	1.3	2.1	1.1
G26-353 AC	68.1	24.9	2.9	1.1	1.7	1.2
G26-353 BC	68.7	23.6	3.3	1.3	2.5	0.6
G26-415 AC	68.6	26.0	1.4	2.0	1.7	0.3
G26-415 BC	58.8	34.0	2.2	1.9	2.2	0.9
Overall Averages	68%	24%	4%	1%	2%	1%

(after Thompson, 1984)

quartzitic origin.

3.2.2 Quartz

Based on appearance, the quartz grains can be divided into three separate populations. Two of these populations are predominant in the lithon, one in the cleavage. The largest population in the lithon is that of detrital quartz grains (figure 3.2a). These range in grain size from 1 - 500 micrometres. Grain shapes range from angular to subrounded and from equant to subequant. Undulatory extinction is present. Individual detrital quartz grains may consist of one or two sub grains.

The second population of quartz present in the lithons is of recrystallized quartz, of which there are two different subpopulations. One is confined to the pressure shadows of the larger detrital grains (figure 3.2b). The size of these quartz grains seldomly exceeds one micrometre. They may be in optical continuity with the detrital grain. The second subpopulation of recrystallized quartz is found in samples that have undergone a considerable amount of ductile strain. In these samples, areas are found in which no recognizable detrital grains remain (figure 3.2c). The quartz in these areas is extensively subgrained, the subgrains being polygonal, with straight line segment boundaries. Grain size is on the micrometre scale and extinction is usually straight, rather than undulatory.

Virtually all of the quartz found in the cleavage is

Figure 3.2

a) Top - Detrital Quartz in lithon

Long axis of Photo (LOP) = 1.3mm

b) Center - Quartz and muscovite in pressure shadows

LOP = 0.5mm

c) Bottom - Subgrained Quartz

LOP = 0.5mm

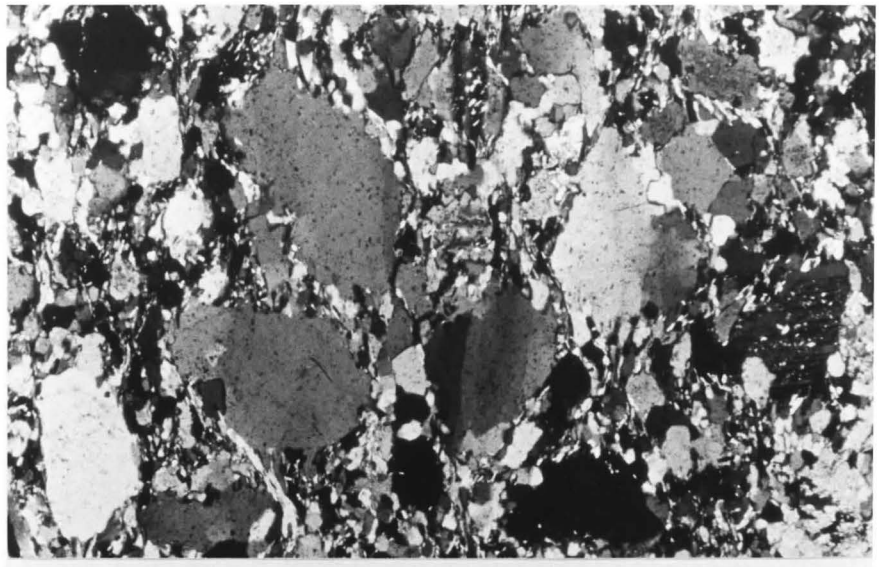

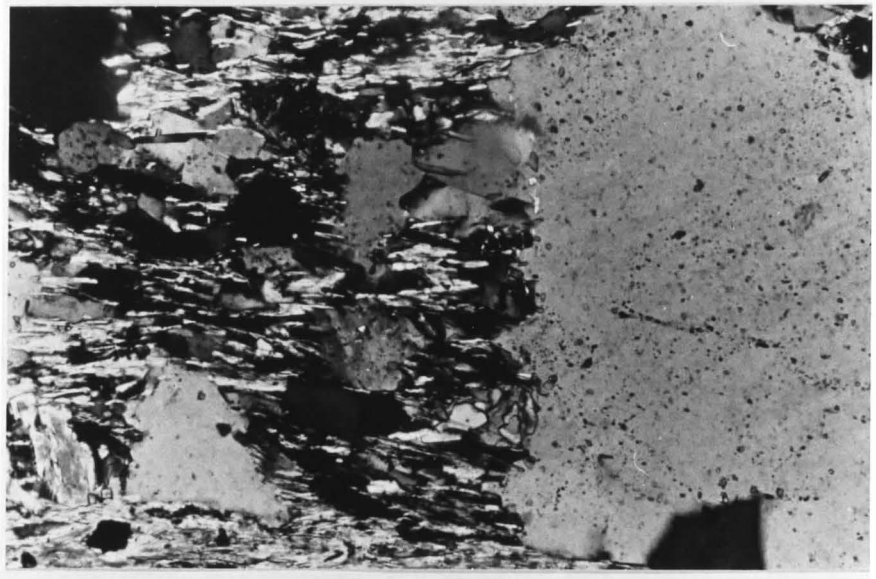

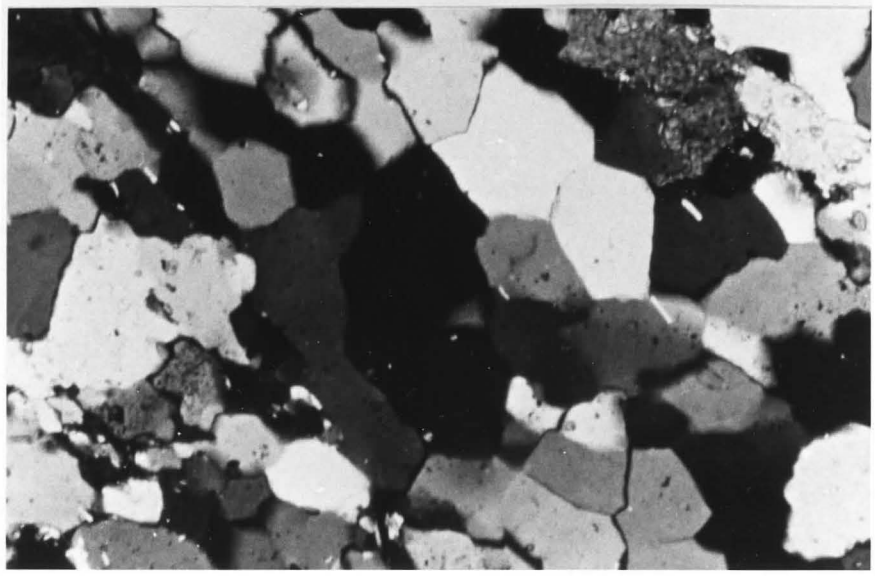

detrital quartz. However, whereas the axial ratios of the detrital quartz in the lithons are relatively low, rarely exceeding 3/1, the axial ratios in the cleavages can be as high as 16/1 (Pryer, 1984). The sides of the grains parallel to the cleavage are often very straight and have quite clearly been modified from their original detrital shape. The absolute length of the long axis of the quartz grains in the cleavage is on average less than that of the quartz grains in the lithons (table 3.3). There may be small pressure shadows parallel to the long axis of the grains.

3.2.3 Phyllosillicates

As mentioned above, chlorite, muscovite and biotite are present. Muscovite accounts for more than 50% of the mica population. Muscovite is present in the lithon as well as in the cleavage, the average grain size in the lithon being somewhat less than that in the cleavage, where it can occur with lengths in excess of 0.5mm (Thompson, 1984). In the lithons, muscovite is common in the pressure shadows of detrital quartz grains.

Chlorite is present throughout the samples, occurring in both lithons and cleavages as very small grains.

Biotite can be found in the lithon as well as in the cleavag. However, proportionally there is more biotite in the lithon than the cleavage (Thompson, 1984). Biotite grain size is usually fine, but a few larger grains (0.5mm) are

Table 3.3

Long axis of quartz grains in

Cleavage and Lithon

Sample Number	Cleavage (mm)	Lithon (mm)
G26-353-BC	0.112 ± 0.0525	0.330 ± 0.133
G20-753	0.134 ± 0.0663	0.216 ± 0.0965
G26-415-AC	0.111 ± 0.0781	0.257 ± 0.116
G26-415-BC 2C	0.148 ± 0.0878	0.232 ± 0.119
G20-753-BC	0.151 ± 0.101	0.208 ± 0.0847
G26-353-BC	0.121 ± 0.0691	0.221 ± 0.116
G19-354-AC	0.156 ± 0.0795	0.250 ± 0.106
G19-354-BC	0.206 ± 0.0929	0.276 ± 0.223
G20-747-AC	0.134 ± 0.0577	0.205 ± 0.727
G26-353-AC	0.155 ± 0.0766	0.187 ± 0.094

present. The relative proportions of micas in the lithon and the cleavage is shown in figure 3.3.

Phyllosilicates may occur in any orientation with respect to the cleavage; however, there is a strong preferred oientation parallel to the cleavage, in both the cleavage and the lithon (Thompson, 1984).

3.2.4 Tourmaline

Tourmaline occurs in spaced cleavage seams as subhedral to euhedral crystals. These can reach sizes up to 20-30 micrometres. The tourmaline appears to be randomly oriented within the cleavage. Probe data (J. Henderson, 1984) are shown in table 3.4.

3.2.5 Cleavage

The cleavage is characterized by zones of high mica content (figure 3.5). The mica content may rise from 10% - 20% in the lithon to more than 90% in the cleavage (figure 3.6a). This increase is due mostly to an increase in white micas. The percentage of dark micas stays constant or decreases. Increases in the mica content are associated with decreases in the quartz content. The shape of quartz grains (figure 3.6b) in the cleavage has been described above. Feldspars in the cleavage seam have a rectangular outline, indicating solution, but do not show axial ratios as large as those of quartz (figure 3.6c).

Cleavage zone widths range from 0.2mm - 3mm. The

Figure 3.3

- variation of white and dark micas in cleavages and lithons.
- dashed line represents white mica.
- solid line represents dark mica.
- cleavage zones are marked by solid bars

(After Thompson, 1984)

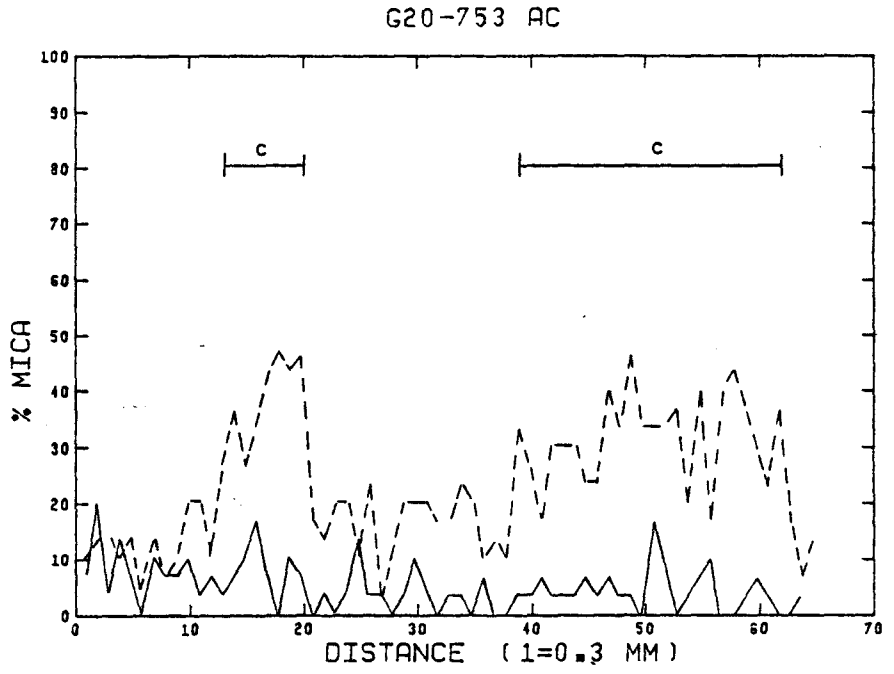
G20-753 AC
% MICA
DISTANCE (1=0.3 MM)
c
c

c=Cleavage

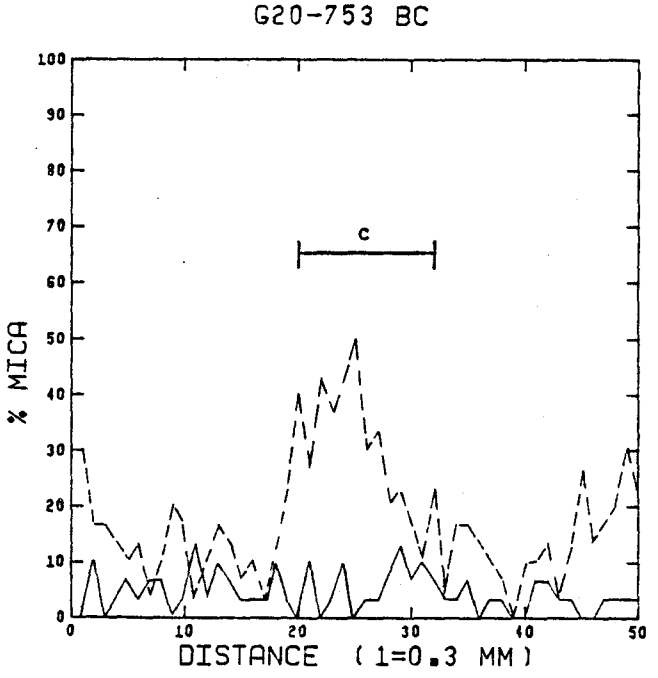
G20-753 BC
% MICA
DISTANCE (1=0.3 MM)
c

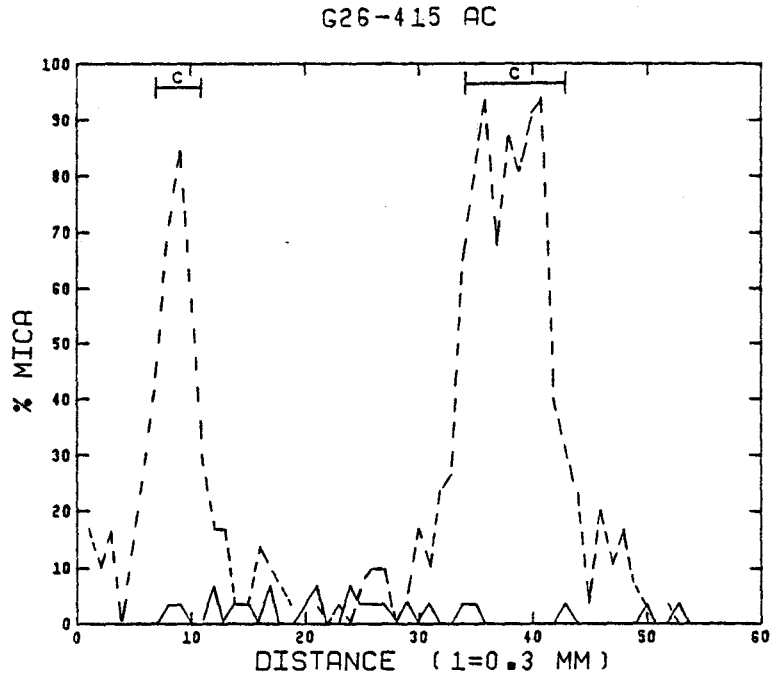
G26-415 AC
C
C
% MICA
100
90
80
70
60
50
40
30
20
10
0
0
10
20
30
40
50
60
DISTANCE (1=0.3 MM)

C=Cleavage

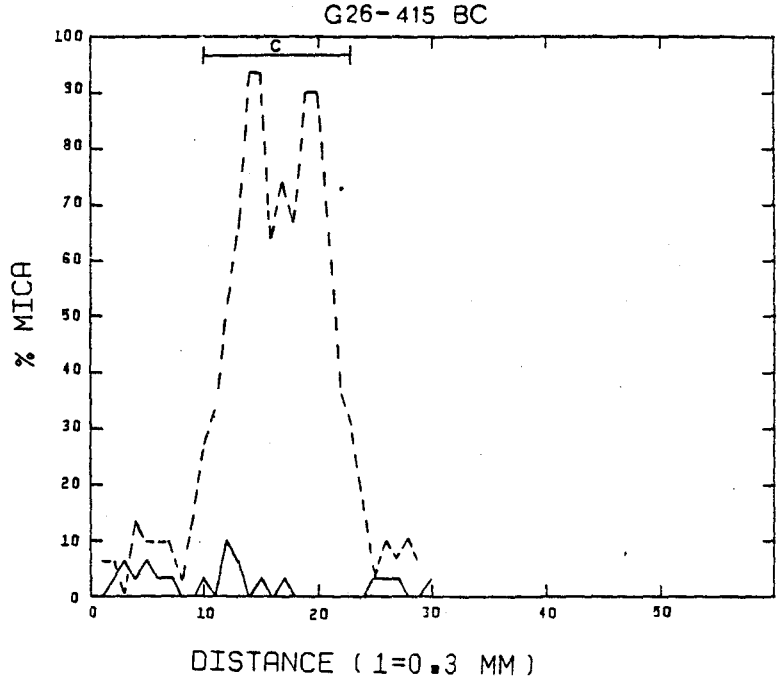
G26-415 BC
C
% MICA
100
90
80
70
60
50
40
30
20
10
0
0
10
20
30
40
50
DISTANCE (1=0.3 MM)

Table 3.4: Microprobe analysis of Tourmaline

Wt.%	1	2	3	4	Av.
	duplicate				
SiO_2	38.05	38.42	36.86	37.18	37.63
TiO_2	1.00	1.83	.68	.36	.97
Al_2O_3	32.45	31.29	32.88	32.72	32.35
Cr_2O_3	.07	.15	.09	.10	.10
FeO	9.02	10.51	8.46	9.49	9.37
MnO	.09	.05	0.00	0.00	.04
MgO	7.07	6.32	6.07	6.17	6.41
CaO	1.01	.18	.36	.08	.41
Na_2O	2.28	2.49	1.96	3.15	2.47
K_2O	.05	.08	.12	.11	.09
TOTALS	91.09	91.32	87.48	89.40	89.82

Figure 3.5

Thin section photograph of cleavage and lithons.

LOP = 4 cm

Figure 3.6

a) Top - Cleavage plane with high mica content (90%).
LOP = 0.5 mm

b) Center - Quartz grain in cleavage.
LOP = 0.5 mm

c) Bottom - Albite grain in cleavage.
LOP = 1.3 mm

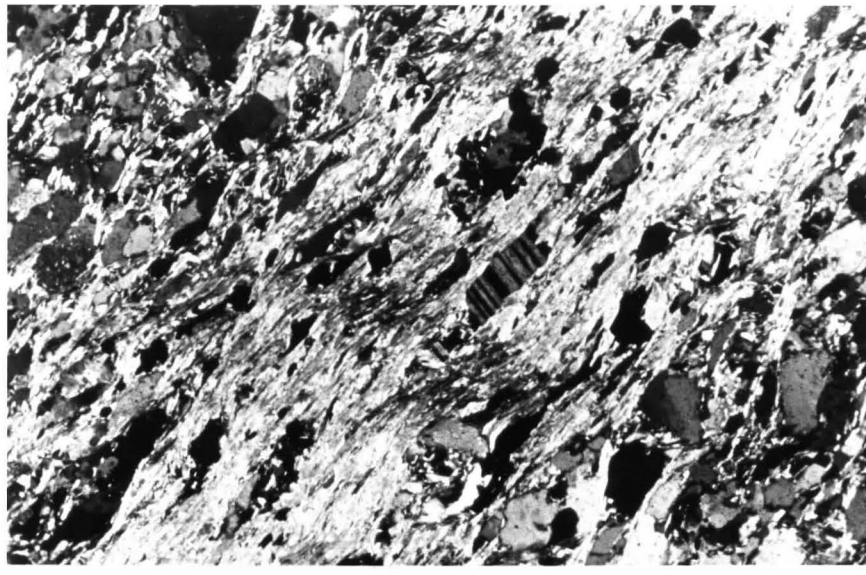

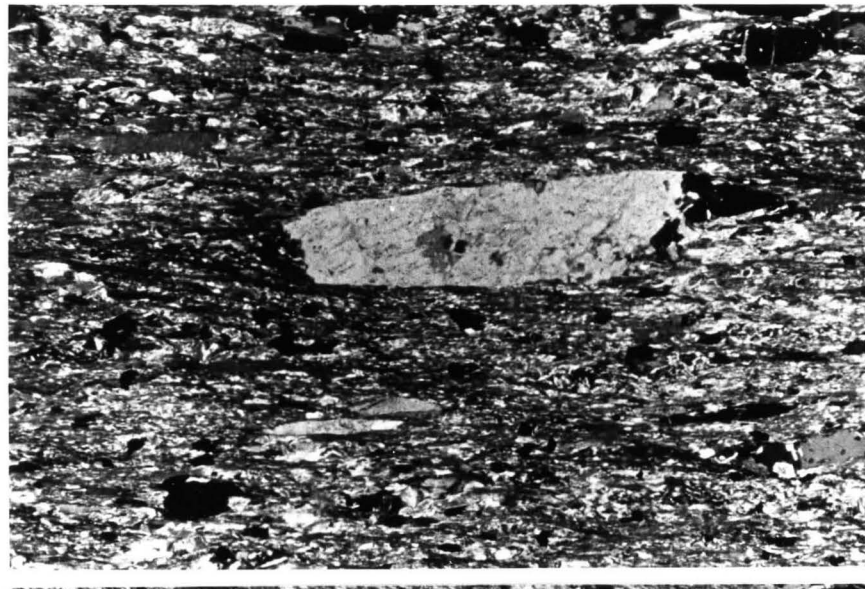

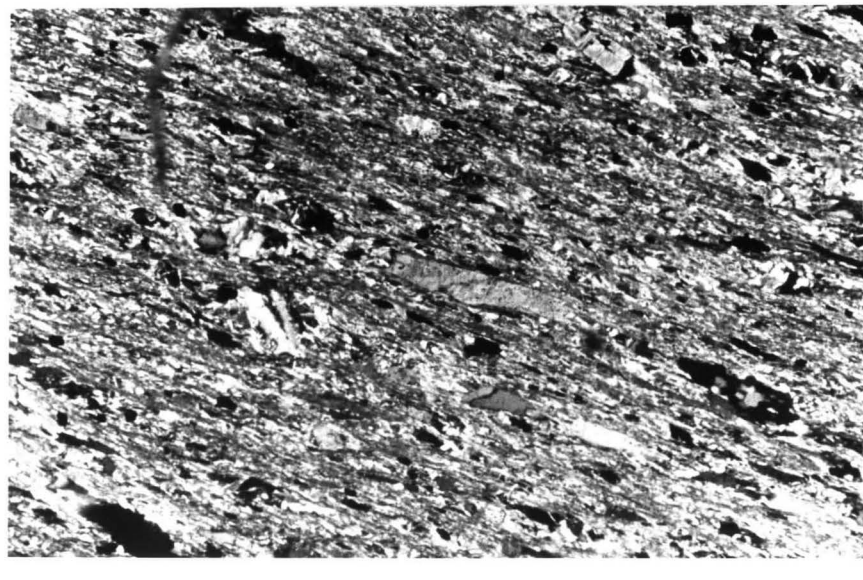

cleavage zones in the Ruth Falls syncline samples are not as well developed as those in the samples from the Goldenville anticline; their widths are at the lower end of the range given. Cleavage zone spacing, as measured in thin sections is approximately 5mm - 15mm. This compares well with the field measurements.

Cleavage zone boundaries may be sharp or gradational. If gradational, the cleavage zone grades into an intermediate area.

3.2.6 Intermediate Areas

Intermediate areas are defined by Pryer (1984) as areas posessing a well developed grain cleavage, without the high mica abundances of the cleavage (figure 3.7). Quartz grains make up more than 50% of the volume of these areas. The quartz grains in an intermediate area are tapered and show axial ratios which are greater than those of quartz grains in the lithons, but not as large as quartz grains in the cleavage (Pryer, 1984). Quartz and mica beards are present and some micas bend around quartz grains, probably in response to local variations in the strain field. Overall however, the orientation of the grain cleavage in intermediate areas is parallel to the orientation of the cleavage zone.

Intermediate areas can be found in three settings, of which two are directly related to the presence of a cleavage zone. Intermediate areas may occur adjacent to

Figure 3.7:

"Intermediate" zones

Top - LOP = 0.5 mm

Center - LOP = 1.3 mm

Bottom - LOP = 0.5 mm

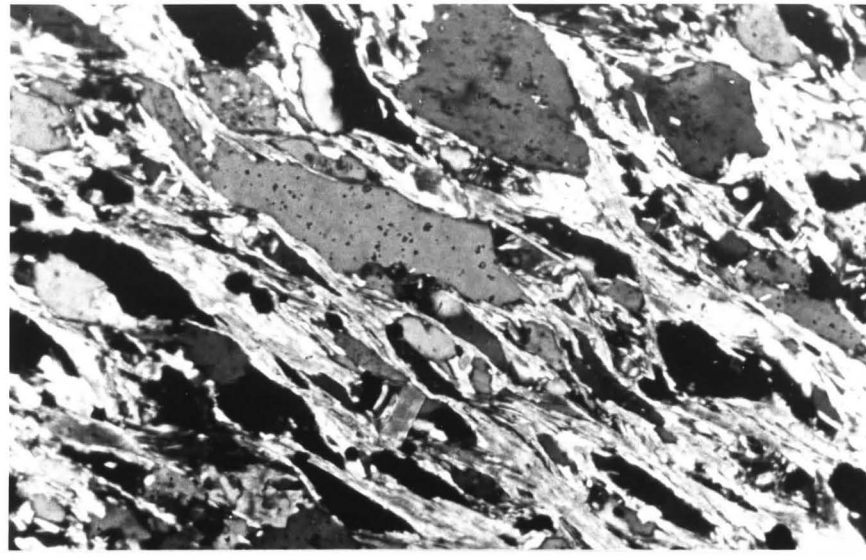

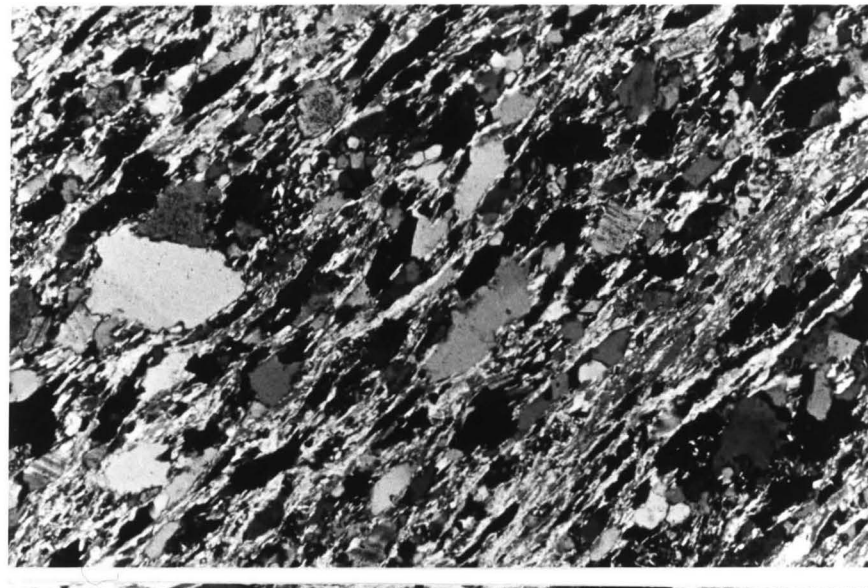

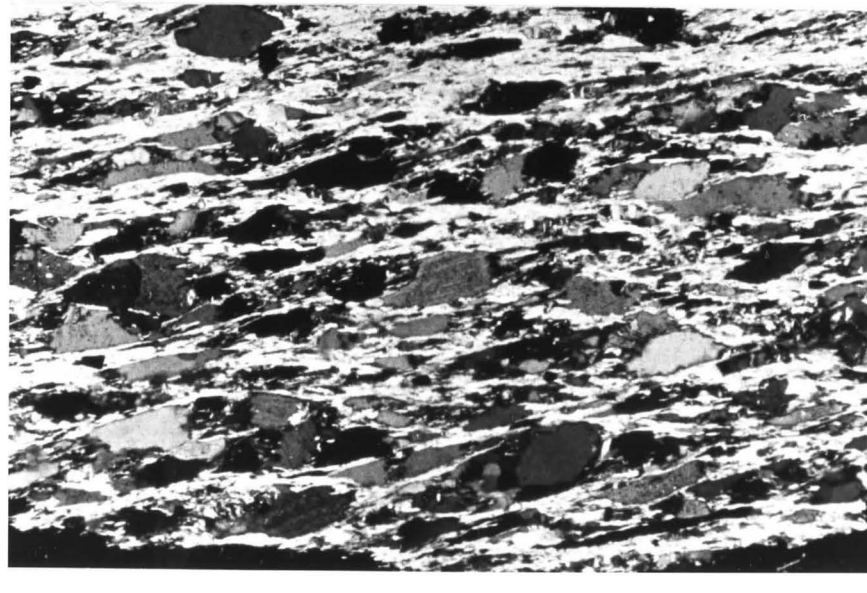

cleavage zones, thus forming a gradational boundary between the cleavage zone and the lithon. They may also occur as islands within a cleavage zone. This setting is thought to have resulted from the convergence of two cleavage zones. Finally, intermediate areas may occur on their own, in a mid- lithon setting; these may be incipient cleavage zones.

3.2.7 Lithons

Lithons always contain more than 50% quartz grains. Detrital quartz grains in the lithons of a sample consistently show the lowest axial ratios found in the sample. These quartz grains show a weak preferred orientation of long axes, parallel to the cleavage (Pryer, 1984). Quartz grains may have quartz and mica beards, grains in which are oriented roughly parallel to the cleavage (figure 3.8a). Micas in the lithons are generally smaller than those in the cleavage (figure 3.8b). In soe places, a grain of muscovite, in excess of 1mm long can be found bent in between and around several quartz grains. Such grains are interpreted as being undoubted detrital muscovite grains (figure 3.8c).

Lithons may also show evidence of ductile deformation. Areas of various sizes may be made up entirely of subgrained quartz. As a very general statement, there is more plastic deformation present in the cores of the folds studied than in the limbs. But it is virtually impossible to quantify this. Minor faults are present in the Ruth Falls

Figure 3.8

a) Top - Quartz and mica beards in lithons.

LOP = 1.3 mm

b) Center - Micas in the lithon.

LOP = 1.3 mm

c) Bottom - Detrital muscovite grains.

LOP = 1.3 mm

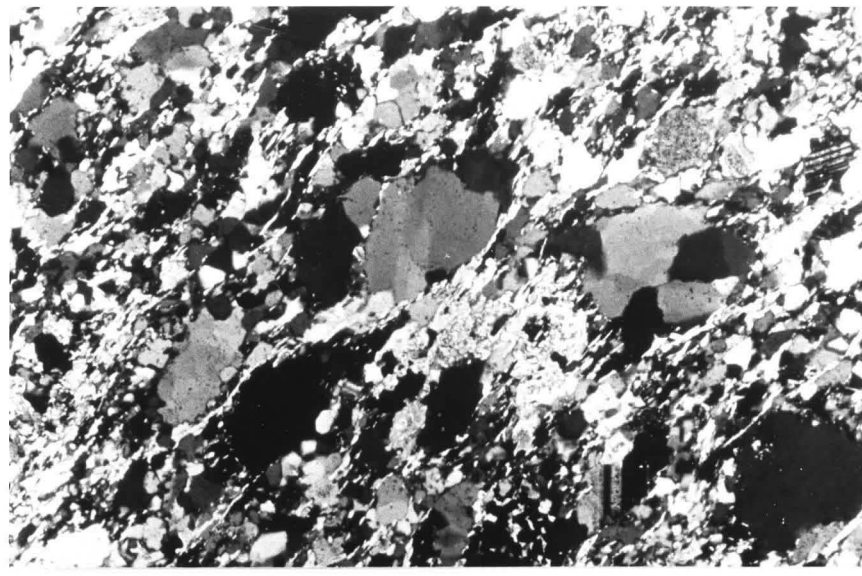

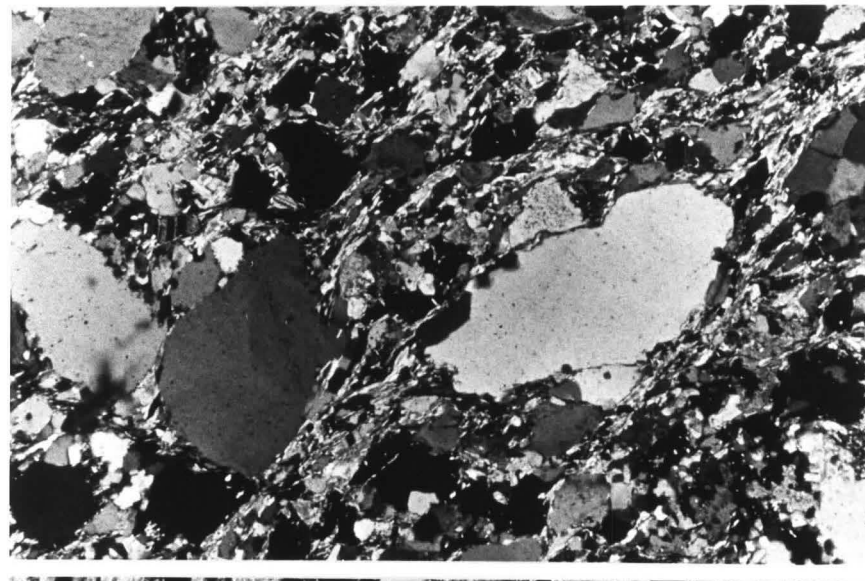

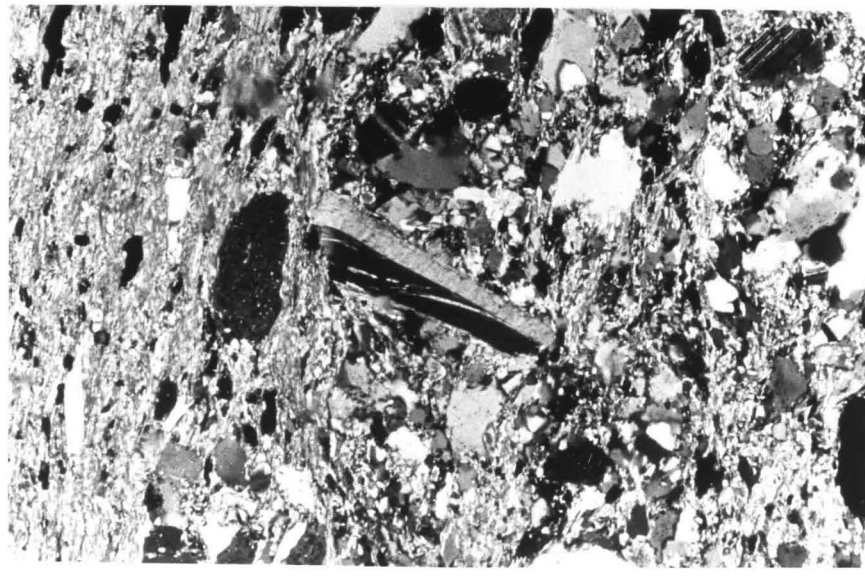

syncline as well as in the Goldenville anticline, and samples taken near these show evidence of plastic deformation as well. Since the location of all minor faults can not be determined, and there is no way to distinguish between plastic deformation caused by faulting or folding, no further inferences are possible.

4. Timing and Nature of the Cleavage

The relative timing of the formation of the cleavage is of great importance if we are to understand the environment of its formation. Fortunately there are pieces of evidence which can be used to give an indication of the timing of the cleavage. Fig 3.1 contains several of these pieces of information.

First, it shows that the cleavage is not fold axial planar. The dip of the cleavage varies consistently with the dip of bedding. The variation itself is consistent throughout the entire map area. The interpretation of these data is that the development of the cleavage was alike throughout the whole map area. The fact that the cleavage is not fold axial planar and fans around the folds suggests that the cleavage developed some time prior to, or early during, the folding and came to its present attitude by rotation during folding.

Another important observation is that the cleavage is parallel to the pipes of sand volcanoes, wherever they are found (figure 4.1). These pipes are water escape structures, which formed during or just after the deposition of the turbidites. Their original orientation will have been within a few degrees of vertical. The cleavage now parallels them in all positions within the folds, suggesting that they

Figure 4.1

Pipes of sand volcanoes (coarse grained) parallel to cleavage (thin dark stripes)

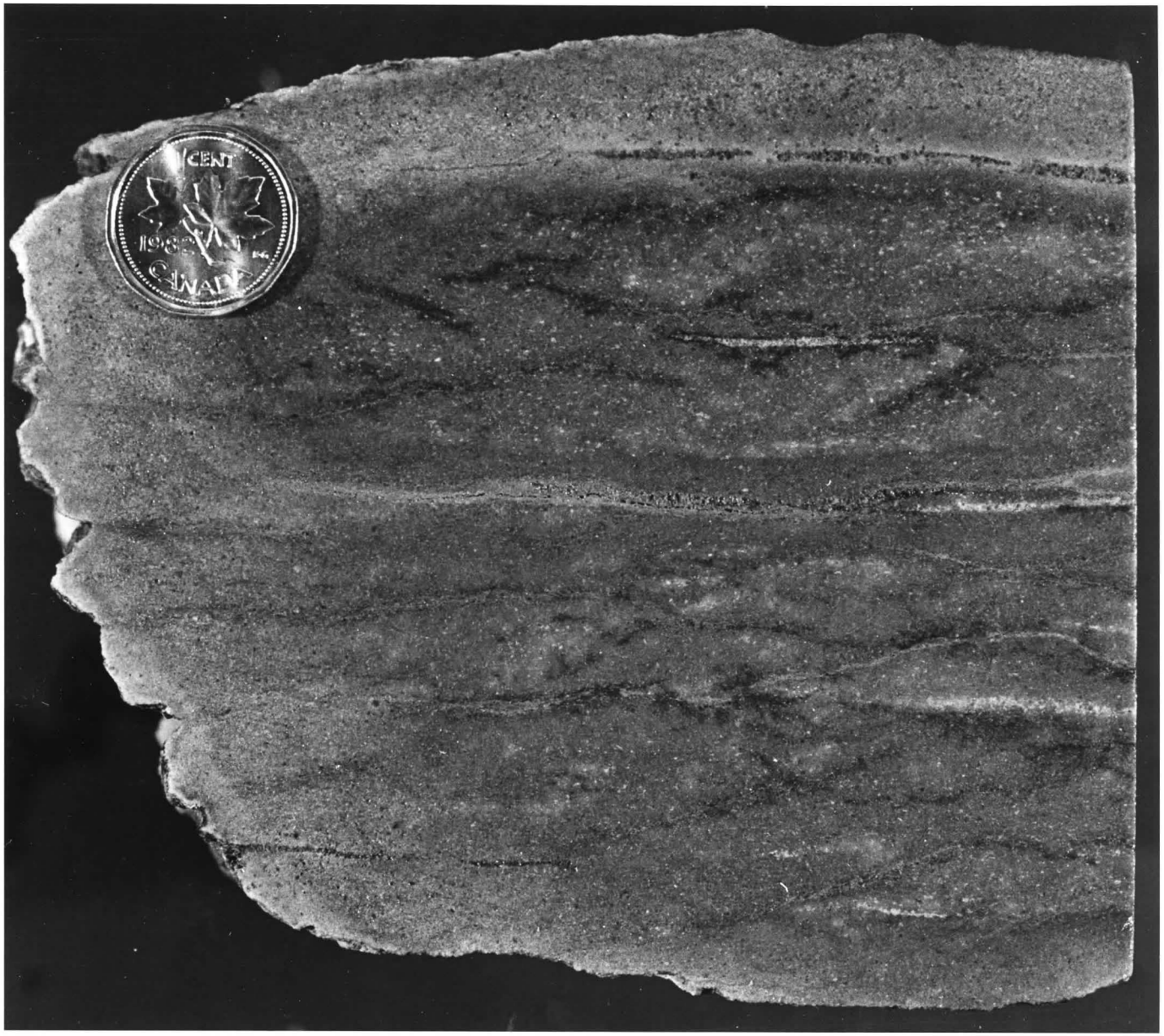
CENT
CANADA

have undergone similar rotation during folding. It also implies that cleavage and water escape structures were parallel originally and that the cleavage initially formed perpendicular to bedding.

Before more inferences about the timing of the cleavage can be made, the nature of the cleavage should be discussed. It has already been mentioned that the axial ratios of quartz grains in the cleavage are higher than those in the intermediate areas, which in turn are higher again than those in the lithons. The long axes of the quartz grains are lined up and the absolute length of the long axis is consistently less in the cleavage than in the lithons (table 3.3). The higher axial ratios within the cleavages are therefore obtained by reducing the width and the lengths of the grains in the cleavages. No sedimentary process could account for this. The explanation therefore must be a tectonic one, which includes a volume loss in quartz. The simplest explanation for the reduction of the grainsize is that parts of the grains have been dissolved. The strongly developed rectangular outlines of some grains in the cleavage support this. Further evidence for solution is given by grain contacts, which have been classified as pressure solution contacts according to Trurnit (1968) (figure 4.2). Pressure solution, which leads to the preferential solution of grains along their more highly stressed contacts would be consistent with the alignment of

Figure 4.2 Pressure solution contacts of grains

Top - quartz grains dissolved into each other.

LOP = 0.5 mm

Center - quartz grains dissolved into each other.

LOP = 0.5 mm

Bottom - Flattened contacts between quartz grains.

LOP = 0.5 mm

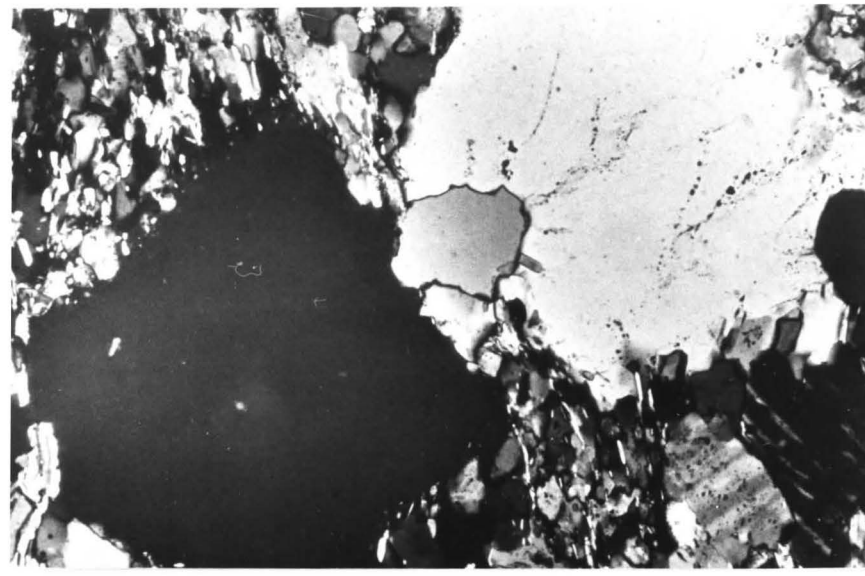

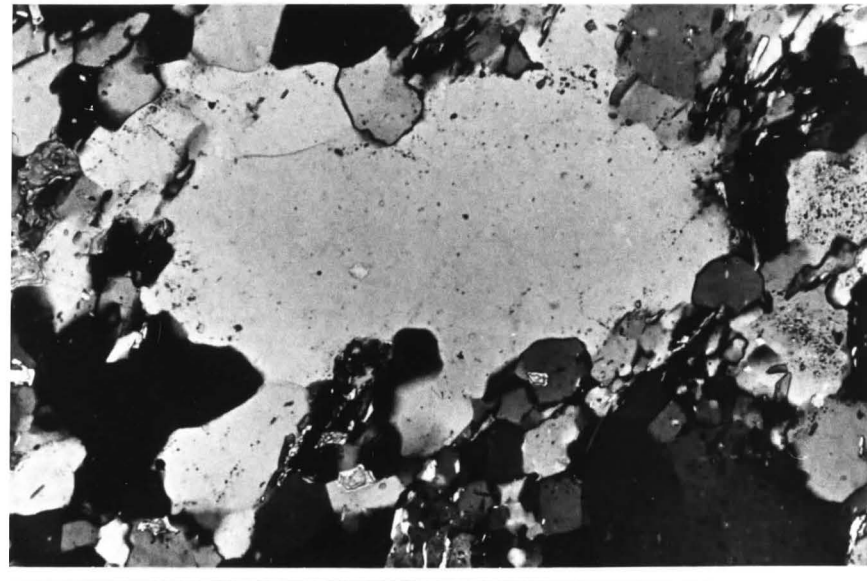

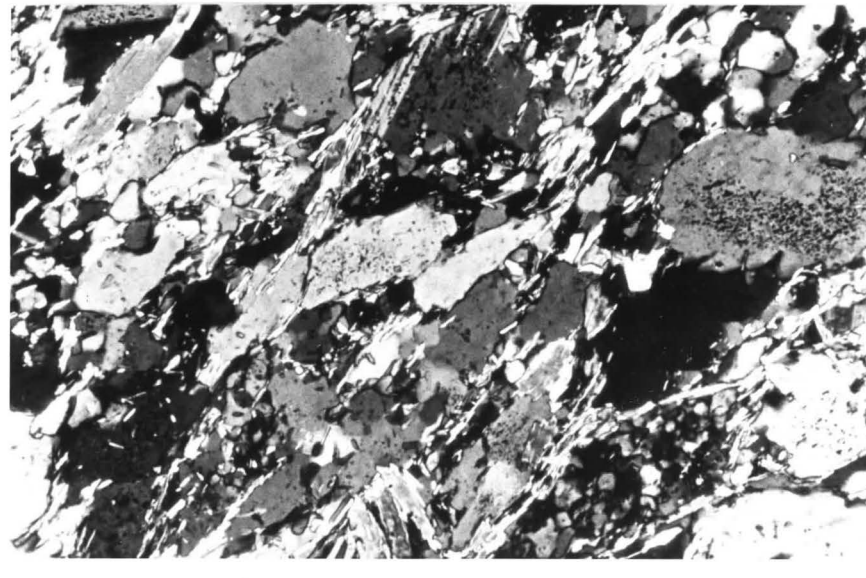

quartz grains, providing no significant amount of subsequent rotation ofindividual grains has occurred. A preferential solution and removal of quartz has to lead to an increase in the percentage of other components since modal analyses are reported as closed arrays. Micas have traditionally been regarded as being relatively insoluble in a pressure solution enviroment, and they are indeed dominant in the cleavage planes. It therefore appears that the cleavage is dominantly of pressure solution origin. The stress field in which a pressure solution cleavage forms would be one in which the major principal stress axis is perpendicular to the cleavage plane.

If the cleavage is formed by only solution of quartz and a simple concentration of detrital micas, the size of the micas and the relative ratio of white to dark micas should be the same in the lithon and the cleavage. This is not the case. The presence of tourmaline in the cleavage planes but not in the lithon also does not conform to a simple model of concentration of everything but quartz. Cleavage formation is therefore clearly more complicated than a simple quartz dissolution- mica concentration process and will be dealt with in more detail later. For now, however it will be sufficient to use this as a simple working model.

The quartz grain shapes lend themselves to strain measurements and estimates of the volume loss that is

associated with the solution of quartz. Measurements by Pryer (1984), based on the assumption that quartz grains were either originally spherical or randomly oriented, are shown in table 4.1 and indicate volume losses for cleavages, lithons and intermediate areas. Not surprisingly, the volume loss in the cleavages is the highest, that in the lithons the lowest. It may be surprising that even the lithons show up to 27% volume loss, since they appear to be relatively undeformed in many cases. These measurements however have to be treated cautiously. The quartz grains need not have been spherical at the time of deposition. Mean grain shape ratios in greywackes may originally range between 0.64/1 and 0.68/1 (Griffith, 1967). An alignment of these grains would therefore already indicate a 32% to 36% volume loss. Parkash (1969) showed that a preferred grain orientation parallel to bedding is common in greywackes. He also showed that imbrications of grains which are common are virtually always at less than 20 degrees to bedding. He found no alignment perpendicular to bedding. Sedimentary processes are therefore not likely to have caused any significant alignment of grains perpendicular to bedding. A horizontal major principal stress system, which would be necessary to form an initially vertical cleavage, may also have caused reorientation of elongate grains. Even though this probably would have been associated with a loss in pore space, it would not represent a true solid volume loss.

Table 4.1 Volume Loss of Goldenville Samples

(after Pryer, 1984)

Sample	% volume loss
G26-415	
Cleavage	-68
Intermediate	-31
Lithon	+5
G26-353	
Cleavage	-71
Intermediate	-40
Lithon	-26
G19-354	
Cleavage	-68
Intermediate	-54
Lithon	-27
G20-753	
Cleavage	-58
Intermediate	-36
Lithon	-18

It can be said that the cleavage formed at least partially due to pressure solution processes and that it is very likely to have formed parallel to water escape structures, at a time when they were still perpendicular or nearly so to bedding. The major principal stress would have been horizontal, which is compatible with the stress system responsible for the folding. Since the cleavage formed perpendicular to the major principal stress, it would be emplaced in the rock before any significant rotation of beds occurred. Otherwise cleavage and water escape structures would not be parallel everywhere. As beds rotated, water escape structures and cleavage rotated to the same degree.

It has already been mentioned that the cleavage is more strongly developed in the core of the fold. A number of explanations are possible.

In the core of the folds the beds did not rotate, but remained horizontal. Providing the stress system did not rotate either, the cleavage would have remained in a favourable position for development in the cores of the folds. In the limbs the cleavage will have been rotated away from its original perpendicular orientation with respect to the major principal stress. This rotation may have put the cleavage into an unfavourable position for any further consistent development. In the core, cleavage development will have continued. A combination of these and other, unknown factors probably all contributed to the development of the

cleavage to its present degree.

The rotation of water escape structures and cleavage during folding can give important clues to the style of folding that took place. The folding could not have been an episode of tangential longitudinal strain, since cleavage and water escape structures would have had to retain their original orientation perpendicular to bedding during folding. Ramsay (1967) analysed an alternative, flexural slip, for folds and developed a theoretical model for the variation of angular shear strain in such folds. This theoretical model curve is superimposed on the Ruth Falls Syncline data set in figure 4.3. It can be seen that there is virtually no correlation between the theoretical model and the field data. Boulter (1982) suggests that homogeneous flattening may occur after the limbs lock up. Such a flattening would lead to a further reduction of the bedding-cleavage angle. It is possible to model the effects of an episode of homogeneous flattening by superimposing different strain values for such flattening onto Ramsay's theoretical curve. This has been done in figure 4.4. The additional strain does not significantly change the curve for low bedding dip values. It does however make a difference for high bedding dip values. The higher the amount of strain added, the smaller the bedding-cleavage angle becomes in areas of high bedding dip. The result is that the theoretical curve is straightened out and becomes more

Figure 4.3

Theoretical curve for flexural slip superimposed on Ruth Falls syncline data set.

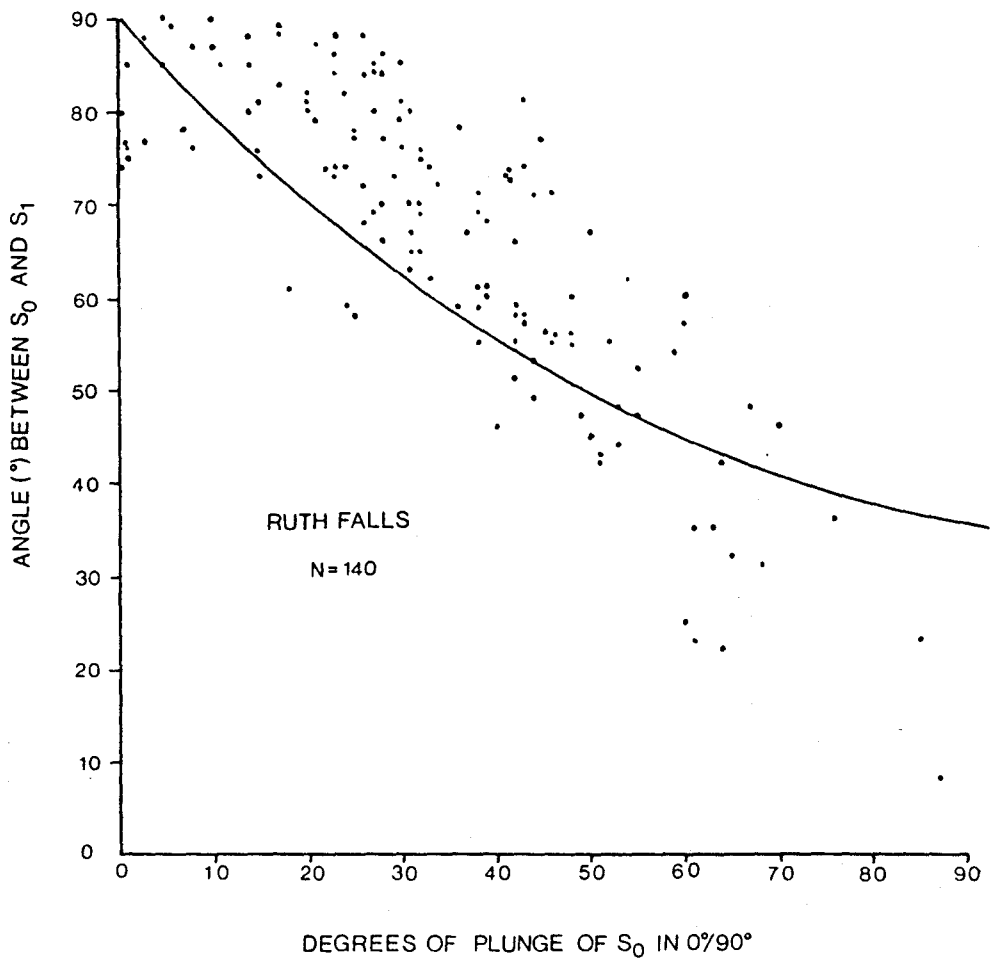
ANGLE (°) BETWEEN S_0 AND S_1
90
80
70
60
50
40
30
20
10
0
RUTH FALLS
N = 140
0
10
20
30
40
50
60
70
80
90
DEGREES OF PLUNGE OF S_0 IN 0°/90°

Figure 4.4

Homogeneous flattening superimposed on theoretical flexural slip curve.

a $-\sqrt{\frac{\lambda_1}{\lambda_2}}$ = 1 (Ramsay's curve)

b $-\sqrt{\frac{\lambda_1}{\lambda_2}}$ = 1.2

c $-\sqrt{\frac{\lambda_1}{\lambda_2}}$ = 1.6

d $-\sqrt{\frac{\lambda_1}{\lambda_2}}$ =2.1

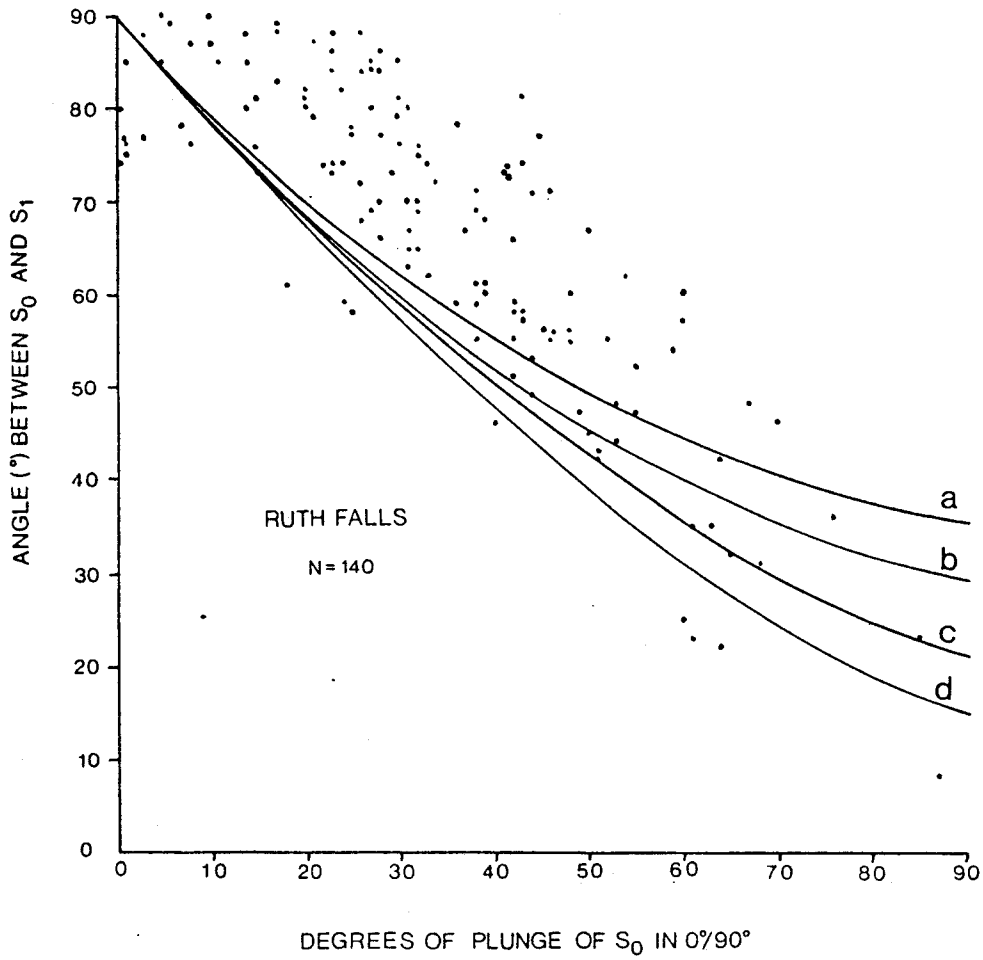
ANGLE (°) BETWEEN S_0 AND S_1
DEGREES OF PLUNGE OF S_0 IN 0°/90°
RUTH FALLS
N = 140
a
b
c
d
0
10
20
30
40
50
60
70
80
90

nearly parallel to the data points, rather than cutting across them. Adding a period of homogenous flattening to the fold history seems therefore reasonable. Most data points lie above the straightened out theoretical curve. This implies that the angular shear observed is less than the values expected. This is not surprising, since the precise influence of the interbedded slates is not known. The slates, which are the incompetent layers in the Meguma package, very likely took up a significant amount of the strain.

On the basis of the available data, it is therefore only possible to state that folds are not due to tangential longitudinal strain or to flexural flow acting alone. Since the effects of a period of homogeneous flattening on the theoretical curve for flexural slip make it fit better to the actual data points, it seems reasonable to propose that such a period of homogeneous flattening did indeed occur in the Meguma Group. Unfortunately no quantification of the flattening strain is possiple with the available data.

5.1 Ruth Falls Chemistry

The development of the cleavage has produced strong mineralogical and therefore chemical inhomogeneities in the rock. It is worthwhile to study the chemical differences associated with such a remarkable mineralogical differentiation. This has been done on the cleavage-lithon scale, as well as on the scale of several hundred metres across a fold.

As stated in the field description, the density of the cleavage varies throughout the fold, cleavage density being higher in core than in limb. Several sample sets have been taken from the Ruth Falls syncline (figure 2.2a,b), representing both core and limb areas. Each sample set was chosen from the same greywacke bed and, as nearly as possible, from the same stratigraphic level in the bed. One sample was taken from the core of the fold and one or two from the limb. Seven beds were sampled in this manner and one sample set was taken across a single bed in one location, in order to check the composition in different levels of one bed. The samples were slabbed perpendicular to the plane of the cleavage and the entire slab, containing several cleavage planes was crushed for analysis. Whole rock analyses were done by X-ray fluorescence while Au, As, Sb and W concentrations were determined by radiochemical

neutron activation analysis (see section 5.3).

Table (5.1.1) gives the normalized whole- rock compositions, including loss on ignition (LOI) for the Ruth Falls samples. Samples A50A - A50D represent the compositions of different levels of the same bed. Sample A50D was taken from a Bouma B or C unit, which was slightly more pelitic than the remainder of the bed. The relatively high CaO content and the large loss on ignition suggest that the bed contained calcite. Samples A50A, A50B, A50C, A50E and A50F contain less than 2% CaO and have less than 2% LOI. They are very similar in other components as well. The maximum difference in their SiO_2 contents is slightly more than 3%, outside the analytical limits of accuracy, which were determined to be about 1% to 2% for SiO_2. Comparison of the other components of all samples, excluding A50D, shows that these too are quite close.

If one now compares the concentrations of elements in the six core- limb sample sets it can be seen that four show a loss in the core of SiO_2, Fe_2O_3 and K_2O, whereas two show a gain reltve to limb. Other components vary nonsystematically. Even though the variations in SiO_2, Fe_2O_3 and K_2O are outside the limits of analytical accuracy, they are still within the limits set by the variations found in samples A50A - A50F, excluding sample A50D.

A comparison of all samples, excluding A50D, shows that the overall composition of the greywacke beds tested is

Table 5.1.1: Ruth Falls Syncline

Normalized Composition Including Loss on Ignition, Whole Rock

Sample	A8	A1	B92	F18	F15	F5A	F14	A45	A55	A54
SiO_2	78.27	78.95	83.06	81.08	79.29	77.30	75.91	77.77	81.32	82.32
AL_2O_3	10.38	10.10	8.63	9.16	9.96	11.28	11.58	10.35	9.41	8.93
Fe_2O_3	2.76	2.70	1.95	2.37	2.82	3.69	4.00	2.67	2.52	2.34
MgO	1.93	1.33	1.03	1.42	0.87	1.30	1.33	1.23	0.95	1.03
CaO	0.68	0.87	0.64	0.94	0.95	0.84	1.02	1.76	1.07	0.73
Na_2O	2.13	2.18	1.91	2.18	2.81	1.88	2.08	2.80	1.93	1.98
K_2O	2.35	2.27	1.48	1.40	1.44	1.62	1.87	1.32	1.13	1.08
TiO_2	0.35	0.50	0.38	0.44	0.46	0.51	0.55	0.41	0.44	0.50
MnO	0.04	0.05	0.05	0.06	0.05	0.06	0.08	0.07	0.07	0.04
P_2O_5	0.05	0.04	0.04	0.06	0.10	0.09	0.09	0.06	0.07	0.07
Loss on ignition	1.06	1.00	0.83	0.89	1.23	1.43	1.48	1.54	1.11	0.94
Total	100.00	100.00	100.00	100.00	100.00	100.00	100.00	100.00	100.00	100.00
Core/ Limb	Core	Limb	Core	Limb	Core	Limb	Core	Limb	Core	Limb

Table 5.1.1: Ruth Falls Syncline

Normalized Composition Including Loss on Ignition, Whole Rock

Sample	A50	A49	A47	A50A	A50C	A50E	A50D	A50F	A50B
SiO_2	79.71	79.52	80.76	80.22	79.46	79.64	64.47	77.74	81.03
Al_2O_3	9.80	9.37	9.06	8.72	9.90	9.52	7.67	10.94	9.31
Fe_2O_3	2.74	2.64	2.42	2.36	2.76	2.68	1.95	3.27	2.42
MgO	1.35	1.55	1.35	2.21	1.35	0.77	1.26	0.96	1.06
CaO	1.14	1.03	0.75	1.12	1.11	1.81	13.00	1.07	1.09
Na_2O	1.97	2.83	2.66	2.76	2.02	2.22	1.63	2.23	1.94
K_2O	1.34	1.22	1.14	0.93	1.35	1.31	1.04	1.67	1.24
TiO_2	0.53	0.49	0.48	0.46	0.53	0.54	0.40	0.60	0.51
MnO	0.07	0.09	0.03	0.06	0.07	0.08	0.26	0.06	0.05
P_2O_5	0.08	0.07	0.07	0.07	0.08	0.09	0.33	0.08	0.08
Loss on ignition	1.26	1.18	1.28	1.07	1.36	1.35	8.00	1.39	1.26
Total	100.00	100.00	100.00	100.00	100.00	100.00	100.00	100.00	100.00
Core/ Limb	Core	Limb	Limb	X	X	X	X	X	X

X - Samples used to check composition of different flow units in one bed.

Table 5.1.1

Normalized Composition

Including Loss on Ignition, Whole Rock

Sample	F12	A53	A52
SiO_2	80.02	80.32	81.61
Al_2O_3	9.86	9.68	9.19
Fe_2O_3	2.81	2.86	2.37
MgO	1.14	1.06	1.09
CaO	0.82	0.78	1.18
Na_2O	2.23	2.15	1.67
K_2O	1.30	1.34	1.01
TiO_2	0.55	0.51	0.46
MnO	0.06	0.06	0.01
P_2O_5	0.07	0.08	0.06
Loss on ignition	1.14	1.18	1.35
Total	100.00	100.00	100.00
Core/ Limb	0	0	0

0 - Bed cannot be properly correlated.

quite similar, regardless of position in the fold. The maximum difference in SiO_2 content is less than 10% and differences in the other components are correspondingly small. The conclusions that can be drawn from this are as follows: 1) Variations in chemical composition between the core and the limb of the same bed are of the same order as variations across that bed, that is, from stratigraphic bottom to top of the bed. The processes operating to produce the cleavage do not produce gross chemical changes of the rock that can easily be determined on this scale. It should be kept in mind that this study compares a less cleaved area, the limb, with a more cleaved area, the core. 2) The overall composition of all Bouma A units sampled in this area is quite similar.

In order to study the chemical differences between the cleavage planes and the lithons, individual cleavage planes and lithons were cut out of sample slabs. Lithons were easily obtained in this manner; there were, however, problems with the sampling of cleavage planes. Cleavage planes are often less than one mm wide, the approximate minimum thickness that can be cut out with the diamond saw blade used. There is therefore a problem of contamination of cleavage material by incorporation of adjacent lithon material.

Table (5.1.2) shows the whole rock chemistry of the six cleavage-lithon pairs analysed. The picture this gives

Table 5.1.2

Ruth Falls Syncline

Normalized Composition Including Loss on Ignition of Lithon-Cleavage

Sample	A1C	A1L	A50C	A50L	F14C	F14L	A49C	A49L
SiO_2	75.10	79.89	67.83	78.74	70.31	74.35	72.54	78.48
Al_2O_3	11.85	9.58	16.08	9.88	13.46	12.22	13.66	9.89
Fe_2O_3	4.13	2.96	4.58	3.19	5.61	4.46	4.03	3.00
MgO	1.23	1.26	1.42	0.97	2.22	1.41	1.37	1.39
CaO	1.08	0.84	1.33	1.47	0.98	1.04	1.15	1.72
Na_2O	1.70	2.04	1.89	2.19	2.09	2.19	2.12	1.87
K_2O	2.74	1.86	3.59	1.35	2.51	2.07	2.50	1.26
TiO_2	0.63	0.49	0.83	0.49	0.63	0.56	0.71	0.50
MnO	0.07	0.07	0.08	0.07	0.12	0.10	0.07	0.08
P_2O_5	0.09	0.06	0.13	0.08	0.08	0.09	0.12	0.08
Loss on ignition	1.38	0.95	2.24	1.57	2.00	1.51	1.72	1.74
Total	100.00	100.00	100.00	100.00	100.00	100.00	100.00	100.00

Table 5.1.2

Ruth Falls Syncline

Normalized Composition Including Loss on Ignition of Lithon-Cleavage

Sample	F5AL	F5AL	F5AC	F5AL	F5AC
SiO_2	74.73	74.29	70.80	74.71	70.22
Al_2O_3	12.21	12.28	14.01	11.87	13.87
Fe_2O_3	4.46	4.55	4.97	4.48	5.32
MgO	1.37	1.38	2.03	1.83	2.08
CaO	1.05	1.06	1.02	0.99	1.13
Na_2O	1.94	2.19	2.16	1.95	2.08
K_2O	1.94	1.95	2.44	1.90	2.76
TiO_2	0.59	0.58	0.64	0.55	0.67
MnO	0.08	0.09	0.09	0.07	0.09
P_2O_5	0.09	0.11	0.12	0.11	0.11
Loss on ignition	1.53	1.53	1.73	1.54	1.67
Total	100.00	100.00	100.00	100.00	100.00

is a little more consistent than that given by the core-limb sets. In comparison to the lithon the cleavage consistently contains less SiO_2 and more Al_2O_3, Fe_2O_3, K_2O and TiO_2. In the majority of the six analyses, MgO and loss on ignition tend to be higher in the cleavage than in the lithon whereas CaO and Na2O show the opposite trend. The values for the concentrations of MnO and P_2O_5 are so low that the analytical errors render the differences meaningless.

These results are not surprising. The cleavage planes are relatively depleted in quartz and enriched in micas, which explains the decrease in SiO_2 and the increases in Al_2O_3, K_2O, Fe_2O_3 and TiO_2.

One of the goals of this project is to estimate the gains and losses of chemical components during the processes which are responsible for the development of the spaced cleavage. Since there is evidence of volume loss in the lithons and more strongly so in the cleavage planes, gains and losses cannot be estimated by directly comparing the results of the whole rock analysis. The analyses have to be standardized to equivalent mass units, which implies that an estimate of the volume loss has to be made. Volume loss estimates using physical strain markers have already been mentioned. Here, the volume loss will be estimated using chemistry alone, through the use of Gresens' (1967) approach.

The basic equation that Gresens derived is used here

in the form of:

$$100(fv(gc/gl)\ Ccn - Cln\ ) = Xn$$

In this equation Ccn and Cln are the values for any component n (eg. SiO_2) in the cleavage and the lithon respectively, as given by the whole rock analysis. Xn represents the actual amount of that component which has been lost or gained from the cleavage. fv is defined as the volume factor. If fv is equal to one, replacement has taken place at constant volume. When fv<1 replacement has taken place with volume loss, in this case indicating that the cleavage has lost volume with respect to the lithon. The ratio gc/gl is the ratio of density of the cleavage over the density of the lithon. This ratio was measured in five samples and was determined to be within 5% -10% of unity. Since the accuracy of the measurements was estimated to be approximately 5% - 10% the density ratio was taken to be unity in all cases. With the density ratio known and the chemical analysis providing the values for Ccn and Cln, one is left with one equation and two unknowns, the volume factor and the actual amount of any component lost or gained by the cleavage. Since the cleavage in the Ruth Falls syncline samples is in many cases very thin and does not contain a sufficient number of pressure dissolved quartz grains, it did not lend itself to the physical strain estimates already mentioned. No independent strain estimate,

or volume factor is therefore available. There is however a method for obtaining volume factor estimates from the chemical analysis alone. It is based on the assumption that the system studied contains several relatively immobile components. By letting Xn = 0 one can calculate a volume factor for each individual component. Since some of these components will have experienced gains or losses they will show a range in volume factors. A clustering of volume factors of several components will indicate that these components have either been lost from or gained to the cleavage to the same extent, or that these components have been relatively immobile. If the assumption is made that these components are relatively immobile, than the cluster of these components will give the true volume factor of the system. The true volume factor of a system gives the overall bulk loss or gain the system has experienced

Figure (5.1.2) is a plot of components vs. volume factor (Xn = 0) for all five cleavage lithon pairs. Applying the above mentioned criteria one can see that TiO_2, Al_2O_3 and FE203 form a relatively tight cluster in all five sample pairs. Since TiO_2 and Al_2O_3 plot closer to each other than Fe_2O_3 the TiO_2 and Al_2O_3 positions were chosen as true volume factors. The true volume factors therefore range from 0.6 to 0.9, which implies a 40% to 10% loss in volume. This has to be interpreted as differential volume loss between lithon and cleavage only, since the chemical method only

Figure 5.1.2

Ruth Falls Syncline volume factors

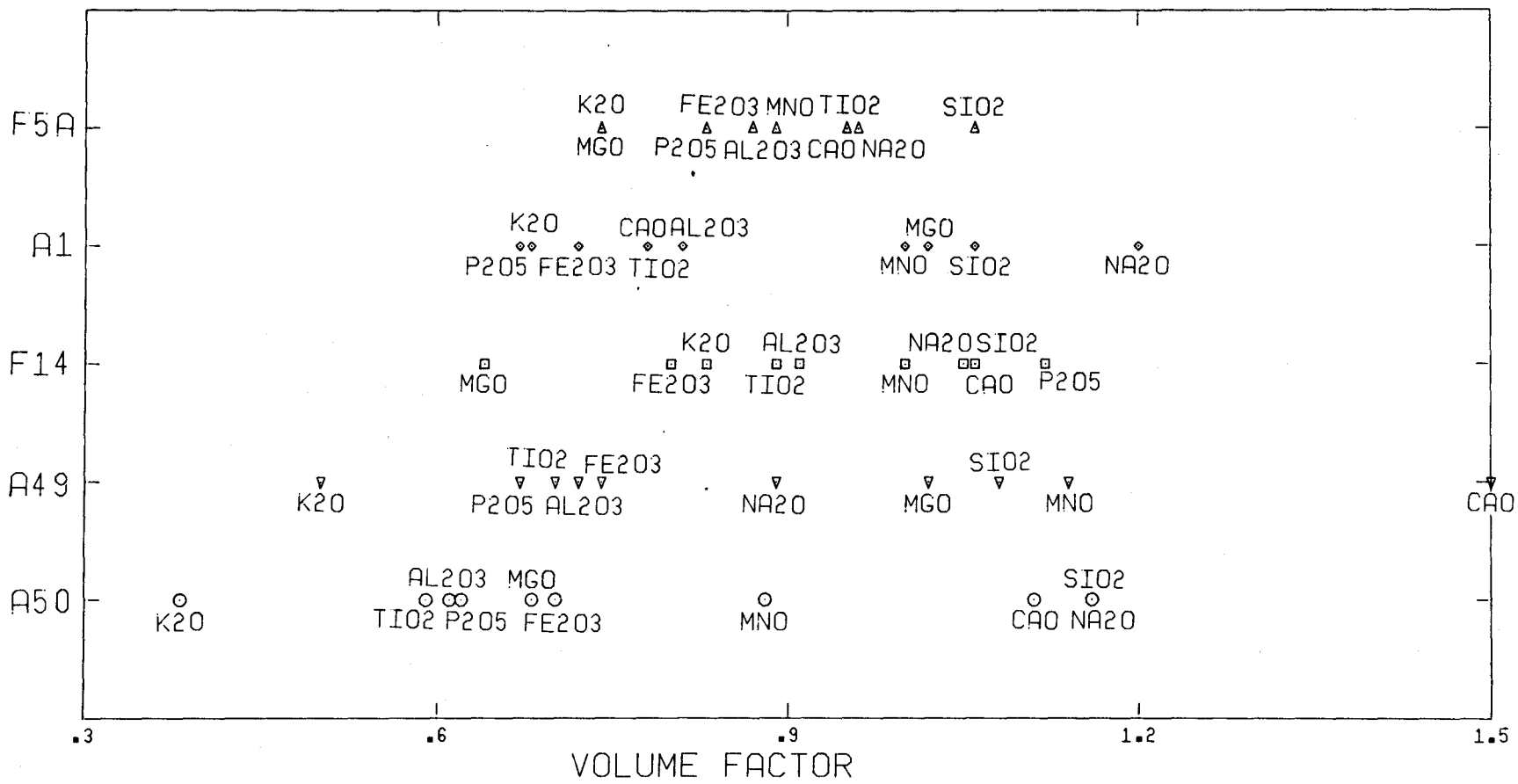
F5A
A1
F14
A49
A50
K2O FE2O3 MNO TIO2 SIO2
MGO P2O5 AL2O3 CAO NA2O
K2O CAO AL2O3 MGO
P2O5 FE2O3 TIO2 MNO SIO2 NA2O
K2O AL2O3 NA2O SIO2
MGO FE2O3 TIO2 MNO CAO P2O5
TIO2 FE2O3 SIO2
K2O P2O5 AL2O3 NA2O MGO MNO CAO
AL2O3 MGO SIO2
K2O TIO2 P2O5 FE2O3 MNO CAO NA2O
.3
.6
.9
1.2
1.5
VOLUME FACTOR

looks at the differences between the two and has no known absolute base. Volume losses in the lithon, as determined by Pryer (1984) cannot be measured by chemical methods. The volume losses between cleavage and lithon measured by Pryer (1984) only on Goldenville samples range between 40% and 76%. The chemical estimates therefore appear to be low. However it has already been mentioned that the cleavage in the Goldenville samples was more extensively developed than in the Ruth Falls syncline samples. These volume loss estimates therefore do not seem unreasonable and the selection of Al_2O_3 and TiO_2 as true volume factors appears to be justified.

Any component which falls to the right (fig 5.1.2) of the true volume factor of the system has suffered a loss from the cleavage with respect to the lithon. SiO_2 and Na2O have suffered losses in every case and CaO in four out of five. MnO and P_2O_5 will not be considered due to the above mentioned inaccuracies. Losses in SiO_2 and CaO can be explained in terms of decreased quartz and calcite content in the cleavage planes. The loss in Na2O can only be explained by stating that the micas in the cleavage must contain proportionally less Na than those in the lithon. There is not enough albite in the rock to account for the observed variation of Na2O.

Any component that has a volume factor less than that of the system, ie. falls to the left of the true volume

factor on the graph, has been added to the cleavage planes, with respect to the lithons. K_2O behaves in this manner in every case. This correlates well with the increased muscovite content in the cleavage. MgO appears to behave very unsystematically.

In summary one can state that Al_2O_3, TiO_2 and probably to a lesser extent Fe_2O_3 have remained relatively immobile during the cleavage formation. SiO_2, Na2O and very likely CaO have been lost from the cleavage during its formation and K_2O has been introduced into it. The behavior of MgO, MnO and P_2O_5 cannot usefully be determined. Relative volume losses between lithon and cleavage range between 10% and 40%. These estimates are made under the assumption that the material dissolved in the cleavage planes was not redeposited in the lithons. Since Pryer (1984) determined that the lithons themselves showed some volume loss, this assumption seems justified. If material from the cleavage planes had been redeposited in the lithons, the directions of movement for the individual components would likely still be correct, but the bulk volume loss estimate would be an overestimate.

By substituting the volume factor estimates back into the original Gresens equation, the absolute amounts of material lost or gained can now be calculated. For sake of simplicity, the volume factor given by Al_2O_3 was used as the true system volume factor for the purposes of calculations.

Even though the volume factors used give the overall loss to the nearest percent, a minimum error of five percent is estimated. This error is partially due to analytical error as well as to the density ratio not being unity, but it is also very unlikely that Al_2O_3 was absolutely immobile during cleavage formation. It seems much more likely that it moved as well, merely at a much slower rate than other components. Table (5.1.3) shows the absolute losses and gains calculated. It is apparent that the vast bulk of material removed from the cleavage is SiO_2. The losses and gains of the other components are relatively minor and almost balance each other out. This is not surprising. In order to achieve significant volume losses in a system which contains more than 70% SiO_2 it is more than likely that a large portion of that volume loss will have to be a loss of SiO2. However the significance of the movements by other components should not be overlooked. These movements clearly indicate that the production of a spaced cleavage is not restricted to the solution of quartz and carbonate alone.

5.2 Goldenville Chemistry

The cleavage zones of samples from the Goldenville anticline are wider than those in the Ruth Falls syncline samples and less quartz rich. Consequently, the chemical differences between cleavage planes and lithons should be more pronounced. Wide cleavage planes also reduce the

Table 5.1.3

Absolute amounts lost or gained by cleavage zone

(g/100g)

	SiO_2	Fe_2O_3	MgO	CaO	Na_2O	K_2O	TiO_2
F5A	-13.49	+0.14	+0.28	-0.05	-0.22	+0.47	+0.01
F50	-37.36	-0.40	-0.10	-0.66	-1.04	+0.84	+0.01
F14	-10.37	+0.65	+0.61	-0.15	-0.29	+0.21	+0.01
A49	-26.25	-0.01	-0.4	-0.89	-0.34	+0.54	+0.01
A1	-19.06	-0.39	-0.29	+0.04	-0.66	+0.36	+0.02

problem of lithon contamination during sampling. Five samples of core, each approximately ten cm long, were selected for analysis. Each piece of core yielded one sample set, consisting of five to six cleavage planes and five to six lithons. The same samples were studied by Pryer (1984) and Thompson (1984). Each cleavage sample and each lithon sample were analysed individually. Only XRF whole rock data are considered in this chapter. Due to the small sample size it was not possible to measure the loss on ignition.

Figure 5.2.1 shows the whole rock major element contents of five individual lithons from sample number G26-415 . As can be seen there is a variation in the CAO content by a factor of five, which probably reflects variations in the lithon carbonate content. Overall however, there is no significant variation in the major element chemistry of the lithons of individual sample sets. Other sample sets show similar agreement.

Figure 5.2.2 depicts the results of the analysis of five individual cleavage planes of the same core sample. Clearly the chemical composition of the cleavage planes is distinctly different from that of the lithons. However the compositions of the five different cleavage planes agree quite closely amongst themselves.

In order to determine how much the major element chemistry of cleavages and lithons of different beds (ie. different core samples) varies, the averages for the

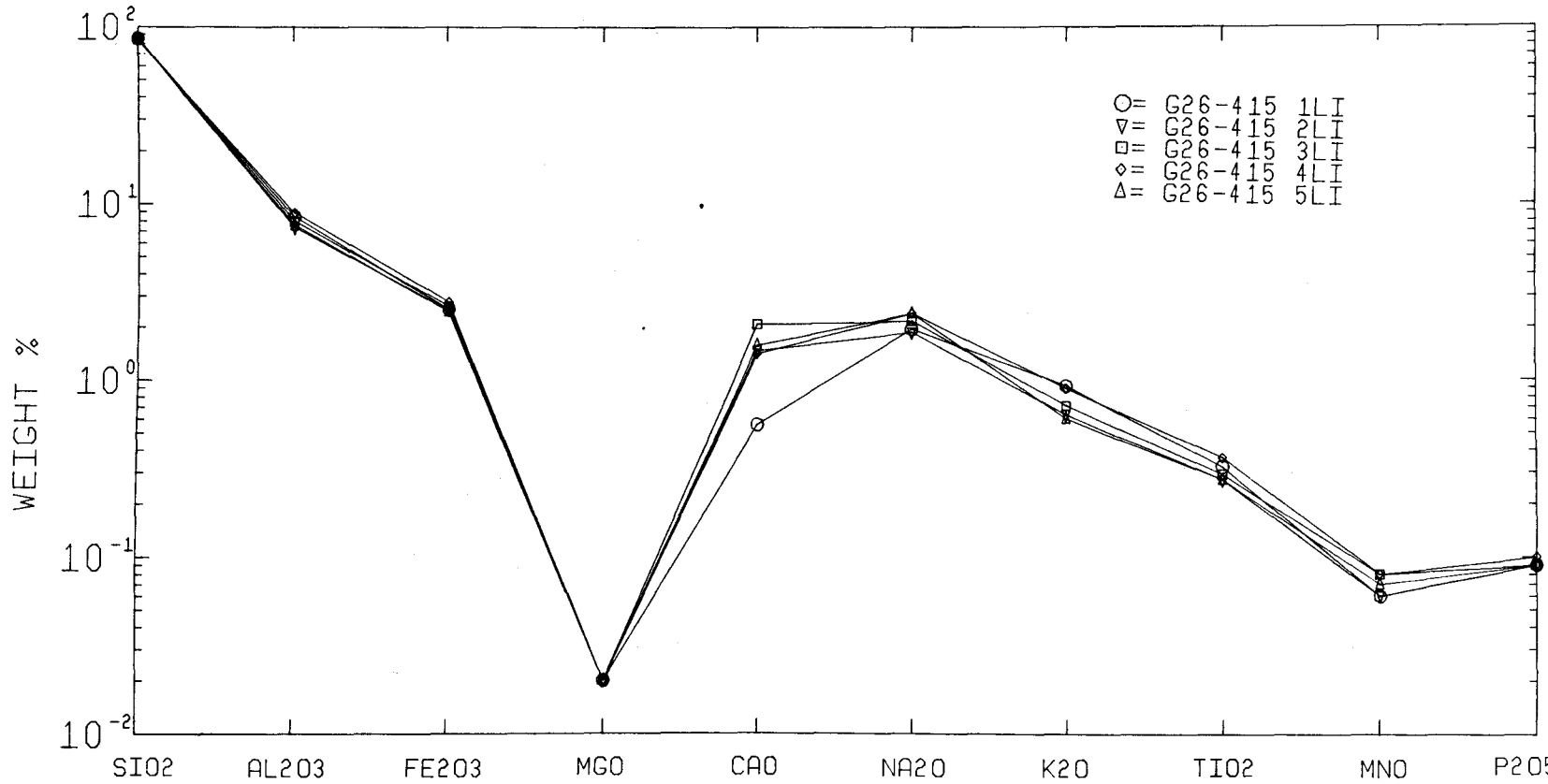

COMPOSITION OF INDIVIDUAL LITHONS OF G26-415

FIGURE 5.2.1

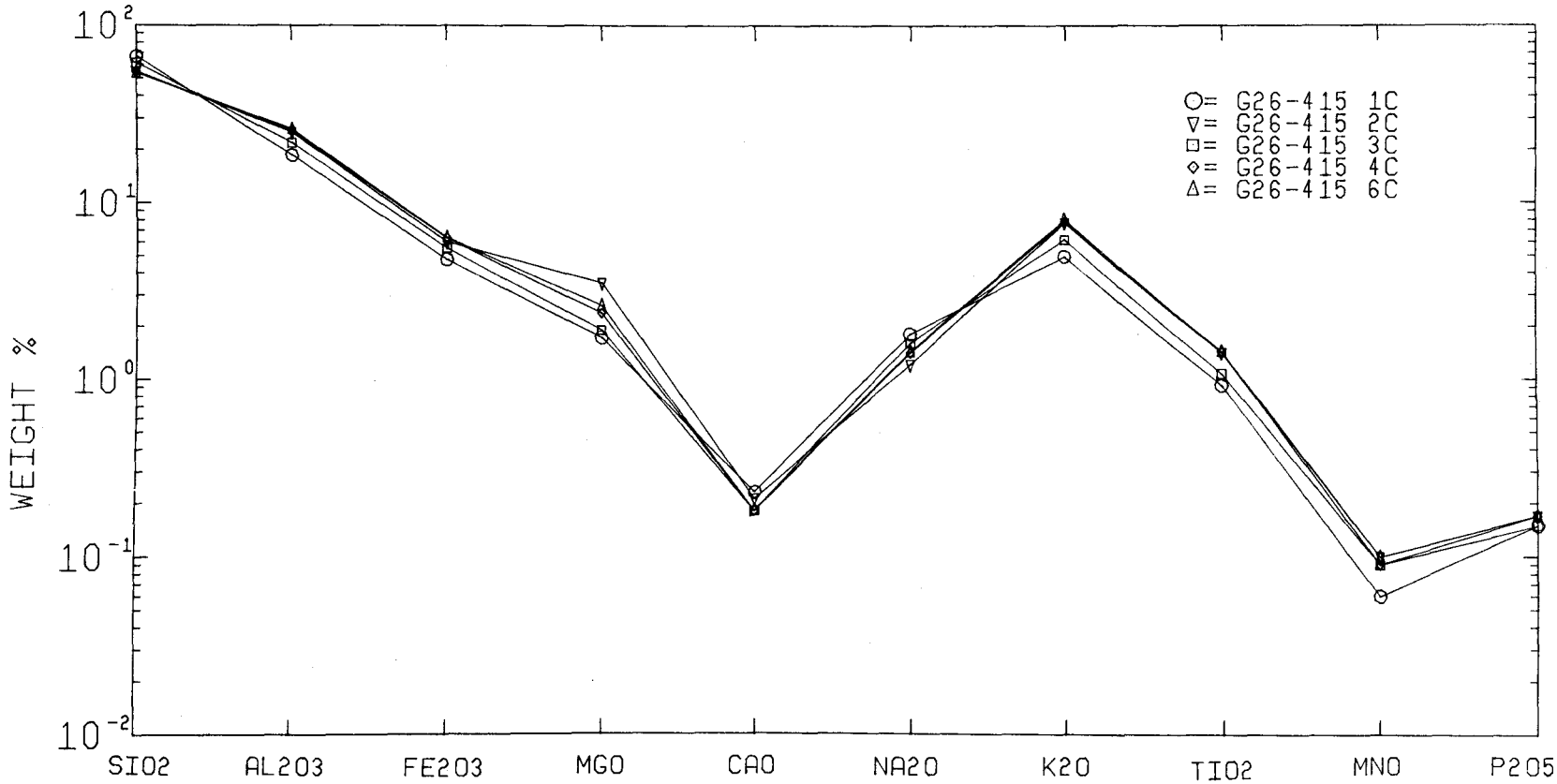

INDIVIDUAL CLEAVAGE COMPOSITIONS OF G26-415

FIGURE 5.2.2

cleavage and lithon suites for each core sample set was calculated. Differences in the development of cleavage planes, ie. differences in the amount of quartz present in the cleavage plane, are reflected in their chemical analysis. For the calculation of the average cleavage plane chemistry for each sample set only those cleavage planes which are chemically alike were used. The reason for this is that the average cleavage plane composition should not reflect the averaged out compositions of several cleavage planes in different stages of development, ie. with different quartz contents, but that it should represent the composition of a cleavage plane in a single stage of development with a consistent quartz content. G26-353-1C, 6C,G20-753-4C, G20-747-1C and G19-354-4C and 5C were therefore omitted from the average cleavage calculations. It is apparent in figure 5.2.3 that the main variation in composition of the lithon averages lies in their MgO content. This variation is between 0.01 wt% and 1 wt% and is probably due to differences in amounts of Mg bearing detrital phases. The bulk of the Mg is probably derived from clays, since the amount of visible detrital grains which are not quartz or feldspar is not large enough to account for a variation of this magnitude. The minor fluctuation in K2O can also be explained by differences in the content of potassium bearing detrital phases. Overall however, the chemical variation between the lithons of the five beds is quite small. The

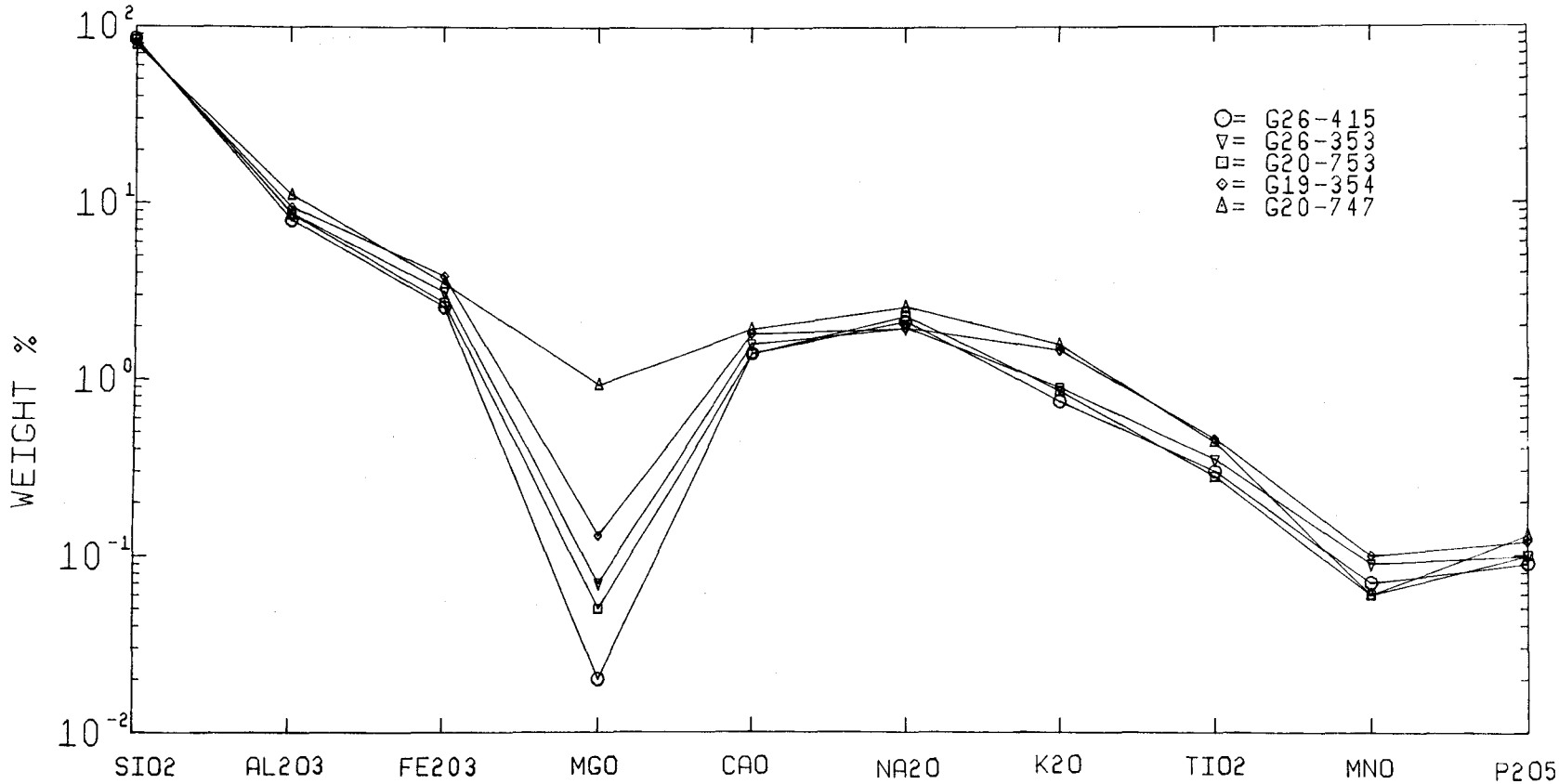

AVERAGE LITHON COMPOSITIONS OF GOLDENVILLE SAMPLE SETS

FIGURE 5.2.3

average compositions of the cleavage planes of all sample sets (fig.5.2.4) are also very similar to each other, especially when we consider that not every cleavage plane is equally well developed. Differences in the degree of development of the cleavage planes, indicated by variations in their mica content, must be reflected in their major element chemistry.

Figure 5.2.5, which directly compares average lithon and cleavage compositions of sample set G26-415, indicates the following changes. The cleavage is enriched in Al_2O_3, K2O, Fe_2O_3, MgO and TiO_2 by 15%, 6.1%, 3.2%, 2.4% and 0.9% respectively with respect to the lithon, whereas SiO_2, CaO and Na_2O are depleted by 26%, 1.4% and 0.6% respectively. The low amounts of MnO and P_2O_5 present and the analytical errors associated with their analysis precluded their use in quantitative results and they are largely ignored in the following discussion. The most interesting difference between the lithons and the cleavages is the large relative percentage increase in MgO and K2O. Other sample sets show similar results. In general, the differences between the Goldenville cleavage planes and lithons are greater than those in the Ruth Falls syncline samples. This was expected, since the Goldenville cleavage planes are better developed.

In an effort to determine the true losses and gains, associated with the cleavage formation the standard Gresens (1966) approach was taken. The densities of the cleavages

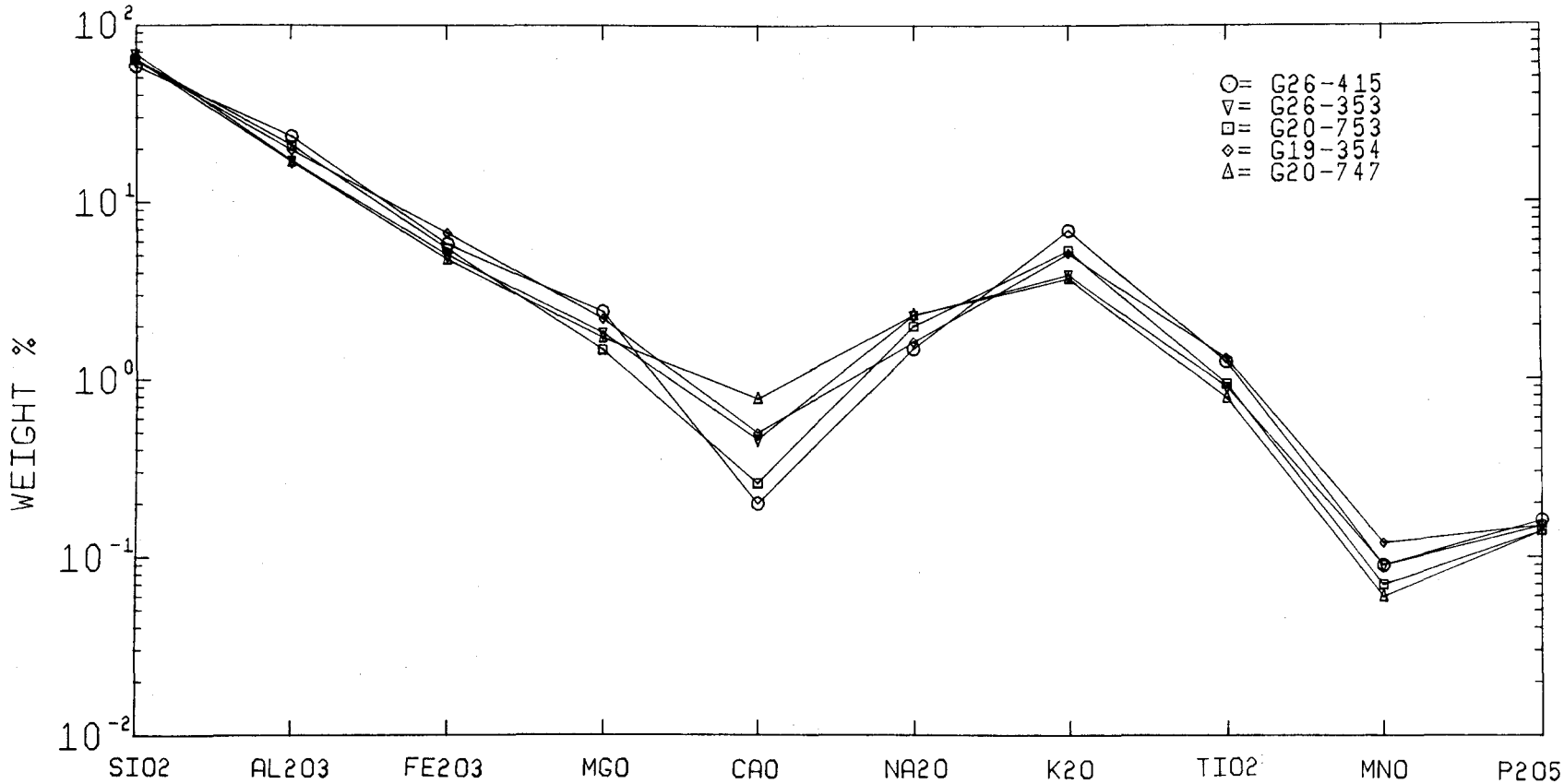

AVERAGE CLEAVAGE COMPOSITIONS OF GOLDENVILLE SAMPLE SETS

FIGURE 5.2.4

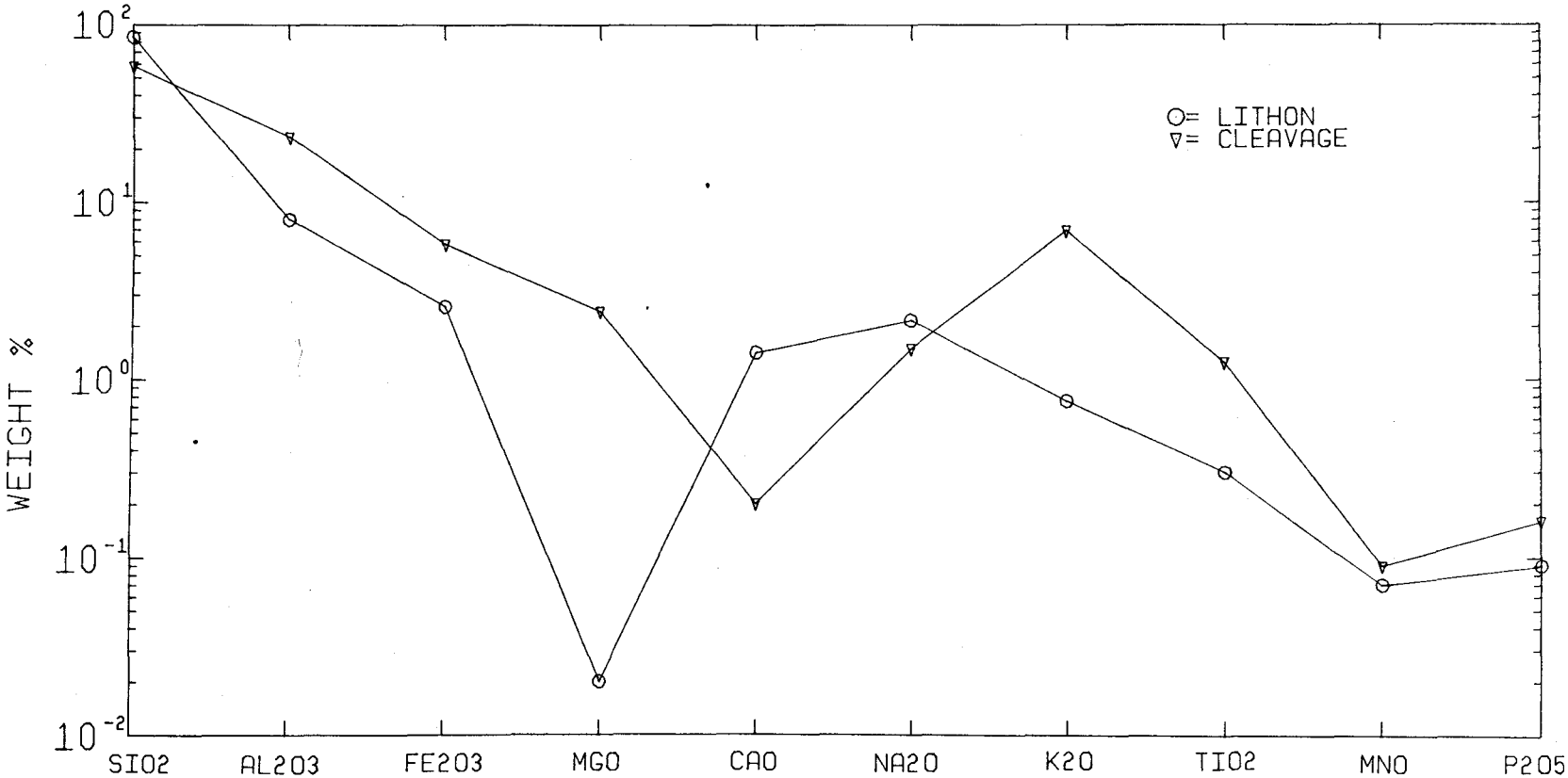

AVERAGE LITHON AND CLEAVAGE COMPOSITIONS OF G26-415

FIGURE 5.2.5

and lithons were found to be the same within the limits of accuracy of measurement. The density ratio used in the Gresens equation was therefore taken as unity as before. Figure 5.2.6 shows the average volume factors for the oxides in all sample sets, assuming no loss or gain to or from the cleavage. The criteria used to choose the true volume factor are the same as in the Ruth Falls syncline study. Even though clustering may not be immediately apparent in figure 5.2.6, TiO_2, Al_2O_3 and Fe_2O_3 are the only oxides that are relatively close to each other in all five cases and maintain relatively consistent component ratios. One can therefore consider the oxides TiO_2, Al_2O_3 and Fe_2O_3 to be the least mobile components in this system. Al_2O_3 is again chosen as the true volume factor for this system, mostly because it has a volume factor intermediate between TiO_2 and Fe_2O_3, but also because it is five to six times more abundant than TiO_2 or Fe_2O_3 and is therefore least influenced by minor internal losses or gains. The true volume factors for the five cases presented here range from between 0.4 and 0.6. This implies that the cleavage represents a forty (volume factor = 0.6) to sixty (volume factor = 0.4) percent volume loss, with respect to the original lithon. These estimates are higher than those from the Ruth Falls syncline, which again is not surprising, since the cleavage in the Goldenville anticline is better developed.

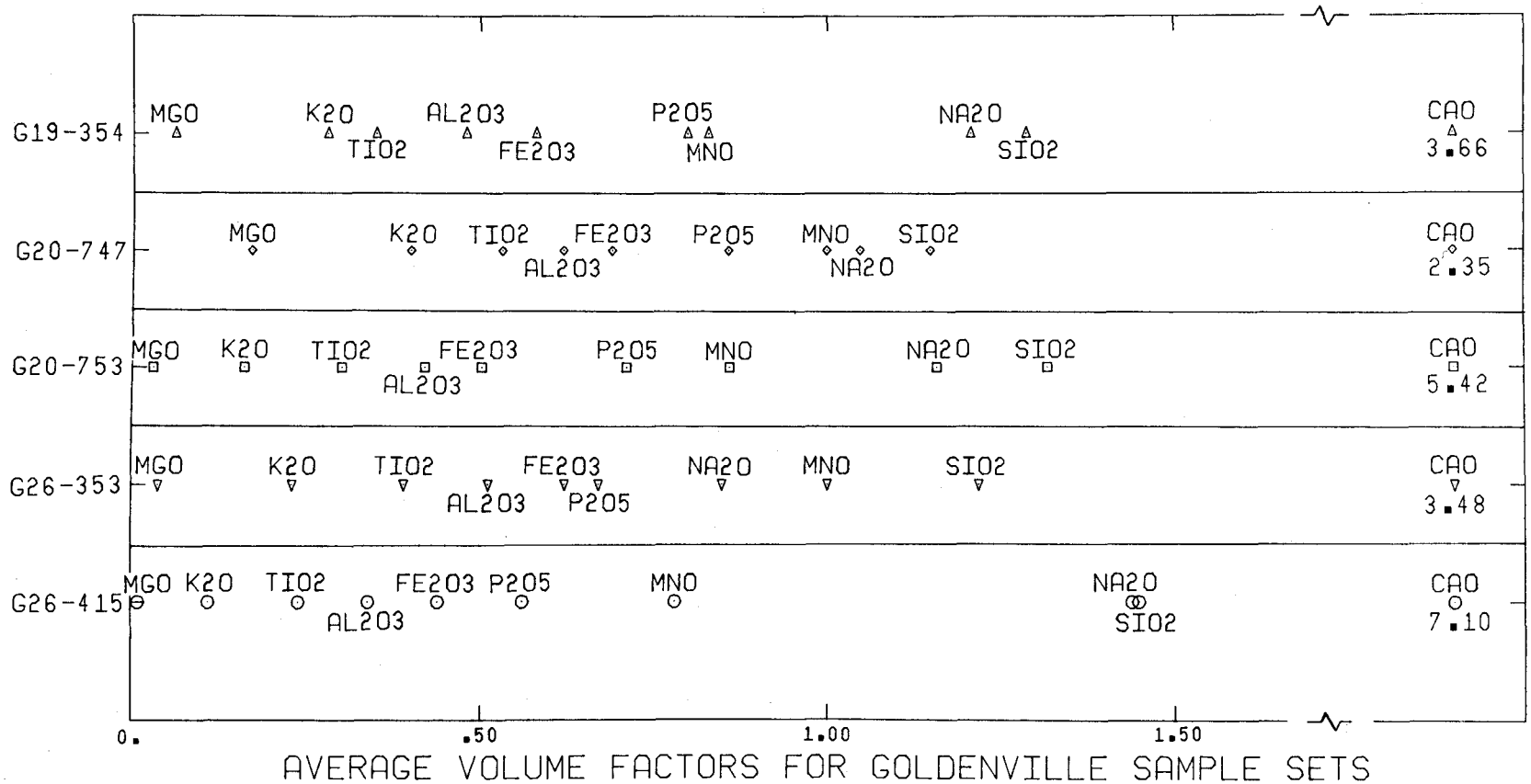
G19-354
MGO
K2O
AL2O3
P2O5
NA2O
CAO
TIO2
FE2O3
MNO
SIO2
3.66
G20-747
MGO
K2O
TIO2
FE2O3
P2O5
MNO
SIO2
AL2O3
NA2O
CAO
2.35
G20-753
MGO
K2O
TIO2
FE2O3
P2O5
MNO
NA2O
SIO2
AL2O3
CAO
5.42
G26-353
MGO
K2O
TIO2
FE2O3
NA2O
MNO
SIO2
AL2O3
P2O5
CAO
3.48
G26-415
MGO
K2O
TIO2
FE2O3
P2O5
MNO
NA2O
AL2O3
SIO2
CAO
7.10
0.
.50
1.00
1.50
AVERAGE VOLUME FACTORS FOR GOLDENVILLE SAMPLE SETS

FIGURE 5.2.6

With the use of a true volume factor one can then use figure 5.2.6 to determine what has been lost from or introduced into the cleavage domain. Any oxides to the right of the true volume factor (Al_2O_3) have been lost from the cleavage during its formation, whereas oxides to the left of the volume factor were introduced to the cleavage during its formation. The distance from the true volume factor gives an indication of the degree to which this loss or gain has taken place.In all cases the results show remarkable similarities. In all cases CaO is the oxide which has been lost to the greatest extent during cleavage formation. (It should be noted that this does not imply that the bulk of the material lost during cleavage formation was CaO but rather that this component has suffered the greatest relative percent loss with respect to its "original" lithon composition). SiO_2 shows the second greatest loss. Again the losses in these two components can easily be demonstrated in thin section by the lack of carbonate and the apparent depletion of quartz in the cleavage plane. The loss of silica is also the largest bulk loss from the cleavage plane. Other oxides lost during the cleavage formation, in decreasing amounts, are Na_2O, MnO and P_2O_5. The sources for these oxides are probably detrital clays which eventually formed the micas of the cleavage. MgO and K2O were indroduced into the cleavage plane and probably contributed to the formation of micas. These chemical changes imply that

micas were actively growing during the cleavage formation and that the bulk composition of the micas in the cleavage is different from the bulk composition of the micas in lithon. This is further supported by the petrography and reflected in the variations in the biotite content between lithons and cleavage. The similarity in the order with which the oxides plot on figure 5.2.6, ie. MgO on the left side to CaO on the right side, demonstrates how remarkably consistent the processes were that led to the chemical evolution of the cleavage. Furthermore the degree to which the oxides are spaced out amongst themselves along the volume factor axis of figure 5.2.6 is dependent upon the volume loss that has occurred. Sample number G20-747, which shows the highest volume factor and therefore represents the smallest volume loss also displays the smallest spread amongst the oxides. On the other hand sample number G26-415 which shows the largest volume loss also displays the largest spread of the oxides. This demonstrates that the chemical movements that take place during the cleavage formation are not random or erratic, but are well controlled and follow certain definite patterns.

The fundamental assumption that these interpretations are based on is that the lithon represents the original source rock. This implies that very little or no deposition of dissolved material has taken place in the lithon. Deposition of material in the lithon would cause the

volume loss to be overestimated. The chemical estimates alone give no clues as to whether deposition has occurred in the lithons. Fortunately volume loss estimates, based solely on the shapes of detrital quartz grains are available as well (Pryer, 1984). Since the chemical volume loss estimates only deal with the differential volume loss between cleavage and lithon, they should be compared with their physical equivalents.

Pryer (1984) estimates a 40% volume loss between cleavage and lithon for sample G20-753. Chemical estimates for the individual cleavage planes, listed in appendix 3, range from 47% - 60%. Physical estimates for samples G19-354 and G26-353 are 41% and 45% respectively, whereas chemical estimates range from 31% - 52% and 31% - 56% respectively. There are physical estimates available for two cleavage planes in sample G26-415. One gives a loss of 76% , with chemical estimates ranging from 57% - 69%. The second cleavage plane, for which a physical estimate is available is specifically identified as G26-415-2C. This allows a comparison of physical and chemical estimates of the same cleavage plane. The physical estimate shows a volume loss of 73% as compared to the chemically calculated volume loss of 68%.

For samples G19-354 and G26-353 the physical estimates are well within the range given by the chemical estimates. For G20-753 and G26-415 the chemical estimates

are somewhat higher than the physical values found. Since the volume loss estimates are derived by two different and independent methods, a difference of less than 10% is not considered significant.

Other physical volume loss estimates, derived by unfolding folded quartz veins located in the cores of several folds, all yield volume loss estimates between 50% and 60% (J. Henderson, 1984 pers. com.).

The conclusion therefore is that physical and chemical estimates of the volume loss between the lithon and the cleavage agree well with each other. No significant amount of redeposition of material dissolved in the cleavage could have occurred in the lithon. This is further supported by physical evidence, which shows a volume loss in the lithon in all but one sample.

The material lost from the cleavage must therefore have been lost from the greywacke beds as a whole.

If material had been lost from the lithons as well as the cleavage, the chemical volume loss estimates would give the minimum amount of material lost.

5.3 Trace Element Geochemistry

5.3.1 Ruth Falls Syncline

All Ruth Falls Syncline samples which were analysed for major elements were also analysed for Au, W, As and Sb radiochemical neutron activation. The abundances of all four

elements were generally very low, never exceeding 8 ppb. The results of all analyses are listed in the appendices. Table 5.3.1 shows the mean values for the whole rock samples, as well as the means for all individual cleavage and lithon samples, for all four elements. In general, the values for the whole rock analyses are lower than the cleavage and lithon values for the sample. This can only be interpreted as an indication of the dispersion of Au, W, As and Sb in the rock. Mean Au, W, As and Sb values for cleavages and lithons do not differ to a great degree, the difference always being less than the standard deviation of the higher value. No reliable conclusions about the chemical migrations of these four elements during cleavage formation can be made on the basis of the Ruth Falls Syncline samples. These samples can be used to demonstrate the background Au, W, As and Sb levels, which can be found in unmineralized Goldenville Formation greywackes.

5.3.2 Goldenville Samples

All Goldenville cleavage and lithon samples were analysed for Au, W, AS and Sb by instrumental neutron activation (appendix 5). For all elements, cleavage and lithon means were calculated for each of the five sample sets. An overall mean for cleavage and lithon values was then calculated using the sample set means. The results are shown in table 5.3.2.

Table 5.3.1: Au, W, As and Sb averages for Ruth Falls Syncline

	Au ppb	W ppb	As ppm	Sb ppm
Whole Rock	1.1 ± 1.0	0.3 ± 0.3	2.0 ± 0.8	0.9 ± 0.4
Cleavage	3.0 ± 2.7	0.1 ± 0.1	2.6 ± 0.8	1.3 ± 0.5
Lithon	2.0 ± 2.0	0.4 ± 0.4	2.1 ± 0.6	1.2 ± 0.4

Table 5.3.2

"Average Au, W, As and Sb values for Goldenville core samples"

	Au ppb		W ppm		As ppm		Sb ppm	
	C*	L*	C	L	C	L	C	L
G20-747	7.2 ± 2.5	6.8 ± 3.0	5.8 ± 0.8	2.3 ± 0.6	170 ± 150	150 ± 170	1.3 ± 1.1	3.9 ± 5.4
G19-354	3.3 ± 1.6	4.5 ± 3.8	8.5 ± 2.5	3.2 ± 0.6	105 ± 85	35 ± 13	1.0 ± 0.8	0.5 ± 0.1
G20-753	4.4 ± 3.5	4.6 ± 2.9	8.7 ± 1.4	1.6 ± 0.4	260 ± 140	85 ± 72	2.1 ± 1.1	0.7 ± 0.5
G26-353	3.6 ± 1.2	4.4 ± 1.2	5.6 ± 1.4	2.5 ± 0.3	95 ± 50	65 ± 50	0.5 ± 0.2	0.3 ± 0.2
G26-415	5.2 ± 1.7	2.4 ± 1.2	8.5 ± 1.9	1.5 ± 0.2	170 ± 150	13 ± 4.6	0.9 ± 0.8	0.2 ± 0.1
	4.7 ± 1.5	3.7 ± 2.3	7.4 ± 1.5	2.2 ± 0.7	160 ± 70	70 ± 55	1.2 ± 0.6	1.1 ± 1.6

* C: Cleavage; L: Lithon

The overall mean values of the Goldenville samples can be compared to those of the Ruth Falls Syncline. Goldenville Au values are only about one ppb above Ruth Falls Syncline means and for Sb, the means for Goldenville and Ruth Falls are virtually identical. Significant differences are present in the means for W and As. In both cases the values of Goldenville samples are higher than those of the Ruth Falls Syncline samples. The large variation in As values is attributed to the sporadic presence of small arsenopyrite crystals in the samples.

There is no consistent partitioning of Au between cleavage and lithon. In three sample sets the lithon mean is greater than the cleavage mean, whereas the remaining two sample sets show that the opposite is the case. Virtually always the difference between the means is less than the standard deviation about the means. There are some indications that Au concentrations may be linked to arsenopyrite. Figure 5.3.1 compares average Au values with average As values. The correlation for the cleavage values are low, but there is a trend for the lithon samples. However, even though the correlation coefficient is 0.92, only five samples are used and more extensive sampling is needed before any firm conclusions can be reached. Differences in the behavior of Au and As during the cleavage development may account for the lack of correlation in the cleavage.

Figure 5.3.1

Plot of Au and As values for Goldenville samples, showing best fit line for lithons.

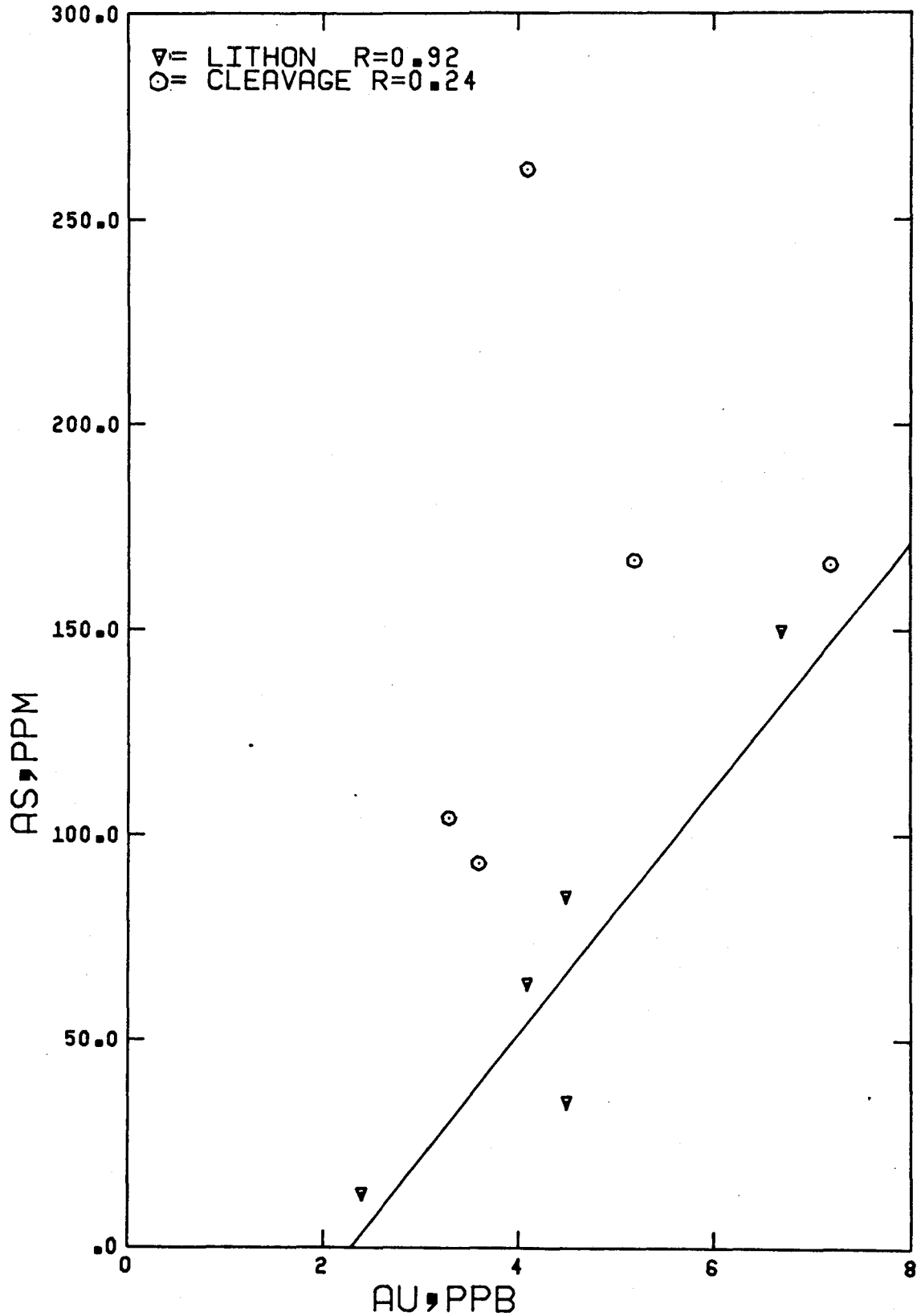
▽= LITHON R=0.92
⊙= CLEAVAGE R=0.24
300.0
250.0
200.0
150.0
100.0
50.0
.0
0
2
4
6
8
AS, PPM
AU, PPB

Generally Au levels are low. It seems unlikely that the Au exists as particulate matter in the rock. It probably occurs in phyllosilicate minerals. The only firm conclusion that can be made is that the background Au levels of the greywackes within a mineralized area are only slightly above those of an unmineralised area.

Mean As values for the cleavage are higher than those in the lithon. Arsenopyrite crystals are responsible for the high, erratic values of As. The cleavage therefore does appear to concentrate As; however the high standard deviations make definite conclusions doubtful.

Sb behaves in a fairly consistent manner. In four out of five sample sets, the lithon mean is less than the cleavage mean, but the overall cleavage and lithon mean of all sample sets are the same.

The distribution of W between cleavage and lithon is consistent. Mean lithon values are always less than mean cleavage values, with the standard deviations being less than the differences between the means. Due to this consistency W can be incorporated into the Gresens calculations. The volume factors obtained for using W range between 0.18 and 0.45 (table 5.3.3). Comparing the W volume factors with the true volume factors of the sample sets, as given by the major elements (fig 5.2.6), W volume factors are consistently less than the true volume facotors. This indicates that W has been introduced into the cleavage

Table 5.3.3

W volume factors of Goldenville samples

Sample	W volume factor
G20-747	0.40
G19-354	0.38
G20-753	0.19
G26-353	0.45
G26-415	0.18

during its formation. Since muscovite can carry W it is not surprising that W should be enriched in the cleavage.

In an effort to determine the behavior of other trace elements during the development of the cleavage the following approach was taken:

A compromise had to be sought, since in most cases three grams of sample, required to make the necessary powder pellets, could not be obtained. A few powder pellets of individual cleavages and lithons were analysed by XRF for Rb, Sr, Y, Zr, Nb, Ce, Nd, La, Ba and Pb.Since these few runs showed significant differences in a number of elements (table 5.3.4), it was thought worthwhile to investigate these differences further.

The major element analyses showed that the chemical compositions of the individual cleavages and lithons of one sample set are very consistent. Since there was not enough sample available to make powder pellets for every individual cleavage and lithon of a sample set, it was therefore decided to make just one powder pellet, representing the cleavage and lithon of each sample set. For this purpose, equal amounts of cleavage sample of one sample set were mixed to produce the pellet representing the cleavage for that sample set. The same was done for the lithons. Duplicate analysis of samples obtained this way showed good agreement. Since the aim of this study is to look at the relative differences between cleavage and lithon, and not at

Table 5.3.4

Trace Element Analysis of individual Goldenville Cleavages and Lithons

Sample	Ce	Nd	La	Ba	Pb	Rb	Sr	Y	Zr	Nb
G20-747-5L	173	24	33	327	14	63	244	36	152	16
G20-747-4L	148	7	35	325	10	64	260	25	153	16
G26-415-5L	9	4	14	65	12	30	165	21	127	16
G26-415-2C	45	45	35	1739	9	250	162	45	457	23
G26-415-2C	43	43	42	1747	10	250	160	43	454	22
G19-354-6L	18	22	22	283	13	60	211	27	227	15
G19-354-5L	15	20	25	259	10	54	216	26	209	14
G26-353-1C	32	46	36	873	19	128	152	32	313	17
G26-353-5L	16	15	20	149	13	36	179	23	147	13
G26-353-6C	41	49	45	1044	15	146	149	32	344	18

the accuracy of absolute values, it was felt that this approach was legitimate. The results of these analyses (appendix 6) were then used to calculate the Gresens volume factors (table 5.3.5) and are graphed in figure 5.3.2. Comparison between these volume factors and the true volume factors of the sample sets can be used to determine any consistancies in the distribution of these trace elements.

Ce, Nd, and La do not show any consistent trends. All three show greatly fluctuating volume factors. It is uncertain wether these fluctuations are due to analytical error or wether they are the result of an inhomogeneous distribution of these elements in the rock. Ce, Nd and La will therefore be ignored in any further discussion. Figure 5.3.3 shows the trace element volume factors for the Goldenville anticline, excluding Ce, Nd and La, but including the W volume factors. For all five sample sets, the volume factors obtained for Rb fall to the left of the true volume factors indicating that Rb was introduced into the cleavage domain. Since the cleavage is a zone of mica concentration and Rb is often associated with micas, this is not a surprising result.

The volume factors obtained by Sr always fall to the right of the true volume factors. Sr has therefore been lost from the cleavage during its formation. Sr probably follows Ca since most of the Sr was likely sited in calcite, which has been lost from the cleavage.

Table 5.3.5

Volume factors of Goldenville composite powder pellets

	G19-354	G20-753	G26-353	G26-415	G20-747
Rb	0.41	0.19	0.33	0.23	0.46
SR	1.35	1.26	1.19	1.11	1.18
Y	0.68	0.56	0.80	0.65	0.08
Zr	0.49	0.41	0.56	0.42	0.64
Nb	0.89	0.83	0.78	0.81	0.88
Ce	0.42	0.15	0.65	0.23	0.37
Nd	0.57	0.00	0.84	0.45	0.29
La	0.43	0.27	0.34	0.47	0.76
Ba	0.36	0.18	0.29	0.19	0.39
Pb	1.07	1.41	1.16	0.91	1.00

Figure 5.3.2

Trace element volume factor of Goldenville complex.

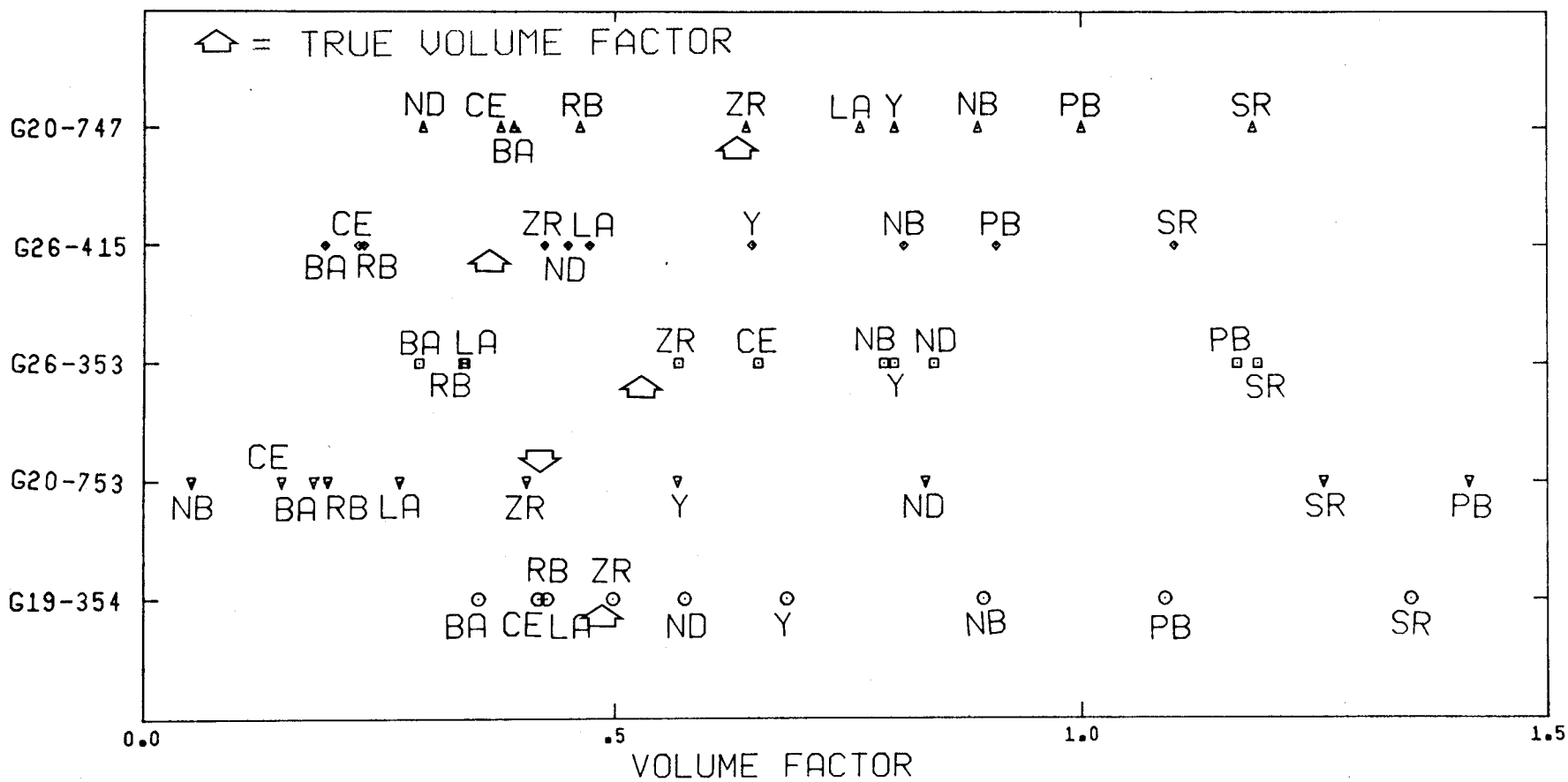
⌂ = TRUE VOLUME FACTOR
G20-747
ND CE RB ZR LA Y NB PB SR
BA
G26-415
CE ZR LA Y NB PB SR
BA RB ND
G26-353
BA LA ZR CE NB ND PB
RB Y SR
G20-753
CE
NB BA RB LA ZR Y ND SR PB
G19-354
RB ZR
BA CE LA ND Y NB PB SR
0.0
.5
1.0
1.5
VOLUME FACTOR

Figure 5.3.3

Trace element volume factors of Goldenville samples, excluding Ce, Nd and La but including W.

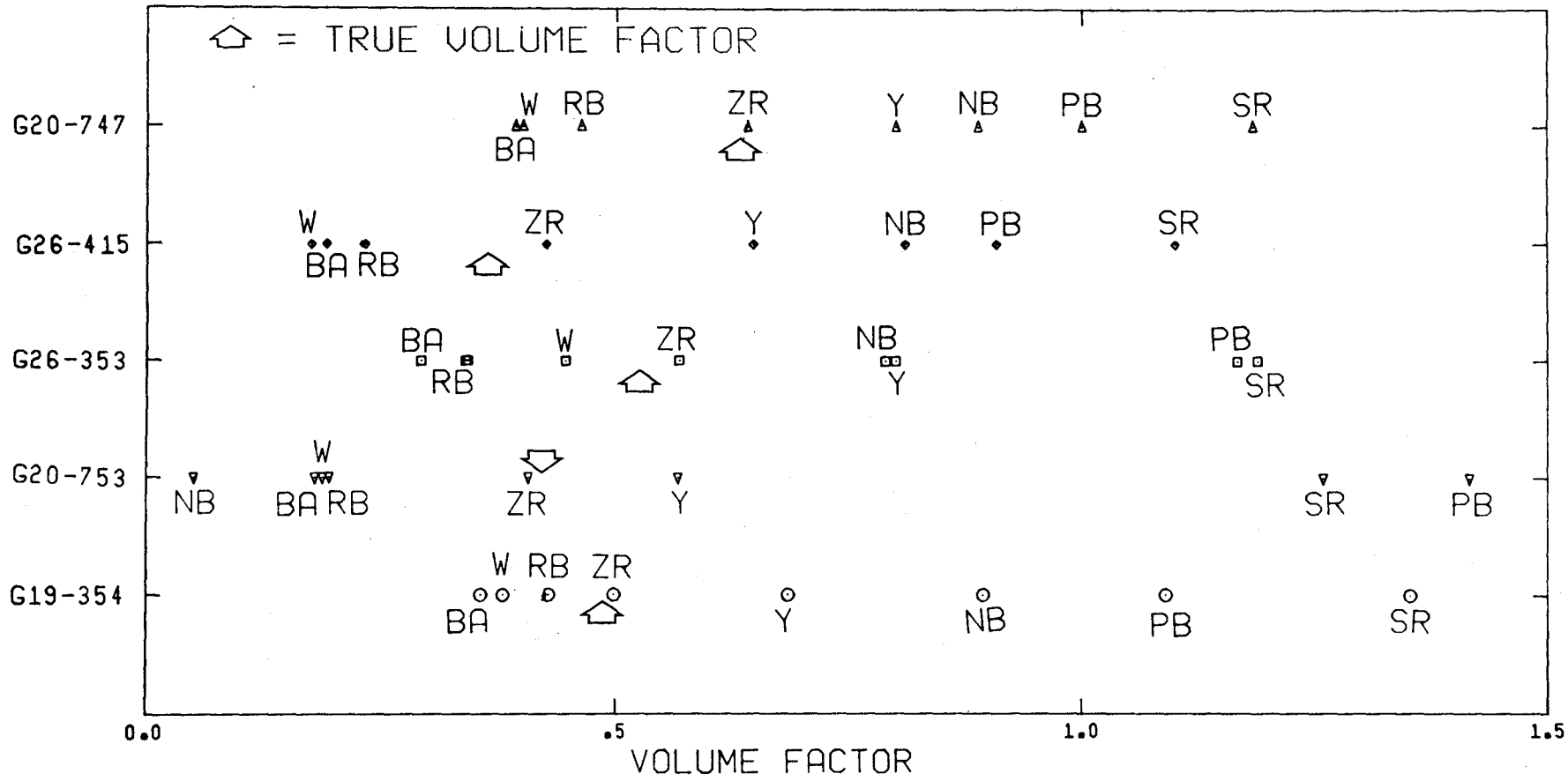
= TRUE VOLUME FACTOR
G20-747
W RB ZR Y NB PB SR
BA
G26-415
W ZR Y NB PB SR
BA RB
G26-353
BA W ZR NB PB
RB Y SR
G20-753
W
NB BA RB ZR Y SR PB
G19-354
W RB ZR
BA Y NB PB SR
0.0
.5
1.0
1.5
VOLUME FACTOR

Y also consistently lies to the right of the true volume factor, but it always falls closer to the true volume factor than Sr. Y has therefore been lost from the cleavage as well.

In four out of five cases the volume factor given by Zr lies in almost the exact position of the true volume factor of the sample sets. Even for sample set G26-415 the Zr volume factor of 0.43 still compares relatively favourably with a true volume factor of 0.34. The Zr is probably located in zircons, which are generally regarded as very resistant to change at greenschist facies. The proximity of Zr to the true volume factor of the samples based upon major elements is further confirmation that the choice of Al_2O_3 as the true volume factor was justified.

Nb has been lost from the cleavage, as is indicated by its consistent position to the right of the true volume factor of the cleavage. The same applies to Pb; however, since the Pb level is at the approximate detection limit, this result has to be treated with caution.

The volume factor for Ba falls consistently to the left of the true volume factor of the sample sets. Ba has therefore been introduced into the cleavage during its formation. Since muscovite can carry Ba this result is not surprising.

In summary, only preliminary suggestions can be made about the behaviour of Au and Sb during the cleavage

development. Even though the levels of As are higher in the cleavage than in the lithon, the patchy occurences of arsenopyrite crystals make any possible conclusion doubtful. The distribution of W, Rb, Sr, Y, Zr, Nb, Ba and Pb however is consistent in all five sample sets. This consistency leads to further comparison. It may be surprising that there is a certain similarity in the order with which the volume factors fall on the graph. With only four exceptions, the order from left to right is, Ba, W, Rb, Zr, Y, Nb, Pb and Sr. All four exceptions show only a reversal between two neighboring elements. This can be taken as further proof that the trace element data gathered in this wayare useful enough for this purpose. It also shows that the chemical movements of several trace elements follow certain well controlled patterns, much in the same way the major elements do.

6. Discussion

Thus far, it has been shown that the chemical development of the cleavage follows certain patterns. This chapter will outline what these patterns are. This discussion will largely be restricted to the major elements which demonstrate these patterns more clearly than the trace elements.

It has already been mentioned that volume factors for the oxides, as plotted in figure 5.2.6, are systematically distributed; MgO always has the smallest volume factor, while CaO consistently has the largest. The spread between these oxides also seems to be controlled by the true volume factor. The sample with the smallest true volume factor, representing the highest volume loss, has the largest spread in the oxides. Two preliminary conclusions are as follows:

(1) The degree of mobility and migration of the oxides increases with increasing volume loss. It is reasonable to assume that increasing volume loss corresponds to the progressive development of the cleavage.

(2) Oxides maintain their relative solubilities with respect to each other, as demonstrated by their order on the graph. This relationship is independent of how far the chemical evolution of the cleavage has progressed.

Up to now, solubilities and the migration of chemical components have only been discussed in terms of the non-dimensional volume factor. Further insight into the processes of cleavage formation may be gained by consideration of the actual amounts of material that have moved. The Gresens approach allows one to calculate the absolute amount of material lost or gained. The results of these calculations are listed in appendix 3 and some examples are given in table 6.1. The most convenient way of thinking about the results of these calculations is to consider a mass of 100g of original rock, equivalent in composition to the present lithons. Choosing one of the examples in table 6.1, one can now consider the changes that have occurred in 100g of original rock, which has undergone a volume loss of 69% to become a cleavage domain. Of the 69g lost, almost 68g were SiO_2. If one combines the loss of SiO_2 with the loss of 1.4g of CaO, 1.7g of Na_2O and 0.6g of Fe_2O_3 the total losses amount to almost 72g out of the original 100g. These losses are somewhat counterbalanced by the introduction of 0.72g of MgO and 1.7g of K_2O into this original volume, the net loss amounting to 69g. The most striking aspect of this compositional change is that virtually 100% of the net loss can be accounted for by the loss in SiO_2. Since SiO_2 accounts for approximately 85% of the original volume it is not surprising that it should account for the bulk of the volume loss, especially since quartz is quite soluble under

Table 6.1

LOSS or GAIN (g/100g) of LITHON

f_v	SiO_2	Fe_2O_3	MgO	CaO	Na_2O	K_2O
0.69	-31.47	-0.31	1.10	-0.58	-0.48	0.66
0.51	-48.14	-0.58	0.73	-1.36	-0.66	1.02
0.43	-55.83	-0.52	0.72	-1.32	-1.37	1.37
0.31	-67.98	-0.60	0.79	-1.36	-1.71	1.73

pressure solution conditions (Eugster, 1981). In none of the analyses does the amount of any single component, lost or gained, other than SiO_2, reach 2g. The development of the cleavage, is therefore dominated by the movement of SiO_2. The somewhat simplistic view, taken in an earlier chapter, that the cleavage developed by the solution of quartz and the concentration of micas is therefore substantially correct. The problem lies with the micas, which clearly are not simply concentrated by virtue of quartz loss. Before their role in the cleavage formation can be adequately discussed, the movements of components other than SiO_2 should be considered further.

It can be assumed that the development of the cleavage is a relatively continuous process. Figures 5.1.2 and 5.2.6 show the chemistry of cleavage development, arrested at two different stages. The greater the volume loss, the further the cleavage development has progressed. Since figures 5.1.2 and 5.2.6 show the average chemistry of several cleavage planes, the results of the analyses of individual cleavage planes would show more stages of cleavage development. Unfortunately, the volume factor is a somewhat abstract measure and a comparison of the actual amounts of the components lost or gained would not be very useful, since the original amounts of the components vary greatly. However, a conversion of the actual amounts lost or gained into a percentage lost or gained, with respect to the

original concentration does lend itself to a comparison.

Figures 6.1a-g show the percentage loss or gain of each individual component, versus the volume factor. The data used for these graphs are the analyses of the individual cleavage planes of both Goldenville and Ruth Falls syncline samples.

Figure 6.1a depicts the percent loss in SiO_2 versus the volume factor. It has already been demonstrated that the movement of SiO_2 dominates the volume loss. Figure 6.1a does therefore not graph two independent variables, which explains the well defined trend shown in this graph. The tight clustering around this line does prove, however, that the errors associated with the analyses are quite small, as far as SiO_2 and Al_2O_3, which is used as the volume factor, are concerned.

The percent loss of CaO, with respect to the volume factor (fig 6.1b), is well defined for low volume factor values. Probably due to analytical error and to scarcity of data for high volume factor values the trend is ill defined in the region of high volume factors. It is therefore not clear whether the data should be interpreted as lying on an exponential curve, or as lying on two intersecting straight line segments. The interpretation of the curve as two straight line segments leads to the conclusion that at some time during cleavage development, corresponding to a volume factor of approximately 0.68, a change in the solubility of

Figure 6.1

a - % Loss SiO_2 vs. v.f.

b - % Loss CaO vs. v.f.

c - % Loss Fe_2O_3 vs. v.f.

d - % Loss Na_2O vs. v.f.

e - % Loss MgO vs. v.f.

f - % Loss TiO_2 vs. v.f.

g - % Loss K_2O vs. v.f.

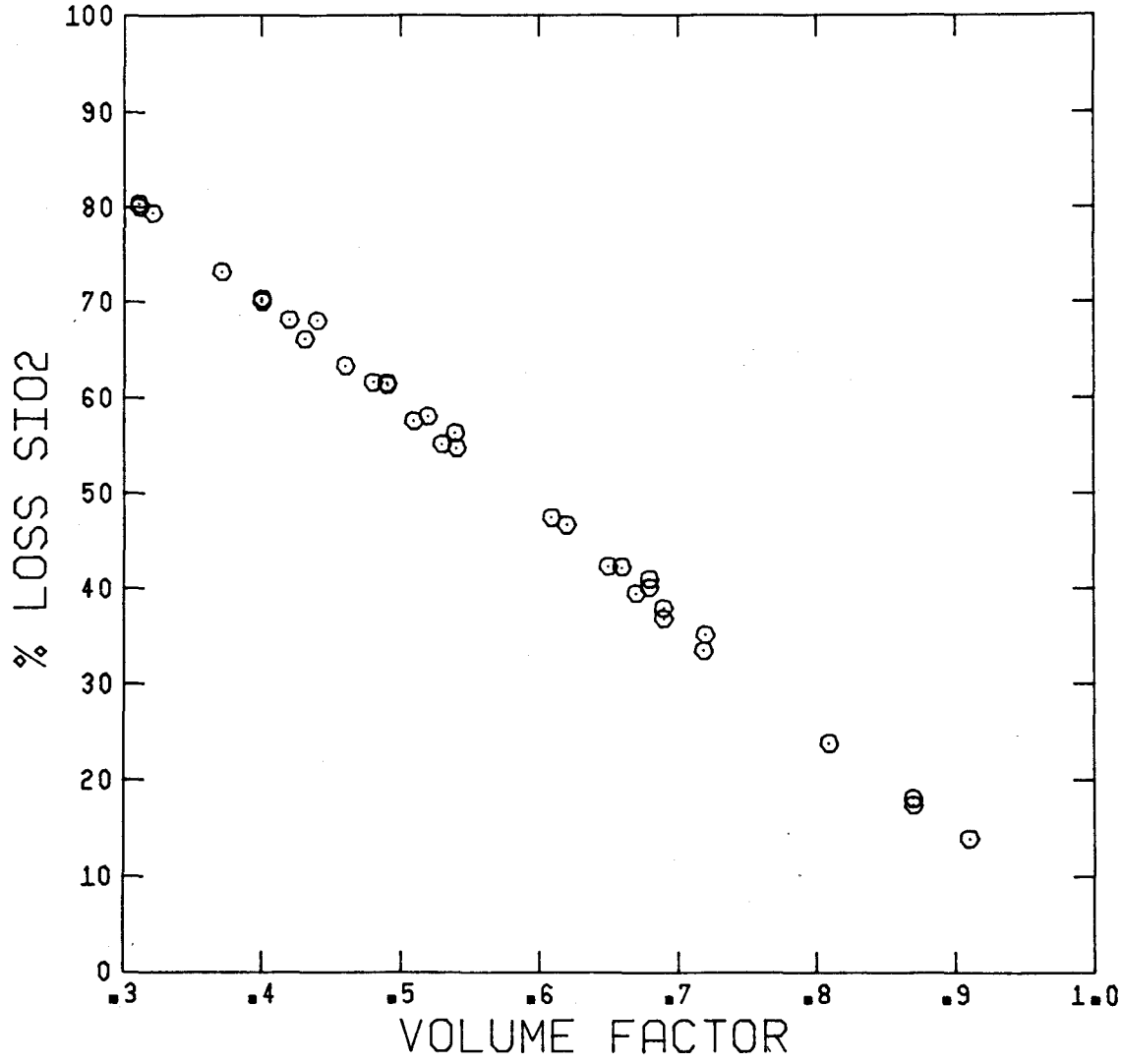
100
90
80
70
60
50
40
30
20
10
0
% LOSS SIO2
.3
.4
.5
.6
.7
.8
.9
1.0
VOLUME FACTOR

6.1a

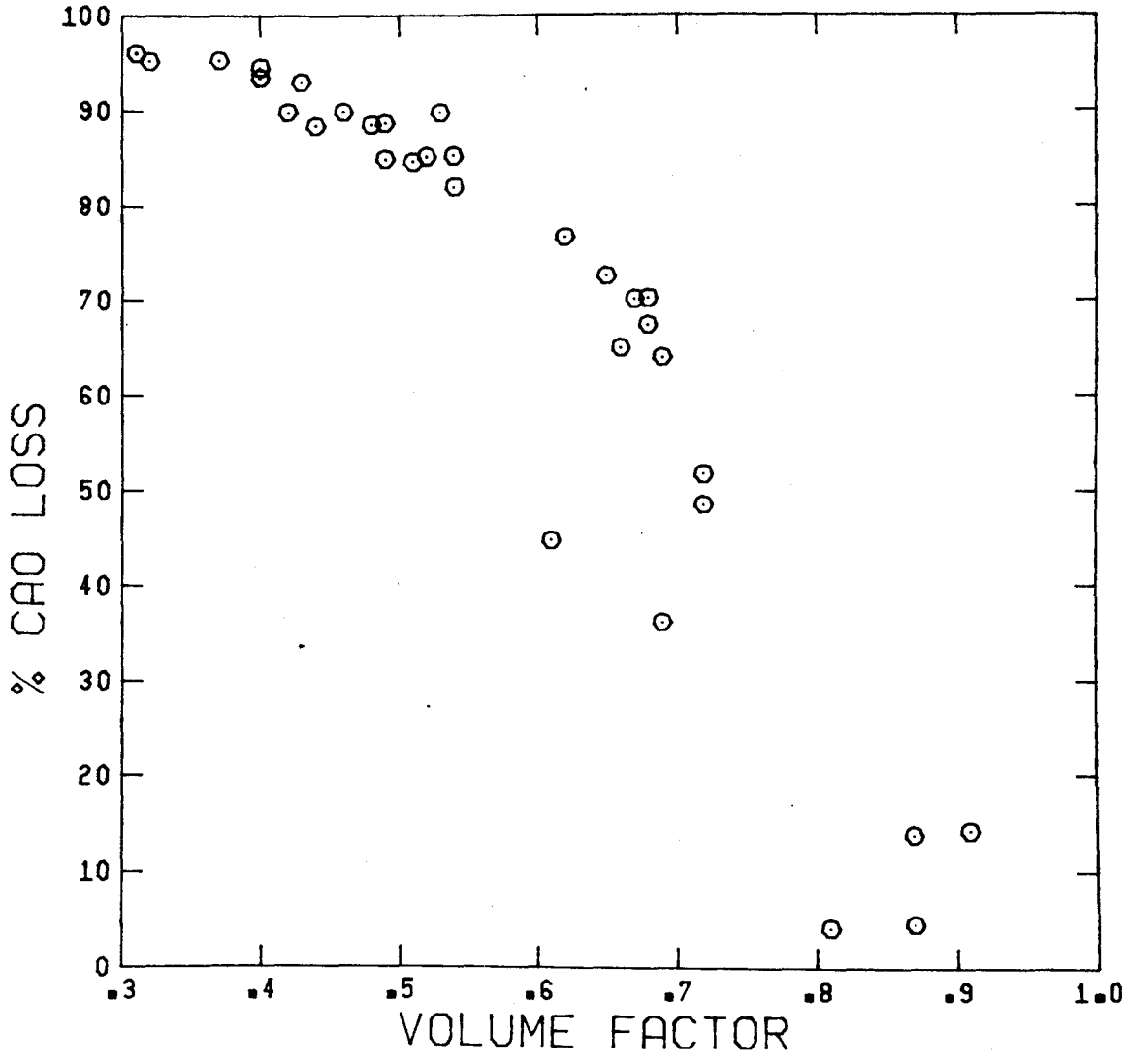
100
90
80
70
60
50
40
30
20
10
0
% CAO LOSS
.3
.4
.5
.6
.7
.8
.9
1.0
VOLUME FACTOR

6.1b

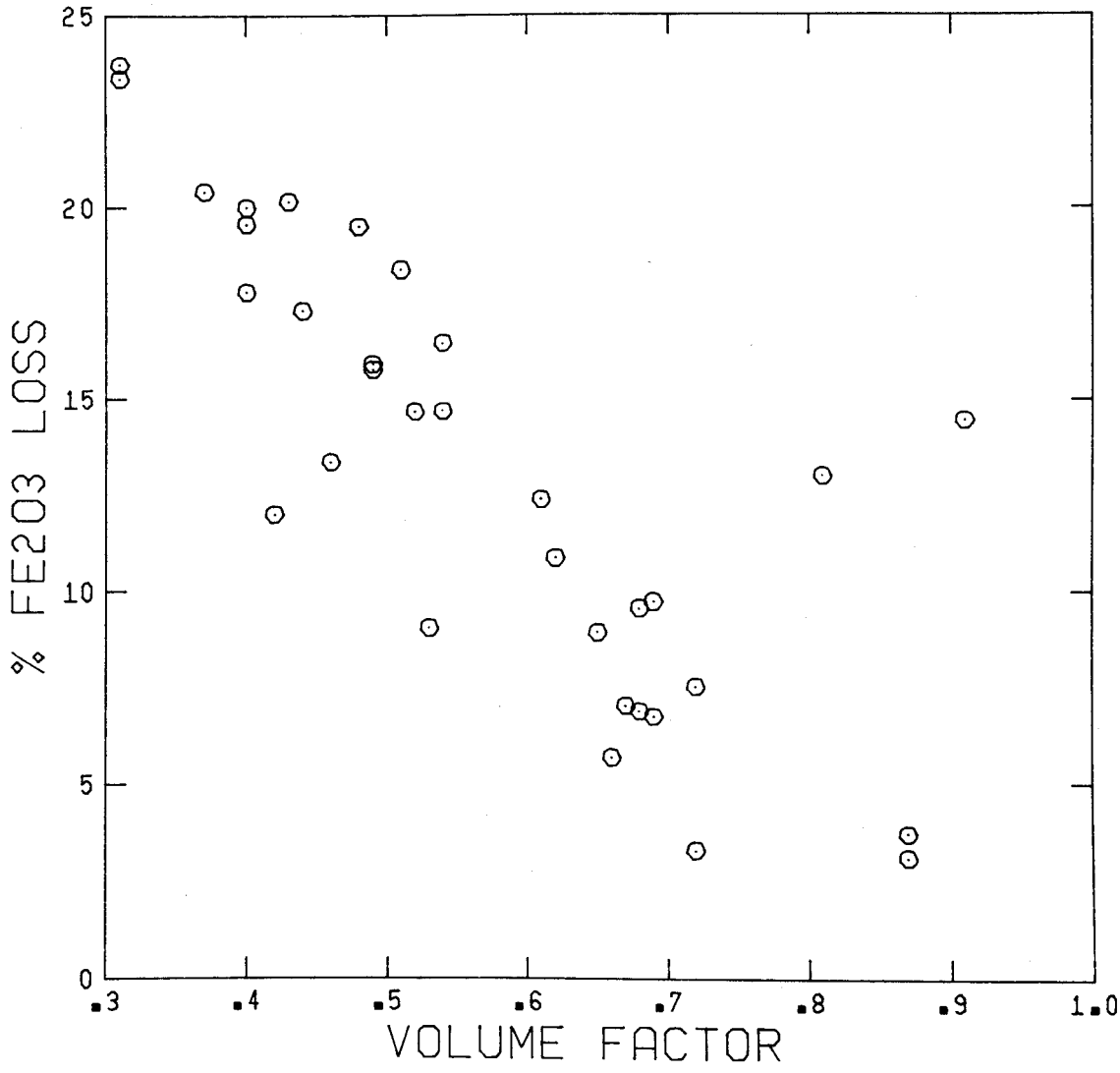

6.1c

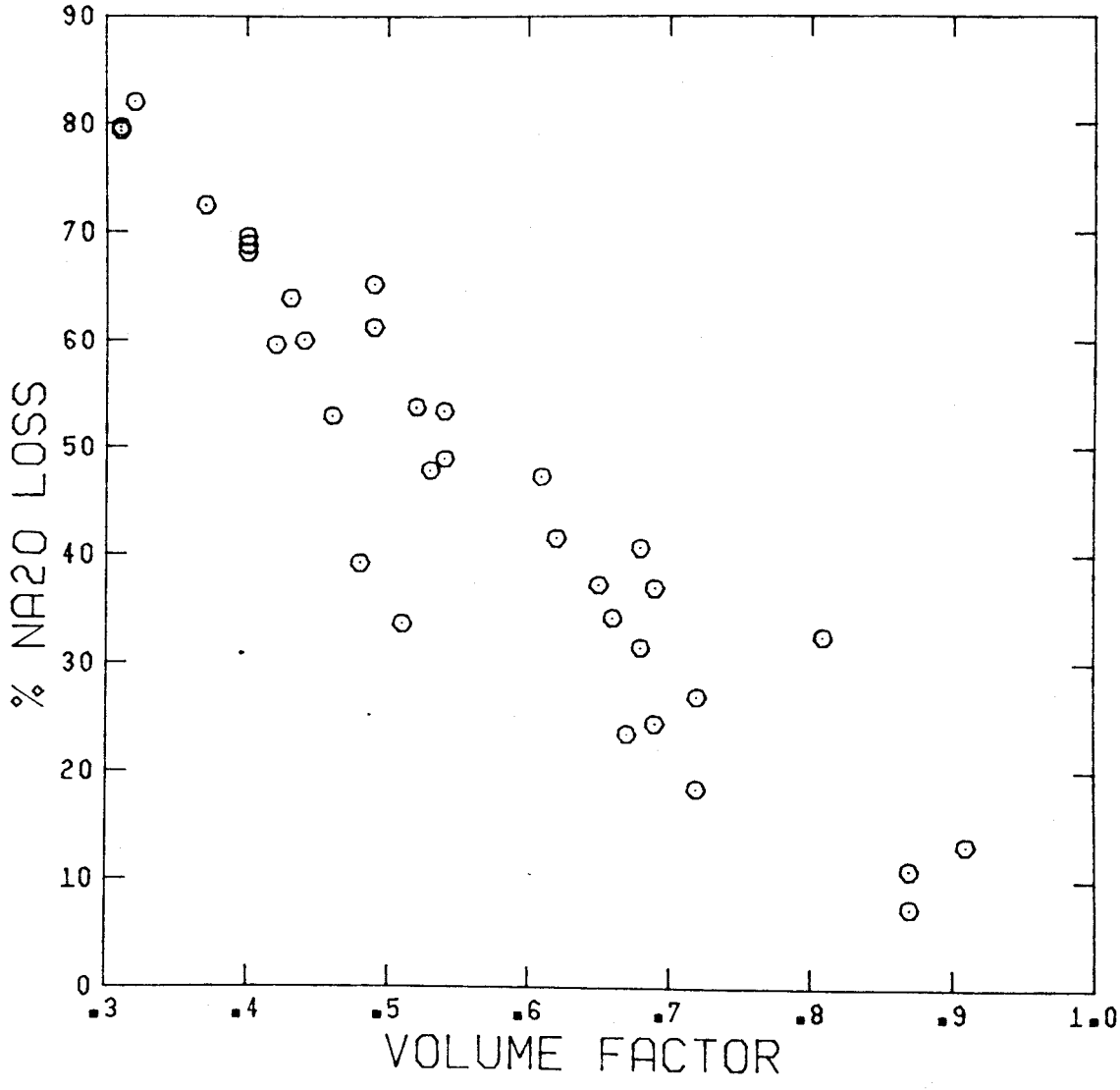

6.1d

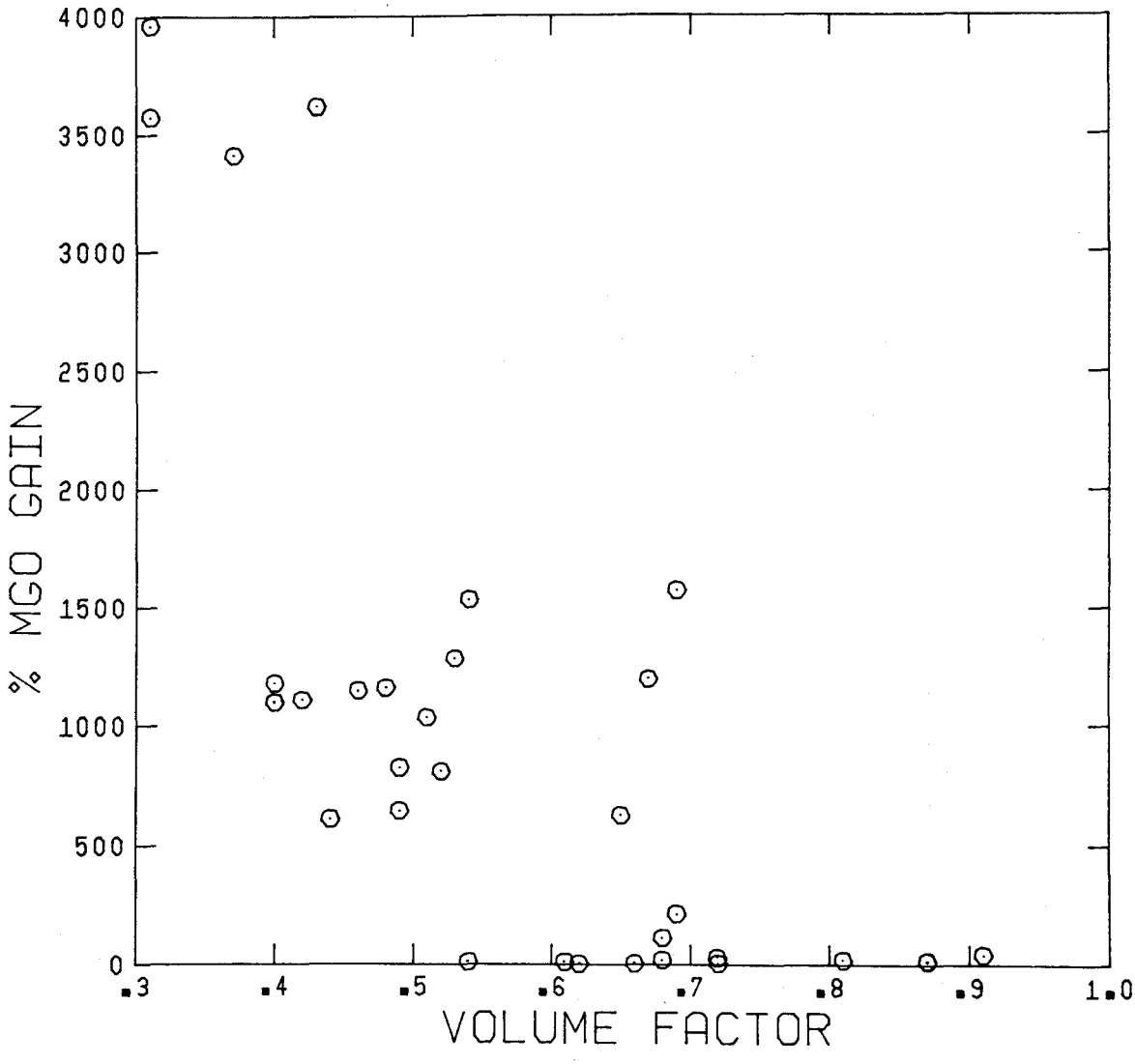
4000
3500
3000
2500
2000
1500
1000
500
0
% MGO GAIN
.3
.4
.5
.6
.7
.8
.9
1.0
VOLUME FACTOR

6.1e

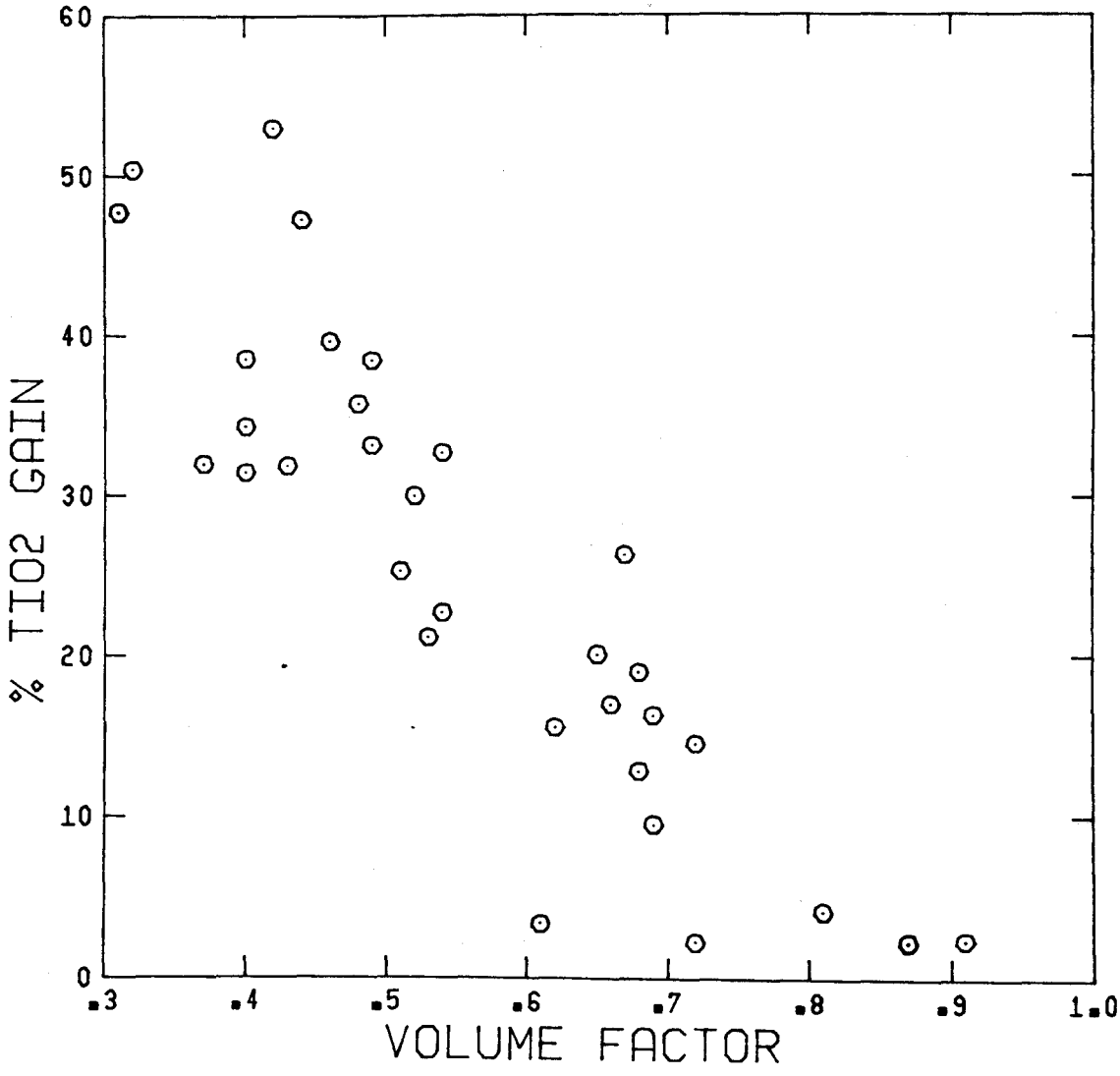

6.1f

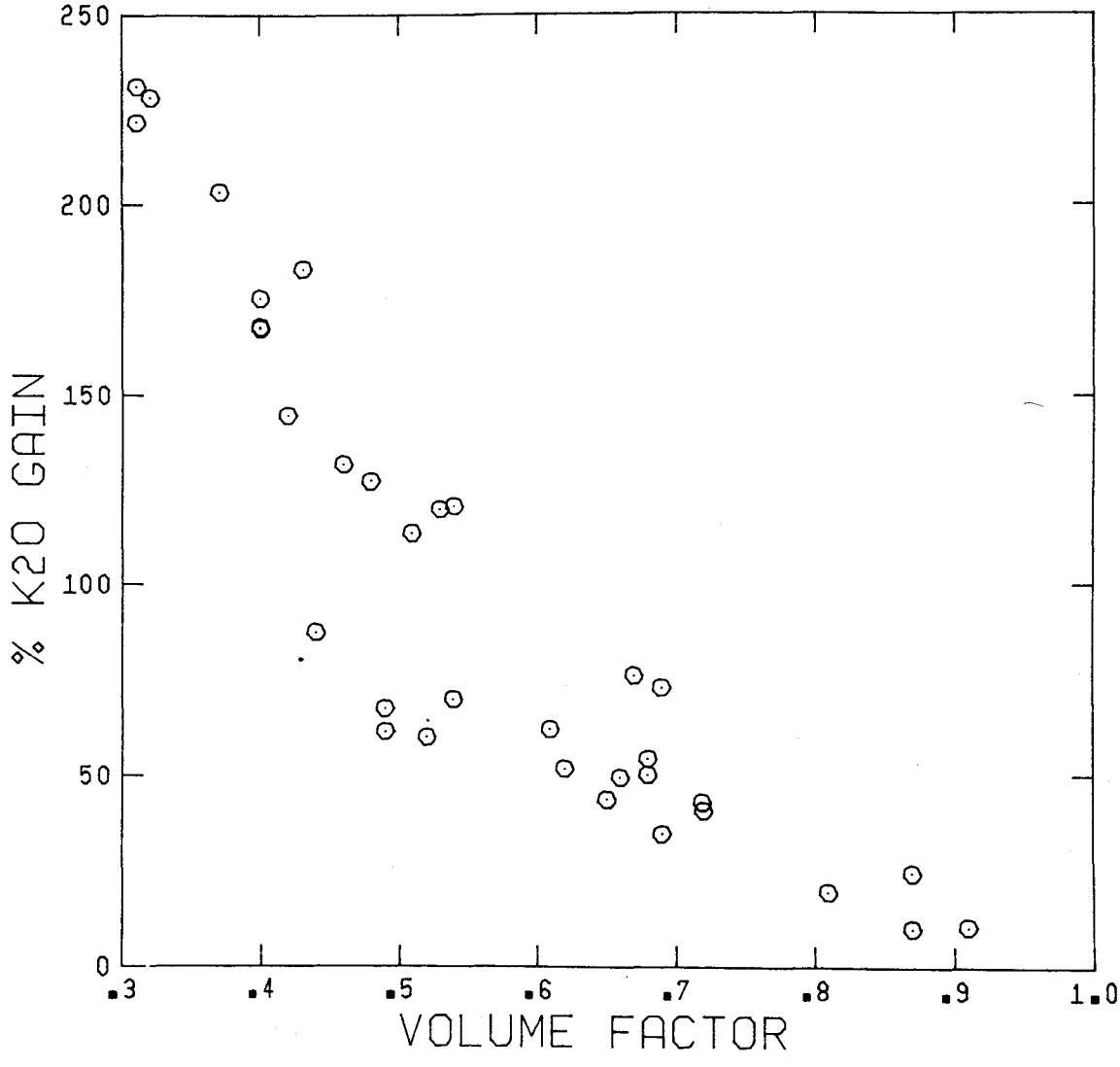

6.1g

CaO occurs. Such a change could be due to a number of factors, including a change in a solution mechanism, the dissolution of a new mineral species or the complete elimination of a mineral. Interpretation of the curve as exponential would mean that the solution of CaO progresses steadily during cleavage development. Since the curve for the loss of SiO_2 and CaO are not the same, the solubility of the relevant minerals (quartz and calcite), are different, regardless of which interpretation is chosen.

The percent loss of Fe_2O_3 versus the volume factor (figure 6.1c), follows a consistent trend, even though a fair amount of scatter is apparent. The scale on which this loss occurs is smaller than those of the previously mentioned oxides, which is not surprising, since Fe_2O_3 is thought to be relatively immobile.

The percent loss of Na_2O versus the volume factor (figure 6.1d), again follows a consistent trend despite some scatter. The remarkable aspect about the trend displayed by Na_2O is that it is the same as that of SiO_2. The interpretation is that any loss of SiO_2 also means a loss of the same percentage of Na_2O with respect to the original Na_2O abundance. It is doubtful that this is a coincidence, especially since comparable behaviour is not displayed by any other oxide. A much more likely interpretation is that the solubilities of SiO_2 and Na_2O in this enviroment are similar, the reasons for which will be discussed in more

detail later.

Figure 6.1e, showing the percent gain of MgO with respect to the volume factor gives no clear trend. The large scatter produced is partially due to large analytical errors at the low abundances of MgO in the lithon, 0.02% to 1.5%. It is possible that the solubility of MgO varies greatly with pressure and temperature or other parameters, or that Mg is hosted by a variety of minerals. Attention should be drawn to the scale of the percent gain, which is on the order of thousands of percent. MgO is clearly very mobile in this enviroment.

The percent gain of TiO_2 with respect to the volume factor (figure 6.1f) follows a consistent trend, with a certain amount of scatter. Compared with MgO and K_2O the scale of these gains is quite small, as can be expected.

Figure 6.1g shows that the gain of K_2O with respect to the volume factor follows a relatively smooth trend. Despite the uncertainty produced by the scatter, the trend does not appear to be linear. The gain in K_2O increases exponentially with increasing volume loss.

Figures 6.1a-g show that the gains or losses of elements with progressive cleavage development are well correlated with volume factors. Possible exceptions, for above mentioned reasons, are MgO and CaO. The similarities displayed by the trends of SiO_2 and Na_2O may point to a connection between these two oxides during cleavage

development. For example, Na is carried in albite, whose dissolution would lead to a loss of both Si and Na. The variation in the trends in the remaining oxides leads to the conclusion that the solubility and migration of each individual component is controlled mainly by the dissolution of a single mineral phase. This gives more support to the notion that the chemical evolution of the cleavage follows certain well defined patterns.

The question which then arises is: how consistent are these patterns? The data examined here come from two locations, geographically approximately 20km apart and from two different geological settings. The samples from both locations appear to be following the same patterns.

A comparison with data coming from outside the Meguma Group is highly desirable. Only one set of chemical data from spaced cleavage planes and lithons has been published. Glasson and Keays (1978) attempted to estimate the amount of Au, Ag, As, Sb, Cu and Zn that has been released from the sedimentary rocks of the slate belt of Central Victoria, Australia, during metamorphism and spaced cleavage development. For this purpose, they analysed spaced cleavage planes and lithons in siltstones and greywackes. The amount of Au, etc., released, was estimated by assuming that Ti, Zr, Y and Ir were the immobile species. The authors concluded that the amount of Au released from the sediments is less than the amount of Au found in the local Au

deposits. No Gresens calculations were attempted in this study.

The Victoria Slate Belt greywackes average 65% quartz, 15% albite, 10% white micas, 5% chlorite and minor amounts of sulphides, carbonate, kaolinite and rock fragments. They therefore differ from the Goldenville greywackes by having a higher feldspar content, a lower percentage of white micas and no biotite. There is also no kaolinite present in the Goldenville greywackes. Judging by the photographs and descriptions of Glasson and Keays, the fabrics of the Australian and Goldenville greywackes are very much alike. The Australian greywackes therefore seem to be suitable for a chemical comparison of the cleavage forming process with the Goldenville samples.

Differences in the modal analyses are reflected in the chemical compositions of the lithons. The Australian lithons show 1.8 wt% to 2.5 wt% MgO, which is higher then any values of Goldenville lithons, wheras the CaO content of the Australian lithons, at 0.2 wt%, is considerably below that of Goldenville lithons. Assuming a cleavage/lithon density ratio of unity, the volume factors of all components of the Australian greywackes can be calculated (appendix 7) and graphed. The results are shown in figure 6.2.

At fist glance few similarities appear between the Australian and Goldenville greywackes. K_2O shows the smallest volume factor and Na_2O the largest, for both the

Figure 6.2

Volume factors of Australian greywackes and siltstones.

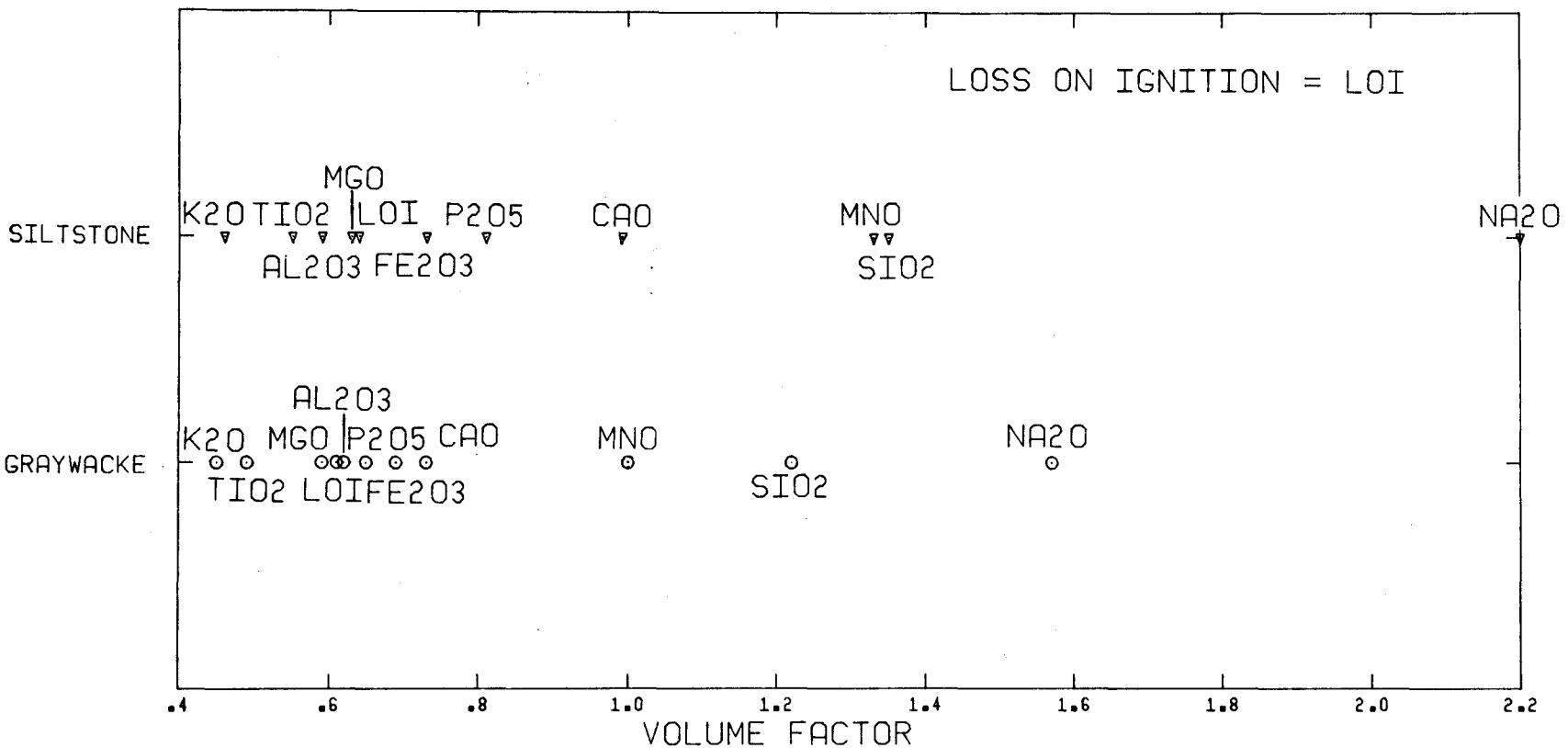
LOSS ON IGNITION = LOI
SILTSTONE
MGO
K2O TIO2 LOI P2O5
CAO
MNO
NA2O
AL2O3 FE2O3
SIO2
AL2O3
GRAYWACKE
K2O MGO P2O5 CAO
MNO
NA2O
TIO2 LOI FE2O3
SIO2
.4
.6
.8
1.0
1.2
1.4
1.6
1.8
2.0
2.2
VOLUME FACTOR

Australian siltstone and greywacke. CaO falls to the left of MnO, MgO plots very close to Al_2O_3 and Fe_2O_3 and P_2O_5 change their relative positions in the two lithologies. These are obvious differences from the Goldenville analyses. However, there are certain similarities. The relative sequence of K_2O, TiO_2, Al_2O_3, Fe_2O_3, MNO and SiO_2 found in the Goldeville samples is present in the Australian analyses as well. The relatively tight clustering of TiO_2, Al_2O_3 and Fe_2O_3, even though not as well defined as in the Goldenville samples, can still be used to determine the volume factor. MgO, plots very close to Al_2O_3 and can be considered as a relatively immobile oxide in the Australian samples. The earlier mentioned differences can be explained at least in part by the differences in the mineral components. The CaO content of 0.22% is probably largely contained in a mineral species less soluble than calcite, in this case albite. It is therefore not as easily released during cleavage development and only shows relatively small percent losses. It is likely that a significant portion of the MgO content of the Australian samples is in the chlorites. In the Goldenville samples, modal analyses (Thompson, 1984) show no significant increase in the chlorite content from the lithon to the cleavage. It may be that MgO only appears to be very mobile in the Goldenville samples because the lithons are virtually devoid of MgO. It has already been mentioned that the large scatter in figure 6.1e, showing the percent gain

of MgO with respect to the volume factor, may be due partially to the large variation in the original MgO abundances. Why and how MgO mobility is linked to its abundance in such a way is not known. The extensive loss of Na_2O can be correlated with the breakdown of albite in the cleavage planes, which is described by Glasson and Keys.

The similarities between the Australian and the Goldenville samples are that TiO_2, Al_2O_3 and Fe_2O_3 are relatively immobile, CaO, MnO, SiO_2 and NaO are lost from the cleavage plane, while K_2O is introduced into the cleavage plane during its development. The chemical evolution of spaced cleavage zones in these two samples progressed therefore along very similar chemical migration lines. The chemical migration patterns found are not accidental, but must be linked with the development of a cleavage.

7. Cleavage Evolution

This chapter will present a model for the development of the spaced pressure solution cleavage in the Megma Group greywackes. The model is based on observations made in the Meguma Group, as well as on the views published in the current literature.

Any model should start by considering what effect diagenesis may have had on the greywackes. Unfortunately nothing can be said about the possible changes which the original clays may have undergone during diagenesis. However, something can be said about porosity changes in the greywackes during diagenesis. If a significant porosity reduction had occurred during diagenesis, it would probably manifest itself through large amounts of quartz overgrowths. These quartz overgrowths would be oriented either randomly or with a preferred horizontal orientation, ie., attached to the vertical sides of the grains. All quartz overgrowth found in the greywackes studied show a tectonic alignment parallel to cleavage. Originally, this alignment will have had a preferred orientation perpendicular to bedding, with the quartz overgrowths attached to the bedding- parallel sides of the grains. In view of the relatively pristine character of the lithons, it seems unlikely that all signs of a significant porosity reduction due to diagenetic

overgrowths could have been destroyed during subsequent deformation. At the onset of deformation, the greywackes had therefore still retained a large percentage of their porosity. The deformation began with the major principal stress, σ_1, being roughly horizontal. This stress caused solution at grain contacts in localised areas within the greywackes.

It is important to understand the role pressure and contact area play during pressure solution. If one considers an effective pressure

$$P'=P-PW$$

to be acting on a volume of greywacke, where P may be the lithostatic pressure during burial or the major principal stress during deformation and PW represents the hydrostatic pressure, then P' has to be integrated over the area of grain contacts, to give an "effective force", F', across those contacts. For a circular contact between two grains

$$<P'>=4/pia2F'$$

where <P'> is the average effective pressure and a the diameter of the contact area. The effective force F' at the contacts therefore decreases as the area of the contacts increases, assuming a relatively constant <P'>. Since the chemical potential driving the solution process is linked to the effective force (Robin, 1978), the chemical potential gradient between the stressed contact area and the stress free areas of the grain decreases with increasing contact area. Pressure solution should

should therefore slow down as grain contacts are enlarged.

Fletcher's (1981) anticrack model for solution surfaces in homogeneous rocks leads to a stress concentration at solution surface tips. However, in a grain aggregate, such as the Meguma greywackes, the solution surface tips of the grain contacts are surrounded by pore space. The strain taken up by the solution along grain contacts may also well be acommodated by the slippage of neighbouring grains past each other. It is therefore not likely that an anticrack type stress concentration would play a significant role at furthering solution at this stage. With the enlargement of grain contacts, the solution of quartz slows down and the amount of strain taken up by the solution decreases. Smaller grain contacts in other areas should therefore begin to dissolve and take up strain. Grain to grain contact solution should therefore sweep through the rock and a continuous grain cleavage should develop, but no spaced cleavage. Since a spaced cleavage has developed, other factors must play an important part in its evolution.

In the original rock, quartz grains were probably surrounded by a matrix of fine quartz grains and clays. As the grain contacts dissolved, the matrix concentrated and the original clays recrystallized into micas. It is during this transformation that the chemical migrations discussed earlier took place. Beach (1979) has discussed possible

reactions, which may take place during cleavage development. The breakdown of albite, considered to be very important by Beach, cannot play a large role here, since its modal abundance is too low. However, some reactions cited by Beach, such as the transformation of mixed illite-montmorillonite to chlorite or muscovite, are probably appropriate here. The formation of chlorite may actually start during diagenesis. The reactions are: mixed illite-montmorillonite to chlorite

$$6Ca_{.5}(Na,K)_{.5}Al_3MgSi_{7.5}Al_{.5}O_{20}(OH)_4 + 25.5Mg^{2+} + 37H_2O \longrightarrow 3.5Mg_9Al_3Si_5Al_3O_{20}(OH)_{16} + 3Ca^{2+} + 3(Na,K)^{+} + 42H^{+} + 27.5SiO_2$$

mixed illite-montmorillonite to muscovite

$$6Ca_{.5}K_{12}Al_3MgSi_{7.5}Al_{.5}O_{20}(OH)_4 + 4K^{+}\ 14H^{+} \longrightarrow 3.5K_2Al_4SI_6Al_2O_{20}(OH)_4\ 3Ca^{2+}\ 6Mg^{2+} + 12H_2O + 24SiO_2$$

The formation of chlorite depends on an introduction of Mg^{2+}, the formation of muscovite on the introduction of K^{+}. Chlorite formation leads to a release of Na^{+} or K^{+}, muscovite formation to a release of Mg^{2+}. Both reactions release Ca^{2+} and SiO_2. Considering the composition of the cleavage plane, the formation of muscovite must be the predominant reaction. The formation of muscovite according to the above stated reaction also increases the pH of the pore fluid. This has a great effect on the solubility of silica, which increases at a pH greater than 8.5 through

dissociation of H_4SiO_4 (Beach, 1979). The presence of Na^+ will also increase the solubility of SiO_2 through the formation of sodium-silica complexes, such as Na_2Si2O_5. This complexing with Na may produce solubilities of silica of approximately 70,000ppm at 250°C, decreasing to zero at 350°C (Row et al., 1967). The temperature is therefore important. Fluid inclusion temperatures of quartz veins emplaced into the rock very early (Graves, 1976) range from 180°C to300°C.

Even though the above stated reactions are merely crude examples, they are probably relevant, as is shown by the loss of NaO_2 and the introduction of MgO and K_2O to the cleavage planes. It is impossible to deduce the exact reactions, since the compositions of the original clays are not known.

The main point of these speculations is that the growth of micas enhances the solubility of SiO_2 and therefore the solution of quartz. It should be noted that the quantities of SiO_2 released by the formation of the micas (see equations) are considerably less than the amount of SiO_2 that is released by the solution of quartz. The solution of quartz along grain contacts, which should have slowed down due to the enlargement of the contact areas, therefore may continue, aided by the chemical changes of the matrix. Some thought should be given to the question why these changes do not aid solution throughout the rock. It

may be that the concentration of the clays in the local area of grain contact solution is responsible for the setting up of an area of concentrated chemical influence, whereas ion concentrations in the lithons are simply too dispersed to influence quartz solution.

The micas grow with their basal planes mostly oriented perpendicular to the major principal stress. Follet (1965) has shown that different crystallographic faces of kaolinite crystals have different charges. The strongest charge is located at the edges of the basal planes, the 110 and 010 faces. It is reasonable to assume that the same applies to muscovite and chlorite crystals. The alignment of micas in the cleavage plane, therefore leads to the development of a "strongly" charged region in the area of the highest concentration of the 110 and 010 mica faces. If the cleavage plane is viewed as having a disk shaped geometry, the "strongly" charged area will be along the edge of the disk. The highest concentrations of free ions can also be expected in this area. Since the concentrations of ions as well as the strength of the charge have to decrease with distance from this area, the cleavage plane edge can be said to be surrounded by a chemical reaction halo which decreases in strength with distance (figure 7.1). This halo is responsible for increasing the solubility of quartz at the cleavage plane boundary. The further development of the cleavage plane takes place where this halo is the strongest,

Figure 7.1

Chemical reaction halo

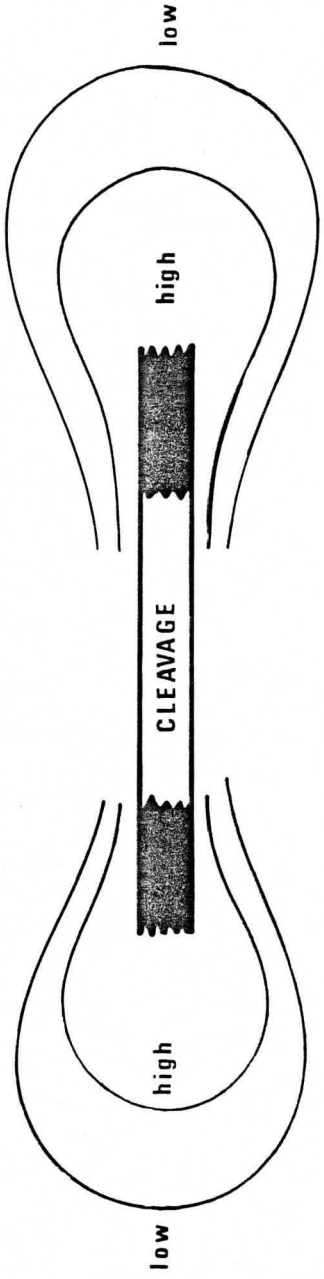
low
high
CLEAVAGE
high
low

at the edge of the cleavage plane. This may explain why even very thin cleavage planes can be continuous over great distances. Cleavage planes also widen, though their width is always very much less than their length. Their edgewise propagation must therefore take place at a greater pace than their widening. It is also possible that, as the growing cleavage plane takes up considerable strain, a Fletcher type anticrack stress concentration develops at the edge of the cleavage plane. The geometry of this stress envelope would be analagous to the proposed chemical halo (Figure 7.2).

Individual cleavage planes almost certainly start as small, unconnected disk shaped structures but in the rock form a connecting network. How then does this network form?

In the Meguma rocks and in many other cases, the cleavage planes actually curve into each other to form the intersections of the rhombs. This would not be expected from the intersection of cleavage planes growing as rectiplanes. Cleavage planes intersecting with each other while following original zones of weaknesses could produce intersections of almost any geometry. However, the majority of cleavage plane intersections show the characteristic curvature towards each other. The above mentioned model offers a possible explanation for this.

A cleavage plane propagating through the rock will have a chemical halo and possibly a stress halo, both of which will be strongest at the cleavage plane margin. As

Figure 7.2

Stress Halo (Stress trajectories at cleavage tip are shown)

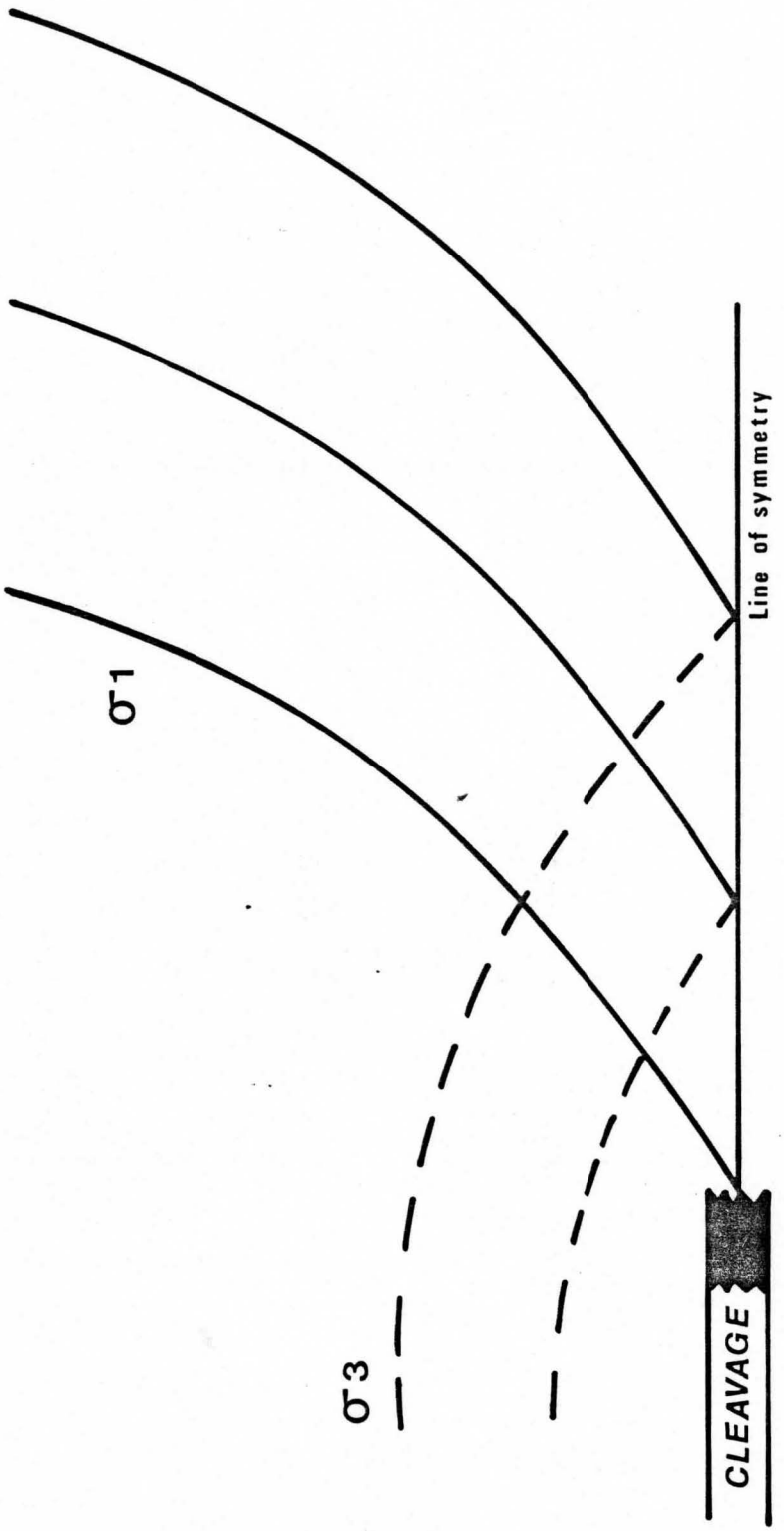
σ1
σ3
Line of symmetry
CLEAVAGE

cleavage planes approach each other, their halos will intersect. This may create an area favourable to dissolution of quartz, which is oriented obliquely to the major principal stress. As solution occurs in this area, the cleavage planes link up (figure 7.3).

The variation in the spacing and intensity of the cleavage planes is dependent upon a number of factors. The magnitude of the stress involved, as well as the time during which the stress is applied, play a large role. The more intense cleavage in the core of the folds may be the result of stress acting on a cleavage which remains in a consistently favourable orientation for a long time. The rotation of the limbs not only took up a lot of strain, but also rotated the cleavage in the limbs away from the major principal stress. Both of these factors may have caused the cleavage development in the limbs to cease. The alignment of the grain cleavage with the spaced cleavage suggest that cleavage development in the limbs stopped early and that the limbs rotated as a single unit.

Another important question is that of material transport. It has been shown that large amounts of material were lost during cleavage development and that most of this material were lost from the greywackes. It is generally agreed that the material removed by pressure solution is transported by a fluid. Pathways must be the cleavage , the lithon or both.

Figure 7.3 Joining of Cleavage Planes

top - chemical halo interaction

bottom - Interaction of stress halos. Solution occurs where the two σ_1 stress trajectories vectorially add up to maximum values.

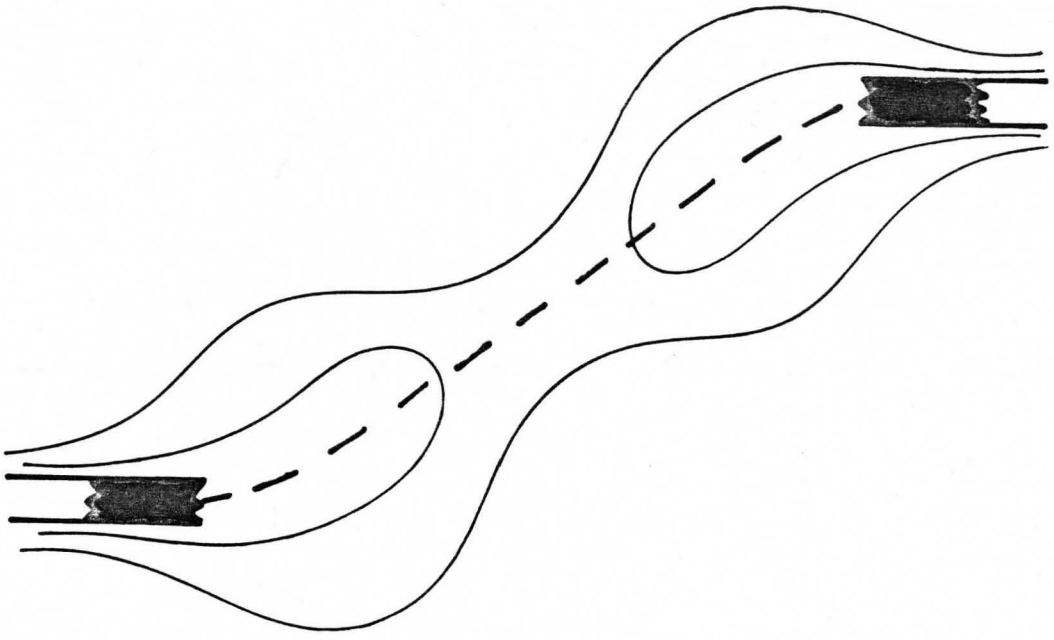

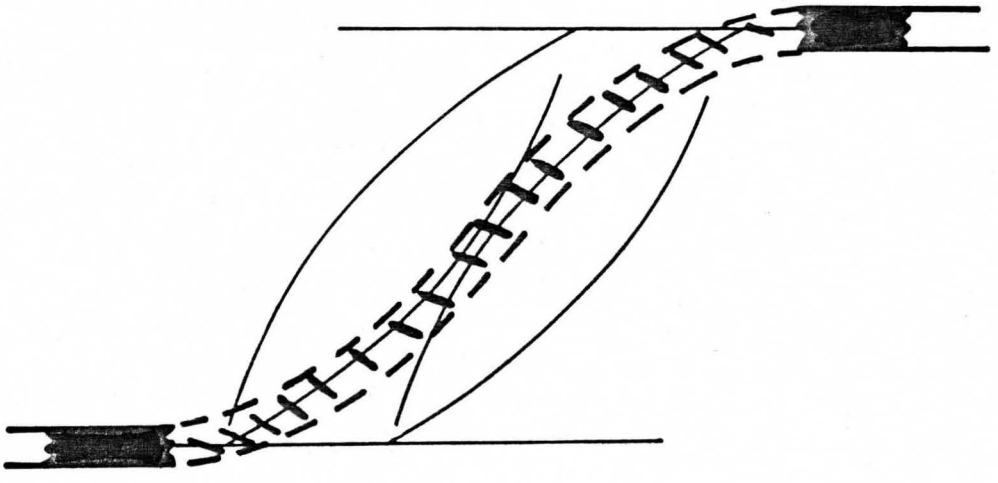

It has already been stated that the greywackes still possessed porespace at the start of deformation. In the greywacke and slate sequence of the Meguma, the greywackes were definitely the fluid reservoir after compaction. Porosity is reduced in the area of grain contact solution. DeBoer (1979) and Rutter (1976) argue for the presence of a thin fluid film, a layer of adsorbed water, between the surfaces of stressed grain boundaries. DeBoer shows that high supersaturations can occur inside the stressed grain-to-grain contacts, but not outside. Rutter's experiments demonstrate that rapid diffusion of solution can occur in the pores, but that diffusion is much slower on stressed contacts. The difference in the rates of diffusion in these experiments, between diffusion through pores and diffussion through stressed contacts was a factor of one million. One more factor is the larger volume of fluid in the lithons compared with the cleavages. Even taking into account the high levels of supersaturation that can occur in the cleavage, the timespan needed to transport a volume of material through the cleavage , would be vastly greater than the time needed to move the same volume through the lithon. Since large amounts of material have been lost from the greywackes, it seems much more likely that most of the diffusion has been through the lithons.

Robin (1979) showed that as long as interlayer diffusion between quartz and mica rich layers is possible,

mobile material migrates to the quartz rich layer. That dissolved material moves into the pore space of the lithon can further be demonstrated if one considers the early stages of cleavage development. Cleavage planes initiate as unconnected plate shaped structures. The dissolved material therefore has to reach the open pore space of the lithon since it has nowhere else to go. The thin fluid layer between the stressed contacts therefore serves to channel the dissolved material to the open pore space of the lithon. The high concentration gradient between the supersaturated fluid of the stressed contacts and the fluid in the lithon will drive dissolved material into the lithon. As long as the lithons are porous and permeable, large scale migration of material dissolved in a fluid will be along the lithons and not the cleavage planes. Only when the porespace and permeability of the lithon has been significantly reduced, does migration through the lithon stop. It is possible that this happens when the cleavage network is fully developed. A lithon bounded everywhere by cleavage planes would be cut off from large scale fluid migrations, defined as being on the order of cm. It is probable that the pore space in the lithon is then reduced by local solution and redeposition. Any subsequent large scale migration of material would be very much slower than migration through the lithon.

8. Conclusions

The chemical evolution of the spaced cleavage follows well defined patterns. The bulk of material removed from the cleavage consists of SiO_2. However, minor amounts of Na_2O, MnO, P_2O_5, Pb, Sr, Nb and Y are also consistently lost from the cleavage. MgO, K_2O, W, Ba and Rb are introduced into the cleavage during its formation, as a result of the crystallization of micas. Al_2O_3, TiO_2, Fe_2O_3 and Zr remain relatively immobile during cleavage formation. These patterns appear to be equally well defined for major and trace elements. The model presented for the cleavage development acounts for the behavior of some of these elements. Dissolution of quartz, carbonate and albite result in the removal of SiO_2, CaO and Na_2O. The crystallization of micas in the cleavage accounts for the introduction of the above mentioned elements into the cleavage planes. The migrations of these elements certainly aid the development of a spaced cleavage, and may be vital for the development of such a cleavage. A comparison with the only other set of data available in the literature, from the slate belt in Central Victoria, Australia, shows a number of similarities. In both the Australian and the Meguma samples SiO_2, CaO, Na_2O and P_2O_5 has been lost from the cleavage, K_2O has been introduced into the cleavage and TiO_2, Al_2O_3 and Fe_2O_3 have

remained relatively immobile. Much more analytical work has to be done on different types of spaced cleavages before the role of all chemical components can be defined. No specific explanations can be offered for the behaviour of some chemical components, such as MnO, P_2O_5 and MgO. This applies especially to the behaviour of some trace elements, namely Au, Sb, As, Ce, Nd and La.

Despite the amount of work that still needs to be done to understand spaced cleavage development, the suggestion may be made that the term pressure solution cleavage is somewhat of a misnomer. Although the cleavage development is undoubtedly initiated by pressure solution at grain contacts, subsequent chemical reactions affecting the solubility of quartz, may play a major role in the development of the cleavage.

REFERENCES

Alvarez, W., Engelder, T., Geiser, P.A. (1978); Classification of solution cleavage in pelagic limestones. Geology, v. 6, pp 263-266.

Beach, A. (1979); Pressure solution as a metamorphic process in deformed terrigenous sedimentary rocks. Lithos, v. 12, pp 51-58.

Boulter, C.A. (1979); On the production of two inclined cleavages during a single fold event; Stirling Range, S.W. Australia. Jour. Struct. Geol., v. 1, pp 207-219.

Clifford, P.M., Crocket, J.H. and Fueten, F. (1983); Distribution and localizaion of gold in Meguma Group rocks, Nova Scotia. Part 1: structural effects and pressure solution preliminary results. Geol. Surv. Canada Paper 83-1B, pp 279-285.

Crocket, J.H., Clifford, P.M., Fueten, F. and Kabir, A. (1983); Distribution and localizaion of gold in Meguma Group rocks, Nova Scotia. Part 2: implications of background geochemistry and cleavage development - a preliminary report. Geol. Surv. Canada Paper 83-1B, pp 285-291.

Cosgrove, J.W. (1976); The formation of crenulation cleavage. Jour. Geol. Soc. London, v. 132, pp 155-178.

de Boer, R.B. (1977); Pressure solution: theory and experiments. Tectonophysics, v. 39, pp 287-301.

Durney, D.W. (1972); Solution transfer, an important geological

deformation mechanism. Nature, v. 235, pp 315-317.

Engelder, T. and Geiser, P. (1979); The relationship between pencil cleavage and lateral shortening within the Devonian section of the Appalachian Plateau, New York. Geology, v. 7, pp 460-464.

Faribault, E.R. (1893); Geogan Sheet. Geol. Surv. Canada, Map 382.

---------- (1895a); Moser's River Sheet. Geol. Surv. Canada, Map 551.

---------- (1895b); Liscomb River Sheet. Geol. Surv. Canada, Map 550.

---------- (1896); Tangier Sheet. Geol. Surv. Canada, Map 565.

---------- (1897a); Sheet Harbour Sheet. Geol. Surv. Canada, Map 592.

---------- (1897b); Fifteen-mile Stream Sheet. Geol. Surv. Canada, Map 607.

Eugster, H.P. (1981); Metamorphic solutions and reactions. Phys. Chem. Earth, v. 13 and 14, pp 461-507

Fletcher, R.C. and Polland, D.D. (1981); Anticrack model for pressure solution surfaces. Geology, v. 9, pp 419-424.

Follett, E.A.C. (1965); The retention of amorphous, colloidal 'Ferric Hydroxide' by Kaolinites. Jour. Soil Sci., v. 16, pp 334-341.

Gibbs, J.W. (1906); The Scientific Papers of J. Williard Gibbs, Volume 1 in Thermodynamics. Longmans, Green and Co., 434p.

Glasson, M.J. and Keays, R.R. (1978); Gold mobilization during cleavage development in sedimentary rocks from the Auriferous Slate Belt of Central Victoria, Australia: some important boundary conditions. Econ. Geol., v. 73, pp 496-511.

Gresens, R.L. (1967); Composition-volume relationships of metasomatism. Chem. Geol., v. 2, pp 47-65.

Gratier, J.P. (1983); Estimation of volume changes by comparative chemical analyses in heterogeneously deformed rocks (holds with mass transfer). Jour. Struct. Geol., v. 5, pp 329-359.

Gray, D.R. (1978); Relationship of crenulation cleavage to finite and incremental strain. Geol. Soc. America Bull., v. 89, pp 577-590.

Griffiths, J.C. (1967); Scientific method in analysis of sediments, in International Series in the Earth and Planetary Sciences. McGraw-Hill Book Company, New York, 508p.

Henderson, J.R. (1983); Analysis of structure as a factor controlling gold mineralization in Nova Scotia. Geol. Surv. Canada Paper 83-1B, pp 13-47.

Parkash, B. (1969); Depositional mechanism of greywackes, Cloridorme Formation (Middle Ordovician), Gaspe, Quebec. unpubl. Ph.D. thesis.

Pryer, L.L. (1984); Strain Measurements from deformed quartz grains in metagreywackes of the Goldenville Formation,

Robin, P.Y.F. (1978); Pressure solution at grain to grain contacts. Geochim. Cosmochim. Acta., v. 42, pp 1383-1389.

Robin, P.F. (1979); Theory of metamorphic segregation and related processes. Geochim. Cosmochim. Acta., v. 43, pp 1587-1600.

Rutter, E.H. (1976); The kinetics of rock deformation by pressure solution. Phil. Trans. Roy. Soc. London, A., v. 283, pp 203-219.

Sorby, H.C. (1863); Uber kalkstein-geschibe mit eindrucken. Jahr. F. Miner., pp. 801-807.

---------- (1908); On the application of quantitative methods to the study of the structure and history of rocks. Geol. Soc. London, Quarterly Journal, v. 64, pp 171-232.

Thompson, M.J. (1984); A petrographic study of pressure solution cleavage in metagreywackes of the Goldenville Formation, Meguma Group, Nova Scotia. unpubl. B.Sc. thesis, 50p.

Trurnit, P. (1968); Pressure solution phenomena in detrital rocks. Sed. Geol., v. 2, pp 89-114.

Williams, P.F. (1972); Development of metamorphic layering and cleavage in low grade metamorphic rocks at Bermagui, Australia. Amer. Jour. Sci., v. 272, pp 1-47.

Appendix 1

Ruth Falls syncline Gresens calculations

vf = volume factor

x = absolute amount lost or gained

x% = percent lost or gained

Sample F5A

	Al	Si	Fe	Mg	Ca	Na	K	Ti	Mn	P
Lithon	12.12	74.58	4.49	1.53	1.03	2.03	1.93	0.057	0.08	0.12
1C vf	0.87	1.05	0.90	0.75	1.01	0.94	0.79	0.89	0.89	1.00
2C	0.87	1.06	0.84	0.74	0.91	0.98	0.70	0.85	0.89	1.09
1C X		-12.98	-0.17	0.24	-0.14	-0.15	0.19	-0.013	-0.0017	-0.016
%X	0.87	-17.41	-3.70	15.43	-13.84	-7.43	9.99	-2.32	-2.13	-13.0
2C X		-13.49	0.14	0.28	-0.048	-0.22	0.47	0.013	-0.0017	-0.024
%X	0.87	-18.09	3.08	18.27	-4.55	-10.86	24.41	2.26	-2.13	-20.25

Sample F14

Lithon	12.22	74.35	4.46	1.41	1.04	2.19	2.07	0.56	0.12	0.09
vf	0.91	1.06	0.80	0.64	1.06	1.05	0.83	0.89	1.00	1.13
X		-10.37	0.65	0.61	-0.15	-0.29	0.21	0.013	-0.11	-0.017
%X	0.91	-13.95	14.46	43.28	-14.25	-13.16	10.34	2.38	-9.0	-19.11

Sample A49

Lithon	9.89	78.48	3.00	1.39	1.72	1.87	1.26	0.50	0.08	0.08
vf	0.72	1.08	0.74	1.02	1.50	0.89	0.50	0.70	1.14	0.67
X		-26.25	-0.098	-0.40	-0.89	-0.34	0.54	0.011	-0.030	0.0064
%X	0.72	-33.45	-3.28	-29.04	-51.86	-18.37	42.86	2.24	-37.0	8.0

Sample A1

Lithon	9.58	79.89	2.96	1.26	0.84	2.04	1.86	0.49	0.07	0.06
vf	0.81	1.06	0.72	1.02	0.78	1.2	0.68	0.78	1.00	0.67
X		-19.06	-0.39	-0.26	0.035	-0.66	0.36	0.020	-0.013	0.013
%X	0.81	-23.86	-13.02	-20.93	4.14	-32.5	19.32	4.14	-19.0	21.5

Sample A50

	Al	Si	Fe	Mg	Ca	Na	K	Ti	Mn	P
Lithon	9.88	78.74	3.19	0.97	1.47	2.19	1.35	0.49	0.07	0.08
vf	0.61	1.16	0.70	0.68	1.11	1.16	0.38	0.59	0.88	0.62
X		-37.36	-0.40	-0.10	-0.66	-1.04	0.84	0.016	-0.021	-0.0007
%X	0.61	-47.45	-12.42	-10.70	-44.81	-47.36	62.22	3.33	-30.29	-0.88

Appendix 2

Normalized whole rock compositions of Goldenville samples

Normalized Compositions of Goldenville Samples

Sample	SiO_2	Al_2O_3	Fe_2O_3	MgO	CaO	Na_2O	K_2O	TiO_2	MnO	P_2O_5	TOTAL
G19-354											
2Li	79.85	9.56	4.04	.23	1.96	2.11	1.56	.48	.10	.11	100.00
3C	64.97	18.24	6.35	2.28	0.52	1.74	4.50	1.15	.11	.15	100.00
3Li	80.15	9.98	4.03	0.14	1.62	1.78	1.60	0.49	.10	.11	100.00
4C	71.48	14.66	5.42	1.46	0.77	1.89	3.23	0.85	.08	.15	100.00
4Li	81.80	9.12	3.65	0.03	1.70	1.76	1.32	0.42	0.08	.11	100.00
5C	73.80	13.84	5.23	0.59	0.95	1.79	2.85	0.73	.09	.13	100.00
5Li	81.51	9.04	3.62	0.04	1.87	2.03	1.26	0.43	.10	.12	100.00
6C	63.28	19.29	6.64	2.46	0.42	1.39	5.00	1.25	.12	.14	100.00
6Li	79.90	9.90	3.96	0.06	1.77	2.21	1.48	0.49	.11	.11	100.00
1C	58.62	21.68	7.27	2.11	0.48	1.78	6.22	1.54	.12	.17	100.00
1Li	80.30	9.40	3.91	0.26	2.05	1.85	1.55	0.46	.09	.13	100.00
2C	63.63	19.24	6.65	1.98	0.56	1.55	4.82	1.30	.12	.15	100.00
G26-415											
1C	66.79	18.60	4.79	1.73	0.23	1.80	4.94	0.92	.06	.15	100.00
1Li	85.14	8.43	2.53	0.02	0.56	1.94	0.92	0.32	.06	.09	100.00
2C	54.55	25.11	6.02	3.53	0.21	1.21	7.69	1.41	.10	.17	100.00
2Li	85.77	7.33	2.50	0.02	1.47	1.86	0.63	0.27	.06	.09	100.00
3C	61.40	21.91	5.55	1.90	0.18	1.60	6.15	1.07	.09	.15	100.00
3Li	83.99	7.94	2.63	0.02	2.08	2.16	0.71	0.29	.08	.09	100.00
4C	54.62	25.59	6.35	2.37	0.18	1.41	7.78	1.43	.09	.17	100.00
4Li	83.10	8.87	2.79	0.02	1.41	2.39	0.89	0.36	.08	.10	100.00
5Li	84.99	7.54	2.45	0.02	1.58	2.39	0.60	0.27	.07	.09	100.00
6C	53.61	26.08	6.38	2.62	0.18	1.43	8.01	1.43	.10	.17	100.00

Normalized Compositions of Goldenville Samples

Sample	SiO_2	Al_2O_3	Fe_2O_3	MgO	CaO	Na_2O	K_2O	TiO_2	MnO	P_2O_5	TOTAL
G26-353											
1C	69.61	16.24	4.87	2.12	0.53	1.86	3.68	0.86	.09	.14	100.00
1Li	84.33	8.02	2.92	0.03	1.88	1.66	0.67	0.31	.08	.09	100.00
2C	75.03	13.04	4.37	1.36	0.71	2.25	2.37	0.66	.10	.13	100.00
2Li	82.12	9.28	3.36	0.11	1.39	2.05	1.14	0.37	.07	.11	100.00
3C	74.78	12.70	4.12	1.70	1.48	2.16	2.26	0.59	.09	.12	100.00
3Li	83.61	8.44	3.01	0.05	1.62	1.97	0.78	0.34	.09	.09	100.00
4C	68.49	17.01	5.04	1.56	0.48	2.56	3.77	0.86	.09	.14	100.00
4Li	82.11	9.09	3.38	0.09	1.63	2.08	1.02	0.39	.10	.10	100.00
5Li	83.20	8.65	3.07	0.06	1.47	2.08	0.91	0.36	.09	.11	100.00
6C	66.53	17.99	5.28	1.84	0.38	2.48	4.26	0.99	.08	.16	100.00
G20-747											
1C	70.51	15.54	4.52	1.39	1.39	2.64	3.09	0.70	.07	.14	100.00
1Li	78.43	11.03	3.47	0.42	1.91	2.58	1.53	0.43	.07	.13	100.00
2C	67.36	17.92	5.06	1.57	0.73	2.45	3.87	0.82	.07	.15	100.00
2Li	80.00	9.84	3.32	0.19	2.44	2.52	1.15	0.36	.07	.11	100.00
3C	67.92	16.70	4.68	2.93	0.93	2.27	3.59	0.77	.07	.14	100.00
3Li	76.57	11.52	4.08	1.40	1.47	2.37	1.82	0.52	.11	.13	100.00
4C	68.94	16.70	4.82	1.65	0.85	2.62	3.49	0.73	.06	.14	100.00
4Li	77.04	11.89	3.65	0.25	1.99	2.62	1.85	0.49	.06	.14	100.00
5C	63.35	20.55	3.56	1.55	0.53	2.24	4.98	1.00	.07	.17	100.00
5Li	77.73	11.76	3.65	0.33	1.45	2.66	1.76	0.47	.05	.13	100.00
6C	68.49	16.95	5.03	1.35	1.03	2.59	3.58	0.78	.06	.15	100.00

Normalized Compositions of Goldenville Samples

Sample	SiO_2	Al_2O_3	Fe_2O_3	MgO	CaO	Na_2O	K_2O	TiO_2	MnO	P_2O_5	TOTAL
G20-753											
1C	63.43	20.57	5.74	1.44	0.34	2.21	5.01	1.02	.09	.15	100.00
1Li	82.57	9.20	2.91	0.06	1.50	2.20	1.08	0.30	.07	.11	100.00
2C	62.03	21.72	5.48	1.60	0.23	1.83	5.92	0.97	.09	.13	100.00
2Li	85.27	7.07	2.31	0.04	2.40	2.17	0.38	0.20	.08	.09	100.00
3C	62.62	21.52	5.51	1.50	0.23	1.75	5.76	0.92	.06	.13	100.00
3Li	83.47	8.82	2.76	0.04	1.20	2.40	0.85	0.30	.07	.09	100.00
4C	70.62	16.43	4.70	1.31	0.27	2.26	3.57	0.64	.05	.13	100.00
4Li	84.01	8.56	2.75	0.05	1.09	2.24	0.88	0.30	.05	.09	100.00
5C	62.34	21.64	5.63	1.50	0.19	1.79	5.75	0.94	.07	.14	100.00
5Li	82.40	9.69	2.97	0.04	0.88	2.48	1.12	0.29	.04	.10	100.00
6C	66.57	18.87	5.16	1.36	0.31	2.35	4.33	0.85	.06	.14	100.00
6Li	84.63	8.06	2.51	0.05	1.51	2.14	0.68	0.28	.05	.10	100.00

Appendix 3

Goldenville Gresen calculations

Lithon = Lithon composition

1Cvf - 6Cvf = volume factors for samples 1C-6C

1Cx - 6Cx = absolute amount lost or gained

1Cx% - 6Cx% = percent lost or gained

SAMPLE G26-415

SAMPLE		Al	Si	Fe	Mg	Ca	Na	K	Ti	Mn	P
Lithon Comp.		8.02	84.60	2.58	0.02	1.42	2.15	0.75	0.30	0.07	0.09
1C vf		0.43	1.27	0.54	0.012	6.17	1.19	0.15	0.33	1.17	0.60
2C vf		0.32	1.55	0.43	0.0057	6.76	1.78	0.098	0.21	0.7	0.53
3C vf		0.37	1.38	0.47	0.011	7.89	1.34	0.12	0.28	0.78	0.60
4C vf		0.31	1.55	0.41	0.0084	7.89	1.52	0.096	0.21	0.78	0.53
6C vf		0.31	1.56	0.40	0.0076	7.89	1.50	0.094	0.21	0.70	0.53
1C	X		-55.83	-0.52	0.72	-1.32	-1.37	1.37	0.096	-0.044	-0.026
	X%		-66.05	-20.17	3619.50	-93.04	-64.00	183.22	31.87	-63.14	-28.33
2C	X		-67.14	-0.65	1.11	-1.35	-1.76	1.71	0.15	-0.038	-0.036
	X%		-79.37	-25.33	5548.00	-95.27	-81.99	228.11	50.4	-54.29	-39.56
3C	X		-61.88	-0.53	0.68	-1.35	-1.56	1.53	0.096	-0.037	-0.035
	X%		-73.15	-20.41	3415.00	-95.31	-72.47	203.40	31.97	-52.42	-38.33
4C	X		-67.67	-0.61	0.72	-1.36	-1.71	1.66	0.14	-0.042	-0.037
	X%		-79.99	-23.70	3573.50	-96.07	-79.67	221.57	47.77	-60.14	-41.44
6C	X		-67.98	-0.60	0.79	-1.36	-1.71	1.73	0.14	-0.039	-0.037
	X%		-80.36	-23.34	3961.00	-96.07	-79.38	231.08	47.77	-55.74	-41.44

Sample G20-747

	Al	Si	Fe	Mg	Ca	Na	K	Ti	Mn	P
Lithon	11.14	78.30	3.52	0.94	1.95	2.60	1.58	0.44	0.06	0.13
1C vf	0.72	1.11	0.78	0.68	1.40	0.99	0.51	0.63	0.86	0.93
2C vf	0.62	1.16	0.70	0.60	2.67	1.06	0.41	0.54	0.86	0.93
3C vf	0.68	1.15	0.75	0.32	2.10	1.15	0.44	0.57	0.86	0.93
4C vf	0.68	1.14	0.73	0.57	2.29	0.99	0.45	0.60	1.00	0.93
5C vf	0.54	1.24	0.63	0.61	3.68	1.16	0.32	0.44	0.86	0.77
6C vf	0.66	1.14	0.70	0.70	1.89	1.00	0.44	0.56	1.00	0.87
1C X	0.72	-27.53	-0.27	0.061	-0.95	-0.70	0.064		-0.0096	-0.029
%X		-35.16	-7.55	6.47	-48.68	-26.89	40.81	14.55	-16.0	-22.46
2C X	0.62	-36.54	-0.38	0.033	-1.50	-1.08	0.82	0.068	-0.017	-0.037
%X		-46.66	-10.88	3.55	-76.79	-41.58	51.86	15.55	-27.67	-28.46
3C X	0.68	-32.11	-0.34	1.05	-1.32	-1.06	0.86	0.084	-0.012	-0.035
%X		-41.02	-9.59	111.96	-67.57	-40.63	54.5	19.0	-20.67	-26.77
4C X	0.68	-31.42	-0.24	0.18	-1.37	-0.82	0.79	0.056	-0.019	-0.035
%X		-40.13	-6.89	19.36	-70.36	-31.48	50.20	12.82	-32.0	-26.77
5C X	0.54	-44.09	-6.52	-0.103	-1.39	1.11	0.10	-0.022	-0.038	
%X		-56.31	-14.70	-10.96	85.32	-53.48	70.20	22.71	-37.0	-29.39
6C X	0.66	-33.10	-0.20	-0.049	-1.27	-0.89	0.78	0.075	-0.020	-0.031
%X		-42.27	-5.69	5.21	-65.14	-34.25	49.54	17.0	-34.0	-23.85

Sample G19-354

	Al	Si	Fe	Mg	Ca	Na	K	Ti	Mn	P
Lithon	9.50	80.59	3.8	0.13	1.83	1.96	1.46	0.46	0.10	0.12
1C vf	0.44	1.38	0.53	0.062	3.81	1.10	0.24	0.30	0.83	0.71
2C vf	0.49	1.27	0.58	0.066	3.27	1.27	0.30	0.35	0.83	0.80
3C vf	0.52	1.24	0.61	0.057	3.52	1.13	0.32	0.40	0.91	0.80
4C vf	0.65	1.13	0.71	0.089	2.38	1.04	0.45	0.54	1.25	0.80
5C vf	0.49	1.27	0.58	0.053	4.36	1.41	0.29	0.37	0.83	0.86
1C X	0.44	-54.80	-0.67	0.80	-1.62	-1.18	1.28	0.22	-0.047	-0.045
%X		-68.0	-17.34	614.15	-88.46	-60.04	87.45	47.30	-47.2	-37.67
2C X	0.49	-49.41	-0.61	0.84	-1.56	-1.20	0.90	0.177	-0.041	-0.047
%X		-61.31	-15.80	646.31	-85.01	-61.25	61.77	38.48	-41.2	-38.75
3C X	0.52	-46.81	-0.57	1.06	-1.56	-1.06	0.88	0.14	-0.043	-0.042
%X		-58.07	-14.68	812.0	-85.22	-53.84	60.27	30.0	-42.8	-35.0
4C X	0.65	-34.13	-0.35	0.82	-1.33	-0.73	0.64	0.093	-0.048	-0.023
%X		-42.35	-8.97	630.0	-72.65	-37.32	43.80	20.11	-48.0	-18.75
5C X	0.69	-29.67	-0.26	6.28	-1.18	-0.73	0.51	0.044	-0.038	-0.03
%X		-36.81	-6.75	213.15	-64.18	-36.69	34.69	9.5	-37.9	-25.25
6C X	0.49	-49.58	-0.62	1.08	-1.62	-1.28	0.99	0.15	-0.041	-0.051
%X		-61.53	-15.93	827.23	-88.75	-65.25	67.81	33.15	-41.2	-42.83

Sample G20-753

	Al	Si	Fe	Mg	Ca	Na	K	Ti	Mn	P
Lithon	8.67	83.54	2.74	0.05	1.41	2.30	0.86	0.28	0.06	0.10
1C vf	0.42	1.32	0.48	0.035	4.15	1.04	0.17	0.28	0.67	0.67
2C vf	0.40	1.35	0.50	0.031	6.13	1.26	0.15	0.29	0.67	0.77
3C vf	0.40	1.34	0.50	0.033	6.13	1.31	0.15	0.30	1.00	0.77
4C vf	0.53	1.18	0.58	0.038	5.22	1.02	0.24	0.44	1.20	0.77
5C vf	0.40	1.34	0.49	0.033	7.42	1.29	0.15	0.30	0.86	0.71
6C vf	0.46	1.26	0.53	0.037	4.55	0.98	0.20	0.33	1.00	0.71
1C X	0.42	-56.90	-0.33	0.56	-1.27	-1.37	1.24	0.15	-0.022	-0.037
%X		-68.11	-12.01	1109.6	-89.87	-59.64	144.67	53.0	-37.0	-37.0
2C X	0.40	-58.73	-0.55	0.59	-1.32	-1.57	1.51	0.11	-0.24	-0.048
%X		-70.30	-20.01	1180.0	-93.48	-68.17	175.35	38.57	-40.0	-48.0
3C X	0.40	-58.49	-0.54	0.55	-1.32	-1.6	1.44	0.088	-0.036	0.048
%X		-70.02	-19.56	1100.0	-93.48	-69.56	167.91	31.43	-60.0	-48.0
4C X	0.53	-46.11	-0.25	0.55	-1.33	-1.58	1.44	0.096	-0.032	-0.44
%X		-55.20	-9.09	1288.6	-89.85	-47.92	120.01	21.14	-55.83	-31.1
5C X	0.40	-58.60	-0.49	0.55	-1.33	-1.58	1.44	0.096	-0.032	-0.044
%X		-70.15	-17.81	1100.0	-94.61	-68.87	167.44	34.29	-53.33	-44.0
6C X	0.46	-52.92	-0.37	1.58	-1.27	-1.22	1.13	0.11	-0.032	-0.036
5X		-63.34	-13.37	1151.2	-89.89	-53.0	131.6	39.64	-54.0	-35.6

Sample G26-353

		Al	Si	Fe	Mg	Ca	Na	K	Ti	Mn	P
Lithon		8.70	83.07	3.15	0.07	1.60	1.97	0.9	0.35	0.09	0.10
1C vf		0.54	1.19	0.65	0.033	3.02	1.06	0.25	0.41	1.00	0.71
2C vf		0.67	1.11	0.72	0.052	2.26	0.88	0.38	0.53	0.9	0.77
3C vf		0.69	1.11	0.77	0.042	1.08	0.91	0.40	0.59	1.00	0.83
4C vf		0.51	1.21	0.63	0.045	3.33	0.78	0.24	0.41	1.00	0.71
6C vf		0.48	1.25	0.60	0.038	4.21	0.79	0.21	0.35	1.13	0.63
1C	X	0.54	-45.48	-0.52	1.08	-1.31	-0.97	1.09	0.11	-0.041	-0.024
	X%		-54.75	-16.51	1535.43	-82.11	-49.02	120.8	32.69	-46.0	-24.4
2C	X	0.67	-32.8	-0.22	0.84	-1.12	-0.46	0.69	0.092	-0.023	-0.013
	X%		-39.49	-7.05	1201.71	-70.27	-23.48	76.43	26.34	-25.56	-12.9
3C	X	0.69	-31.47	-0.31	1.10	-0.58	-0.48	0.66	0.057	-0.028	-0.017
	X%		-37.89	-9.75	1575.71	-36.18	-24.35	73.27	16.31	-31.0	-17.2
4C	X	0.51	-48.14	-0.58	0.73	-1.36	-0.66	1.02	0.089	-0.044	-0.029
	X%		-57.95	-18.4	1036.57	-84.7	-33.73	113.63	25.31	-49.0	-28.6
6C	X	0.48	-51.14	-0.62	0.81	-1.42	-0.77	1.15	0.13	-0.052	-0.023
	X%		-61.56	-19.54	1161.71	-88.6	-39.27	127.2	35.77	-57.33	-23.2

Appendix 4

Au, W, As and Sb values for Ruth Falls Syncline Samples

Sample	Au (ppb) Actual	Au (ppb) cy	W (ppm) Actual	W (ppm) cy	As (ppm) Actual	As (ppm) cy	Sb (ppm) Actual	Sb (ppm) cy
A1	0.5		0.1		1.9		0.9	
A8	0.8		0.1		2.1		0.9	
F15	1.2		0.2		1.2		0.6	
A45	0.8		0.3		2.1		1.1	
A47	0.6		0.5		1.7		1.9	
A49	0.5		0.3		1.5		0.9	
A50	0.8		0.1		2.9		1.3	
A50A	0.4		0.3		2.1		0.5	
A50E	1.4		0.2		1.9		0.4	
A52	2.7		0.2		1.5		0.8	
A53	0.9		1.2		3.8		1.4	
A54	0.3		0.4		3.6		1.2	
A55	0.2		0.2		1.0		0.3	
B-92	0.4		0.3		1.7		0.6	
F5A	0.5		0.2		1.1		0.5	
F12	3.5		0.2		1.5		0.5	
F14	3.2		0.4		3.2		1.3	
F18	1.2		1.6		2.5		1.1	
A1C	2.1		0.4		4.3		2.2	
A1L	1.1		0.4		3.0		1.5	
F5A(1)C	5.8		0.2		2.0		0.9	
F5A(1)L	1.3		0.3		1.6		1.1	
F5A(2)C	7.3		0.2		1.0		0.9	
F5A(2)L	1.6		0.4		1.6		0.7	
F14C	1.5		0.1		2.2		0.8	
F14L	6.1		1.2		2.9		1.0	
A49C	1.2		0.1		2.6		1.8	
A49L	0.6		0.1		1.7		1.4	
A50C	0.6		0.0		3.0		1.7	
A50L	1.3		0.1		2.4		1.9	
18A50C	0.5		0.1		2.1		3.0	
20A50D	0.5		0.0		2.6		1.9	
21A50F	0.7		0.1		4.9		2.6	
22A50B	0.5		0.1		2.7		2.1	

cy - chemical yield
C - cleavage
L - Lithon

Appendix 5

Au, W, Sb and As values for Goldenville samples

Au, W, As and Sb values for Goldenville samples

Sample	Au ppb	W ppm	As ppm	Sb ppm
G20-747				
1C	8.3	4.7	23	0.3
1Li	8.6	2.7	35	13.4
2C	8.8	6.1	173	1.8
2Li	6.3	1.3	36	0.5
3C	9.3	6.1	30	0.5
3Li	10.6	2.8	385	3.2
4C	4.4	5.1	417	3.4
4Li	2.9	2.5	24	0.2
5C	8.9	6.9	82	0.6
5Li	5.3	2.4	274	2.4
6C	3.8	6.2	134	1.1
G19-354				
1C	4.0	11.9	143	1.5
1Li	.2	3.4	25	0.6
2C	3.2	9.2	85	0.9
2Li	11.4	2.9	47	0.5
3C	.2	8.5	4	0.2
3Li	3.9	3.3	25	0.4
4C	3.5	6.0	55	0.6
4Li	5.4	3.1	18	0.4
5C	4.5	5.4	250	2.3
5Li	2.0	2.2	47	0.5
6C	4.3	10.3	91	0.9
6Li	4.4	3.8	47	0.4

Au, W, As and Sb values for Goldenville samples

Sample	Au ppb	W ppm	As ppm	Sb ppm
G20-753				
1C	6.1	9	420	3.5
1Li	2.0	2	160	1.4
2C	1	9	355	2.8
2Li	0.4	1	25	0.3
3C	6.2	11	345	2.5
3Li	6.8	1	13	0.2
4C	1.4	7	25	0.5
4Li	6.5	2	65	0.9
5C	9.1	10	210	1.8
5Li	4.2	1	65	0.6
6C	1	7	215	1.4
6Li	7.4	2	190	1.3

Sample	Au ppb	W ppm	As ppm	Sb ppm
G26-353				
1C	2.4	5	110	0.7
1Li	3.0	2	20	0.2
2C	5.3	4	60	0.5
2Li	5.6	3	70	0.4
3C	2.6	4	50	0.4
3Li	5.4	3	15	0.1
4C	4.3	7	80	0.4
4Li	4.5	3	90	0.4
5Li	3.4	2	130	0.5
6C	3.4	7	170	0.7

Au, W, As and Sb values for Goldenville samples

Sample	Au ppb	W ppm	As ppm	Sb ppm
G26-415				
1C	7.3	6	95	0.6
1Li	4.7	2	20	0.3
2C	4.2	8	165	0.9
2Li	2.1	1	15	0.3
3C	2.8	7	25	0.3
3Li	2.6	2	15	0.3
4C	6.2	10	420	2.3
4Li	2.8	2	9	0.1
5Li	1.2	1	15	0.2
6C	5.6	11	130	0.6
6Li	1.5	1	8	0.1

Appendix 6

Goldenville Trace Element Analysis
of Composite Powder Pellets

	G19-354		G20-753		G26-353		G26-415		G20-747	
	C	Li	C	Li	C	Li	C	Li	C	Li
Rb	153	64	191	37	112	38	159	37	138	64
Sr	153	207	173	218	158	188	156	173	212	251
Y	38	26	37	21	30	24	34	22	30	24
Zr	462	230	283	115	278	158	322	137	234	150
Nb	19	17	18	15	19	15	21	17	18	16
Ce	98	41	110	16	55	36	53	12	82	31
Nd	40	23	48	0	19	16	20	9	27	8
La	56	24	48	13	41	14	38	18	38	29
Ba	995	354	1235	221	774	226	1064	204	933	389
Pb	11	12	12	17	12	14	11	10	11	11

Appendix 7

Composition and volume factors of Australian greywackes and siltstones

Graywacke

	SiO	Ti	Al	Fe	Mn	Mg	Ca	Na	K	P_2O_5	Loss
Lithon	76.56	0.44	10.88	3.54	0.04	1.87	0.24	1.88	2.02	0.15	3.34
Cleavage	62.87	0.90	17.52	5.17	0.04	3.16	0.33	1.20	4.43	0.23	5.50
vf	1.22	0.49	0.62	0.69	1	0.59	0.73	1.57	0.45	0.65	0.61

Siltstone

	Si	Ti	Al	Fe	Mn	Mg	Ca	Na	K	P_2O_5	Loss
Lithon	69.4	0.53	13.52	6	0.08	2.49	0.22	1.21	2.88	0.13	3.52
Cleavage	51.5	0.96	22.65	8.28	0.06	3.95	0.22	0.55	6.26	0.16	5.53
vf	1.35	0.55	0.59	0.73	1.33	0.63	1	2.2	0.46	0.81	0.64

Appendix 8

Accuracy and Precision Estimates

Element	Method	Precision	Accuracy	Detection limit
SiO_2	XRF(FP)	< 2%	< 2%	0.1%
Al_2O_3		< 2%	< 2%	0.1%
Fe_2O_3		< 2%	< 2%	0.1%
MgO		< 2%	< 2%	0.1%
CaO		< 2%	< 2%	0.1%
Na_2O		< 2%	< 2%	1.1%
K_2O		< 2%	< 2%	0.05%
TiO_2		< 2%	< 2%	0.01%
MnO		< 2%	< 2%	0.05%
P_2O_5		< 2%	< 2%	0.05%
L.O.I.		< 5%		
	RNAA			
Au		0.1 ppb		
Sb				
W				
As		200ppb		
	INAA			
Au		25%	<10%	1ppb
Sb		40%	<10%	0.1ppb
W		12%	<10%	0.1ppb
As		10%	<10%	0.1ppb
	XRF(PP)			
Rb		7%	<10%	5ppm
Sr		<5%	<10%	10ppm
Y		<5%	<10%	
Zn		6%	<10%	20ppm
Nb		5%	<10%	10?ppm
Ce		12%	<10%	10?ppm
Nd		5%	<10%	10?ppm
La		10%	<10%	10ppm
Ba		6%	<10%	10?ppm
Pb		20%	<10%	10?ppm